Louisiana State University
LSU Digital Commons

LSU Master's Theses Graduate School

8-21-2018

Development Strategies For a Fractured, Heavy Oil Reservoir - Results From Numerical Simulations

German Albertovich Abzaletdinov
Louisiana State University and Agricultural and Mechanical College, gabzal1@lsu.edu

Follow this and additional works at: https://digitalcommons.lsu.edu/gradschool_theses
Part of the Petroleum Engineering Commons

Recommended Citation

Abzaletdinov, German Albertovich, "Development Strategies For a Fractured, Heavy Oil Reservoir - Results From Numerical Simulations" (2018). *LSU Master's Theses*. 4792.
https://digitalcommons.lsu.edu/gradschool_theses/4792

This Thesis is brought to you for free and open access by the Graduate School at LSU Digital Commons. It has been accepted for inclusion in LSU Master's Theses by an authorized graduate school editor of LSU Digital Commons. For more information, please contact gradetd@lsu.edu.

DEVELOPMENT STRATEGIES FOR A FRACTURED, HEAVY OIL RESERVOIR – RESULTS FROM NUMERICAL SIMULATIONS

A Thesis

Submitted to the Graduate Faculty of the
Louisiana State University and
Agricultural and Mechanical College
in partial fulfilment of the
requirements for the degree of
Master of Science in Petroleum Engineering

in

The department of Petroleum Engineering

by
German Albertovich Abzaletdinov
B.S., Ukhta State Technical University, Russia, 2016
December 2018

ACKNOWLEDGEMENTS

I am greatly thankful to Dr. Ipsita Gupta, my advisor who had an undefeatable confidence in me and who provided support and advice during my stay in the United States. She had guided me in my work, and supported me on my choice of career path.

Thanks are due to Dr. Sergey Durkin from Ukhta State Technical University for technical guidance and discussions on reservoir simulations, and help with data without which this research would not have been possible

Also, I owe a debt of gratitude to my committee members – Dr. Mileva Radonjic and Dr. Dandina Rao for their feedback and suggestions on my work.

Thanks to my wonderful friends the contribution of whom cannot be exaggerated – Dr. Denis Klimenko, Florencia Vasquez, Sulav Dhakal, Hope Asala, Makuachukwu Mbaegbu, William Dazet, Denys Maksymov, Iryna Zema and Liliana Avaroma.

I would like to thank Computer Modelling Group for license donation, and LSU's High-Perfomace Computing Facility for permission to run a supercomputer to simulate my models.

This work is dedicated to my dearest parents, and sister.

TABLE OF CONTENTS

ACKNOWLEDGEMENTS.......... ii

LIST OF TABLES iv

LIST OF FIGURES.......... v

NOMENCLATURE ix

ABSTRACT x

CHAPTER 1. INTRODUCTION.......... 1

CHAPTER 2. BACKGROUND AND LITERATURE REVIEW 4
  2.1 Naturally fractured reservoirs.......... 5
  2.2 Heavy oil reservoirs 9
  2.3 Development of naturally fractured heavy oilfields in different countries.......... 13
  2.4 Numerical simulation of naturally fractured systems 15
  2.5 SAGD in naturally fractured reservoirs and other EOR techniques to increase oil recovery.......... 18

CHAPTER 3. YAREGA HEAVY OIL FIELD 22
  3.1 Geology of YHOF 22
  3.2 Reservoir fluid properties.......... 26
  3.3 History of oilfield development.......... 29
  3.4 Geology of reservoir N.......... 30

CHAPTER 4. RESEARCH GOALS AND OBJECTIVES.......... 37

CHAPTER 5. METHODOLOGY.......... 39

CHAPTER 6. RESULTS AND DISCUSSION.......... 52
  6.1 Simulation results from 2-dimensional model 54
  6.2 Numerical simulations for sector N of YHOF oilfield.......... 61

CHAPTER 7. EFFICIENCY VALIDATION OF FISHTAIL WELL DESIGN BASED ON HISTORY MATCHED DATA.......... 88
  7.1 History matching procedure.......... 90

CHAPTER 8. CONCLUSIONS 100

REFERENCES.......... 102

VITA.......... 109

LIST OF TABLES

Table 1. Historical timeline for YHOF development. 2

Table 2. Examples of heavy oilfields and their development strategies. 12

Table 3. Physical-chemical properties of degasified oil from YHOF. 26

Table 4. Physical and chemical properties of water from formation III. 27

Table 5. Properties and composition of formation oil from well #49p........................27

Table 6. Oil densities and viscosities with temperature – heavy oils from YHOF 28

Table 7. Geological and physical characteristics of reservoir N. 32

Table 8. Governing equations. 40

LIST OF FIGURES

Figure 1. Fracture formation occurring with (a) and without (b) the offset of the layers (Golf-Racht, 1986). 8

Figure 2. World distribution of world oil reserves in accordance with oil density (from Ruzin et al., 2015) 9

Figure 3. Porosity distribution in reservoir N (Ruzin et al, 2015). 24

Figure 4. Permeability distribution in reservoir N (Ruzin et al, 2015). 25

Figure 5. Porosity-permeability relationship model for numerical simulation of reservoir N (Ruzin et al, 2015). 25

Figure 6. Schematic map of YHOF (scheme from YaregaRuda). 31

Figure 7. Oil density and viscosity with temperature – fluids from reservoir N (Ruzin et al, 2015). 33

Figure 8. Geologic cross section of YHOF (Ruzin et al, 2015). 34

Figure 9. Stratigraphy of YHOF (Ruzin et al, 2015) 35

Figure 10. Modern thermomining methods currently being used in YHOF (Chertenkov et al, 2012). 36

Figure 11. Single porosity approach for numerical simulation of naturally fractured reservoirs 41

Figure 12. Schematic representation of flow in dual porosity and dual permeability media. 41

Figure 13. Simple 2-layer 2-dimentional representation of dual media distribution. 44

Figure 14. 20-thousand 2-dimentional single porosity model. 44

Figure 15. Testing of various steam-injection modes. 44

Figure 16. Visual representation of initiation of early water/steam breakthrough. 46

Figure 17. Testing of a preliminary thermogel injection technique. 46

Figure 18. Inverted 5-point dual porosity dual permeability development model. 47

Figure 19. Initial oil saturation of sector from reservoir N. 47

Figure 20. Porosity distribution of a sector from reservoir N. 48

Figure 21. Permeability distribution of sector from oilfield N. 48

Figure 22. Tested development models for the sector of oilfield N. 50

Figure 23. Fishtail well design for cyclic steaming. 50

Figure 24. SuperMike-II supercomputer at LSU. 51

Figure 25. Temperature distribution in a test 2.7 million SAGD model. 52

Figure 26. Example of a grid block size sensitivity analysis. 53

Figure 27. Results of 2-layer 2-dimentional 200-grid block model simulation. 55

Figure 28. Results of various steam injection modes simulation. 56

Figure 29. Results of the simulation for a 20-thousand grid block 2-dimentional model. 57

Figure 30. Visual representation of preliminary thermogel plugging a fractured zone next to an injector well. 58

Figure 31. Results of preliminary thermogel injection in a 2-dimentional model. 59

Figure 32. Results of inverted 5 – point dual porosity simulation. 60

Figure 33. Average pressure and temperature trends for different grid block sizes. 62

Figure 34. Cumulative oil and liquid trends for different grid block sizes. 63

Figure 35. Watercut trends for different grid block sizes. 64

Figure 36. “Typical” and “untypical” behavior trends for single and double porosity systems. 65

Figure 37. Comparison of hot and cold water injection and primary depletion approaches. 67

Figure 38. Comparison between efficiency of hot water and steam injection. 68

Figure 39. The influence of the effect of fracture permeability on recovery factor. 70

Figure 40. The influence of the effect of fracture spacing on recovery factor. 71

Figure 41. The influence of the effect of steam injection pressure on recovery factor. 72

Figure 42. Thermogel injection into injector and producer well surrounding area to enhance oil recovery. 74

Figure 43. Steam/water movement in a fractured reservoir from thermogel injection. 74

Figure 44. Results of thermogel injection into a wellbore surrounding area. 75

Figure 45. Visual representation of thermogel injection into the entire zone between wells in SAGD pair. 76

Figure 46. Results of thermogel injection into the entire zone between the wells in SAGD pair. 77

Figure 47. Results of the model with 3 additional vertical producer wells. 79

Figure 48. Results of the model with 5 vertical producers. 80

Figure 49. Results of the model with 5 horizontal injectors. 81

Figure 50. Results of cyclic steam stimulation using SAGD wells. 83

Figure 51. Comparison of oil recovery using fishtail well design and other EOR techniques. 86

Figure 52. Production parameters of a fishtail well design approach. 87

Figure 53. Oil saturation distribution of sector X of YHOF..................................89

Figure 54. Porosity distribution of sector X of YHOF...89

Figure 55. Permeability distribution of sector X of YHOF....................................90

Figure 56. Real monthly steam injection history profile for sector X of YHOF...91

Figure 57. Oil and water production profile that provides the best match with real data...92

Figure 58. History matching errors for cumulative oil production for sector X of YHOF...93

Figure 59. History matching errors for cumulative water production for sector X of YHOF...93

Figure 60. Fishtail well design implemented in sector X of YHOF.........................94

Figure 61. Comparison between SAGD and fishtail well-design in respect of oil recovery factor 97

Figure 62. Comparison between SAGD and fishtail well design in respect of cumulative steam/oil ratio....98

Figure 63. Comparison between SAGD and fishtail well design in respect of water cut....99

NOMENCLATURE

cp – centipoise

T – temperature

u – velocity

k – permeability

μ – viscosity

p – pressure

x – distance

r – radius

ϕ – porosity

c_t – total compressibility

∇ – divergence

ρ – density

g – gravitational acceleration

Q – heat content

U – internal energy

H_f – enthalpy of fluid

ABSTRACT

This research is focused on studying reservoir “N” in the Yarega heavy oilfield (YHOF) for development strategies and production optimization. YHOF is a naturally fractured heavy oil field where only very recently SAGD technology has been introduced. The motivation for this research is derived from the fact that SAGD employed in this field has so far resulted in early steam breakthrough leading to producer abandonment and new drilling, thus increasing costs. This study explores numerically different static and dynamic reservoir characterization models (single porosity versus dual porosity systems), and subsequent pressure-production history matched reservoir simulation for understanding heat and mass transfer mechanisms. Thereafter, different drilling and production scenarios are tested for candidate selection for the highest recovery and production optimization.

Results from the 3 dimensional sector model suggest that while all effective development technologies in this reservoir should be based on thermal methods of oil recovery, cyclic steam injection inhibited early breakthrough and thus can eliminate or reduce risk for well abandonment from the same cause. Based on results from this research, we however recommend the testing of a fishtail well development plan with cyclic steam injection that includes a 10-day steam injection, 10-day soaking period, and 10-day production period. In comparison to continuous steam injection recovery (4.5% over three years), we anticipate a 7% recovery from this technology implementation and testing.

CHAPTER 1. INTRODUCTION

Yarega Oilfield is a heavy oil field in Komi Republic of Russia, where the first strain of oil is said to have been discovered in 1664 in the waters from the Ukhta River that had oil slicks (Chertenkov et al., 2012). The first well in the region was drilled in 1937, the first in-situ oil mined in 1939, and till 1954 oil mining was the primary mechanism of recovery (Chekonin et al., 2012). Although thermal stimulation of the oil was proposed as early as 1937 by oilfield geologist, I.N. Strizhev, it was not until 1968 that the first steam operation was conducted. By 1972, commercial production of oil from thermal oil-mine recovery was established, and production from Yarega oil rose from 4 % from the in-situ mining techniques to 33% from thermal mining (Chekonin et al., 2012; Chertenkov et al., 2012). Steam-assisted gravity drainage (SAGD) was introduced in the region in 2006 (Chertenkov et al., 2014), and annual production increased to 3.5 million metric tons (25 million barrels) (Chekonin et al., 2012) by 2011.

This research is focused on studying a reservoir (henceforth called reservoir "N") in Yarega heavy oilfield (YHOF) for development strategies and production optimization. YHOF is a naturally fractured heavy oil field where only very recently SAGD technology has been introduced. This study explores numerically different static and dynamic reservoir characterization models (single porosity versus dual porosity systems), and subsequent pressure-production history matched reservoir simulation for understanding heat and mass transfer mechanisms. Thereafter, different drilling and production scenarios are tested for candidate selection for the highest recovery and production optimization.

It is to be noted that the most recent methods of SAGD production from this region uses the drilling technology of opposing injectors and producers. In fact, the world's first opposing SAGD horizontal drilling was performed in this oilfield in 2011-2012 (Chertenkov et al., 2014). The uniqueness of this research is that:

a) it is the first dual porosity reservoir simulation of this area to quantify and understand the impact of the different SAGD methods currently employed in this area, and that

b) it goes beyond current SAGD technology to propose and recommend a new method of drilling and production in the region (the SAGD fish tail) using results from a dual porosity/dual permeability reservoir model and history-matched simulation runs.

Table 1. Historical timeline for YHOF development (from: Chertenkov et al., 2014).

1932	YHOF pool was discovered
1937	Construction of mine #1 was initiated
1939	Start of oil production from mine #1
1942	Construction of mine #3 was initiated
1948	Construction of mine #2 was initiated
1939 - 1954	Mining as per Ukhta system
1954	Mining as per slant well system
1968	First pilot tests of thermal mining technology
1972	Commercial application of thermal mining was initiated
1973 - 1990	Oil production as per commingled system
1998	First pilot tests of surface/sub-surface production system

(table cont'd.)

2003	Acceptance of a new technological system in YHOF currently being used in surface/sub-surface production system
2004	First pilot tests of drilling SAGD wells in YHOF
2006	First time in YHOF three pairs of horizontal wells were drilled from the same location for SAGD technology
2011 - 2012	First in the world opposing SAGD wells from two different locations were drilled
2013	Commencement of opposing SAGD wells using rack type slant rigs

CHAPTER 2. BACKGROUND AND LITERATURE REVIEW

Fractures are one of the most abundant geologic features in the upper layer of Earth’s crust. They can be observed on outcrops and in the subsurface (seismic/well log data) and it is likely that the majority of reservoirs contain some natural fractures (Narr et al, 2006). Development of such naturally fractured reservoirs generally requires an approach different from the ones used in the development of conventional reservoirs. One of the most significant difficulties pertaining to the development of fractured reservoirs is the heterogeneity of properties of the rock (for examples, porosity and permeability) in matrix versus fractures. Thereby, such fractured reservoirs can be introduced as dual porosity reservoirs, where first media (matrix) and second media (fractures) have distinct different capacitive and conductive properties (Warren et al, 1963).

In addition to this, if the fractured reservoirs host heavy oil (high viscosity and molecular weight of the hydrocarbons), the complexity of producing from these reservoirs increases multiple fold as the resistance to motion for heavy oils is much higher than for usual light oils and requires different development techniques (Ruzin et al, 2015). There is a great number of various enhanced oil recovery techniques being currently used in the industry, such as gas injection, thermal and chemical injection. However, one of the most widely used techniques for heavy oils is steam or hot water flooding that increases mobility of the heavy oil to flow into the producer (Alvarado, 2010).

Today, in the age of significant development of computational capabilities, reservoir simulation of flow in naturally fractured heavy oil reservoirs are routinely performed, and development plans and forecasting of determinative parameters such as oil production, temperature and pressure distribution regularly conducted. Despite rapid development of reservoir simulation technologies, however, there still exists a considerable level of uncertainty in the development of naturally fractured reservoirs that leads to inevitable discrepancy between forecasted and actual oil production (Ruzin et al, 2015). The problem behind this uncertainty is ineffective development of matrix zones (due to their low permeability and reduced mobility of the oil) containing primary oil reserves and rapid depletion of fractures and their subsequent water encroachment that leads to oil being trapped in low permeability matrix, resulting in poor recovery in naturally fractured heavy oilfields (Witherspoon, 1981). The simulations are likely unable to capture this because of poor reservoir characterization, and the use of single porosity models for computational efficiency. Therefore, the biggest problem associated with the development of fractured heavy oilfields is sweeping low permeability matrix zones for increased recovery, and effectively capturing that physics in numerical simulation models.

This research focuses on developing a naturally-fractured heavy oil reservoir in an oilfield located in Russia using numerical simulations of coupled heat and fluid flow during stream-assisted gravity drainage (SAGD – described in detail in a later section). Data for this study was donated by Ukhta State Technical University in Russia. For the purpose of this thesis, the oilfield will be called oilfield “N”.

2.1 Naturally fractured reservoirs

It is well known that fractures in naturally fractured reservoirs may have a significant effect on production approach and process-dependent parameters (Khelifa et al, 2014). Such reservoirs have various types of fractures, from macrofractures predetermining main paths of fluid flow to almost not contributing to microfractures that may almost not contribute to flow (Saidi, 1983). Permeability of fractures is a complicated property to determine, and has a wide range of variation from reservoir to reservoir, and within a single reservoir. For oil field development, however, it is essential to understand and predict the response of the reservoir to production in terms of fluid flow through the permeable pathways. Fractures in oil and gas reservoirs may appear in any direction, but generally have a dominant direction for the macrofractures that correlate with the regional stress directions (Saidi, 1983). The number of fractures in the reservoir depends on the distribution of mechanical stresses in the rock and its strength properties. Long, large fractures are called macrofractures. If the rock has high vales of porosity, fractures can have shorter lengths and smaller fracture opening and are called microfractures. The main difference between these two types of fractures is related to fracture size. Generally, macrofractures are those having large opening (more than 100 micrometers) and significant length, while microfractures are the ones having limited opening and length (Song, 1998). Sometimes microfractures can form a so-called fracture network which in some cases are similar to conventional porous media. Based on direct observations, fractures can be separated into closed and open fractures. Fracture closure is related to water circulation and sediment deposition that can plug fractures with minerals like anhydrite and others. At the same time, fractures closed at surface condition may be open at reservoir conditions due to pressure effect on fracture walls (Song, 1998).

Naturally fractured reservoirs may often be very productive in the initial stages of development but have a high tendency to rapidly decline in production. One of the main reasons for this is water/steam breakthrough, a very undesirable occurrence that occurs often (Bratton et al, 2006). It is important to account for the presence of fractures in a reservoir because they affect reservoir performance. Also, before start of production at the stage of drilling, natural fractures may cause severe economic loses and technical difficulties, for instance caused by loss of circulation. Another, though less severe problem may occur when the permeability of fractures is reduced due to significant mud filtrate or cement invasion (Narr, 2006).

Study of naturally fractured reservoirs requires the study of the relationship between fracture formation and interlinked geological processes occurring at the same time. This requires the development of fracture formation theory and reasonable methodology for characteristics of features pertaining to fractured reservoirs. Fracture formation predominantly has a tectonic origin. Sometimes it can be related to various speed of diagenesis and lithification of precipitations in different places. It is important to understand that assessment of fracture related parameters is more complicated procedure than assessment of porosity or permeability of a typical porous reservoir (Pickup, 1994). Fracture detection and assessment occurs during various operations at the time of exploration and oilfield development. Methodology includes such operations as drilling, well logging, core sampling and its tests. The most qualitative and quantitative information regarding fractures can be obtained from cores. All the above listed methods, with correct application, allow to describe naturally fractured reservoirs, assess the system of existing fractures and also obtain individual dependencies that could be extrapolated throughout the entire reservoir/formation.

According to various theories, fracture can be characterized with different definitions. From a geomechanical point of view, fracture is a surface where discontinuity or cohesion of the material (rock) occurred. Fracture classification (whether it is a fault, micro or macro fracture, etc.) depends on scale of the study. Fracture formation can occur with and without the offset of the layers (Golf-Racht, 1986) as shown in figure 1. If there is offset, the fracture is called a fault.

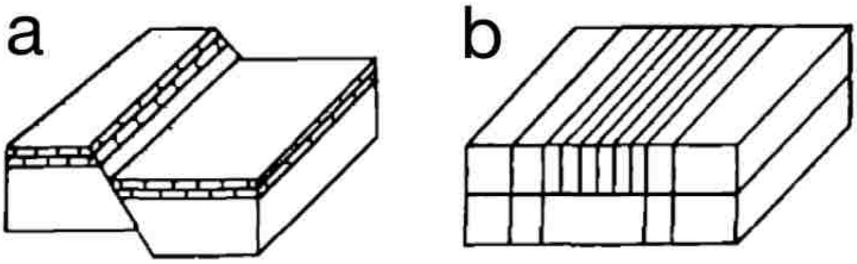

Figure 1. Fracture formation occurring with (a) and without (b) the offset of the layers (Golf-Racht, 1986)

Stearns and Friedman formulated two distinct categories of fractures: fractures “genetically” associated with folding and fractures related to formation of local structures, in other words regional fractures (Stearns et all, 1972). Cook, in his study of Sydney basin came to the conclusion that earlier developed disconnected fractures could remain during later geological stages, such as consolidation or burial of precipitations (Cook et al, 1970). Based on field observations it is possible to conclude that fracture-structural dependencies are closely associated with separation of fractures into two distinct categories:

a) Fractures associated with geometry of the structure, - fractures having constant orientation and well-ordered propagation throughout the entire area of observation.

b) Fractures, not associated with geometry of the structure, - fractures having irregular/non-symmetric or curved discontinuities without any orientation pattern. This type of fractures is associated with various kinds of surface phenomena (landslip, formation subsidence due to gravity, etc.) (McQuillan, 1973).

Fractures crossing the entire lengths of oil-bearing formations separate certain volumes of low-permeability zones that are called “matrix”. Each block in such system in not hydro-dynamically connected to adjacent matrix blocks. Physically, matrix blocks may have several points of contact but hydrodynamic connection in such points is limited. Matrix blocks are characterized with shape, volume and height. Fracture systems are characterized with dip, extension and distribution. Usually, matrix blocks have irregular shapes but during problem solving these shapes are reduced to simplest geometrical figures (cubes, elongated and flat rectangular) (Makurat, 1996).

2.2 Heavy oil reservoirs

In conditions of a constantly increasing deficit of unrecoverable resources, the problem of full-scale heavy oilfield development becomes more significant. World heavy oil and bitumen reserves are assessed to be 750 billion tons. Potentially recoverable reserves compose about 200 billion tons, which is two times higher than the amount of proved reserves in the countries of OPEC. Diagram below depicts the distribution of world oil reserves in accordance with oil density (Ruzin et al, 2015).

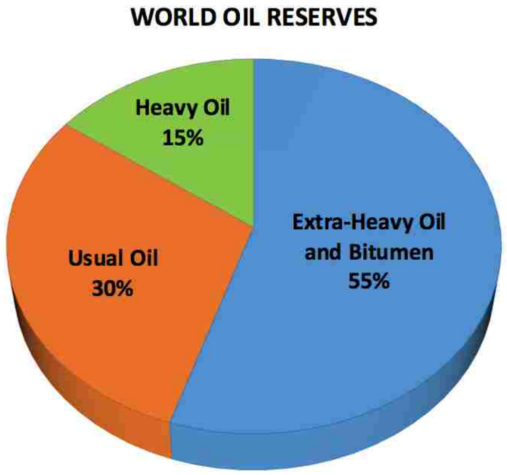

Figure 2. World distribution of world oil reserves in accordance with oil density (from Ruzin et al., 2015)

The largest amounts of oil reserves are located in Venezuela and Canada. Cumulative heavy oil reserves of Orinoco Belt basin in Venezuela and in Alberta province in Canada compose more than 70% of world heavy oil reserves. Other countries having large heavy oil and bitumen reserves are United States (28 billion m^3), Russia (10-20 billion m^3), Indonesia (2.5 billion m^3), China (1.5 billion m^3). Overall, 1680 heavy oilfields were discovered in the history of petroleum industry. Experience gained over multiple decades of heavy oil development indicates that application of conventional technologies for heavy oil extraction (having viscosity higher than 100 mPa·sec) does not allow to increase oil recovery factor higher than 10-15%. In case of heavy oil development having viscosity higher than 1000 mPa·sec, application of conventional methods for effective oil recovery is impossible (Ruzin et al, 2015). Effective recovery of large heavy oil reserves and bitumen is thus one of the priorities of the petroleum industry. Despite the fact that heavy oil reserves significantly exceed the reserves of usual oil, its potential is not used sufficiently.

Thermal methods are found to be the most effective for development of heavy oil reserves. Thermal methods of oilfield development include: steam flooding, fire flooding, hot water flooding, cyclic steaming and combination of listed methods with other physical and chemical techniques. About 60-70% of world oil production using enhanced oil recovery techniques is obtained with a help of thermal methods. Technologies based on thermal recovery methods have a great variety. While choosing an effective technology for a specific heavy oilfield, it is crucial to consider not only the geological characteristic of the oilfield but also certain factors involved in oil recovery using different methods. An effective technology should be based on the most important factors increasing oil recovery (Thakur, 1997).

Crude oil can be classified according to a great number of parameters including its density, viscosity, hydrogen sulfide content and other. During world oil congress in Houston in 1987, the following classification of oil in accordance with its density and viscosity was suggested (SPE National Report, 1987):

- Light oils – density less than 870 kg/m^3 (31.1° API)
- Usual oils – density between 870 – 920 kg/m^3 (22.3 – 31.1° API)

- Heavy oils – density between 920 – 1000 kg/m^3 (10 – 22.3° API)
- Extra-heavy oils – density higher than 1000 kg/m^3 (10.1° API), viscosity less than 10000 mPa·s (10000 cp)
- Natural bitumen – density higher than 1000 kg/m^3 (10.1° API), viscosity higher than 10000 mPa·s (10000 cp)

Natural bitumen stays in a formation in stiffened state, whereas extra-heavy oil is movable. Figure 2 shows world distribution of oils in accordance with the above classification. It is interesting to note that extra-heavy oil and bitumen reserves contribute to more than half of world oil reserves.

The development of oilfields containing extra-heavy oils requires the determination of rheological characteristics of oil. The primary difficulty that predetermines the choice of development in a heavy oil field is the extremely high flow resistance of the formation saturated with non-mobile oil. This does not permit application of conventional and the most effective water flooding technologies, and strategies. Numerous laboratory experiments, field pilot studies and commercial exploitation of heavy oil reserves across the world have demonstrated that extra-heavy oil flows only after being “warmed up”, even in highly permeable formations (Briggs, 1988).

Thus, almost all approaches for development of high-viscosity oilfields are based on thermal methods. Thermal conductivity is one of the most crucial physical rock property responsible for heat distribution throughout the reservoir during thermal development of these oilfields. During injection of a heat-transfer agent (steam or hot water), highly permeable zones rapidly get filled with the agent (convection) and later, low-permeability zones warm up due to conduction (Creaux, 2005).

Table below provides examples of various oilfields containing heavy oil/bitumen that are developed using different techniques, from primary recovery to EOR approaches (Ruzin et al, 2015).

Table 2. Examples of heavy oilfields and their development strategies

#	Country	Oilfield	Oil Reserves (millions of m^3)	°API	T(°C)	Viscosity (mPa*s)	Depth (m)	Development Technology
1	Cuba	Varadero	?	10	65	200	1500	Primary recovery
2	Cuba	Santa Cruz	?	15.8	50	up to 750	1500	Primary recovery
3	Russia	Usinskoye	740	18	23	710	1260	Steam flooding, CSS
4	Kuwait	Wafra	>1590	15	37	250	600	Steam flooding
5	Canada	Grosmont	50500	7	11	1.6*10e6	600	CSS
6	China	Cao-20	2.9	1	59	4610	942	CSS
7	Kongo	Emerude	>109	22	?	100	350	Steam flooding
8	France	Lacq superieur	19.9	22	?	200	650	Steam and hot water flooding
9	Italy	Rospo Mare	159	12	70	30	1310	Hot water flooding
10	Oman	Quarn Alam	186	16	?	220	215	Steam flooding
11	Turkey	Ikiztepe	20.2	11	49	936	1350	Steam flooding
12	Brazil	Campos	300	12	40	936	900	Primary recovery
13	Egypt	Issaran	79.5	11.5	34	4000	671	Primary recovery
14	Iran	Sarvak	2.7	13	60	2279	1200	Primary recovery

2.3 Development of naturally fractured heavy oilfields in different countries

Grosmont formation in Alberta, Canada contains high-viscosity bitumen reserves. Bitumen recovery from Grosmont formation began in the 1970s. Of the various methods tested, cyclic steam stimulations were found to be the most effective. One of the wells, 10A-5-88-19W4 produced about 100,000 bbls of oil after 10 cycles with cumulative steam-oil ratio of 6. Later, a modern SAGD field implementation was run. A cumulative steam-oil ratio of 2.5 was observed. Recovery factor exceeded 50% (Edmunds et al, 2009).

An overview of steam-injection projects in fractured carbonate reservoirs in the Middle East presents a description of effective currently used technologies. In Qarn Alam field in Oman, steam assisted oil gas gravity drainage in implemented. The pilot test began in 1996 with a plan to reach maximum steam injection in 2009. Mukhaizna field is developed using SAGD since 2007. Two pilot tests, first in 1982 and second in 1986 were conducted in Ratqa Lower Fars field in Kuwait using Cyclic Steam Stimulation. Results of the tests show that the field is suitable for thermal recovery techniques (Al Yousef et al, 2013).

Bamboo heavy oilfield is located in Muglad basin and has area of 144 square kilometers. It has depths ranging from 1000 to 1700 meters, and viscosity has a wide range of variation, from 70 to 3000 cp. Primary depletion allowed for recovery factor to reach 18%, or 506 million stock tank barrels. Due to enhanced oil recovery techniques oil recovery factor exceeded 75%. However, water cut is a big problem that makes the development process more complicated. Initially, oil rate amounted to nearly 20,000 STB/day, however after increase of water production rates due to water breakthroughs, oil rate decreased significantly and currently is about 8000 STB/day. Water cut value is constantly increasing and is about 80% at present (Faroq, 2016).

After relatively non-sufficient primary recovery, the option of thermal injection seemed to be attractive. However, “Huff and Puff” injection of chemicals was found to be the most effective. Chemical enhanced oil recovery process consisted of cyclic injection of chemicals into the formation that generated an oil-rich colloidal dispersion which decreased viscosity value significantly (Farog et al, 2016).

Applicability of vapor extraction processes (VAPEX) in naturally fractured heavy oil Iranian reservoir was studied by Azin et al. VAPEX process for EOR was originally developed by Butler and Morys and supposed to be an alternative to SAGD technology. VAPEX includes a generation of a pure hydrocarbon vapor and its injection into heavy oil for viscosity and density reduction. This technology can be applied in the reservoirs where because of any reasons SAGD cannot be implemented. However, there are limitations in VAPEX technology associated with injection pressures. Similar to SAGD, in naturally fractured reservoirs during high-pressure injection the risk of breakthrough increases significantly leading to decreased oil production (Azin, 2005).

Analogous evaluation of steam injection applicability in Iranian fractured oil fields was conducted by Bahonar. A case study was conducted using data of a naturally fractured carbonate oilfield having 3.6 billion barrels of initial oil in place. Oil has very high density (7.24 °API) and very high viscosity (2700 cp). Conducted analysis indicates that steam injection can help to increase recovery factor up to 12%. It was determined that increase in steam quality caused a slight, almost insignificant increase in oil recovery. Also it was observed that maximum recovery could be achieved by keeping injection rates as low as possible (Bahonar, 2007).

Russkoye oilfield is located in Russia and has large heavy oil reserves: 1.3 billion ton of oil in place. Except high oil density and viscosity, development process is complicated by high heterogeneity of the formation. Pilot tests conducted in the oilfield included cold and hot water injection, and various completion implications. After two years of hot water injection, water cut increased from 20 to 45%. Four months after the start of cold water injection, water breakthrough occurred which resulted in water cut increase till 99% and well shut-in (Vologodskiy, 2013).

2.4 Numerical simulation of naturally fractured systems

Behavior of naturally fractured reservoirs has been extensively studied since the 1960s and the first time, a numerical model for simulation of naturally fractured reservoirs was presented was by Warren and Root in 1963. The concept of dual porosity media was introduced. (Warren and Root, 1963). Later, an additional numerical approach was developed by Kazemi (Kazemi, 1976). Difficulty associated with the calculation of mass transfer between matrix and fractures in numerical simulation of naturally fractured reservoirs was emphasized by Sonler (1988). A new technique was developed that allowed to estimate matrix-fracture mass exchange with the consideration of gravity forces for multiphase flow. Later, it became possible to include the effect of capillary pressures and interfacial tension for matrix-fractures mass transfer calculations (Gabitto, 1998). Another study of capillary continuity between grids in numerical simulation of NFR was conducted by Labastie et al in 1991. In their study, the nature of conditions under whichcontinuity between grid blocks existed was determined. A conventional dual porosity dual permeability model using a special approach for describing fracture-matrix flow formulation was developed in the 1990s (Sabathier et al, 1998). This methodology showed the possibility of cooperative work of petroleum engineers and geophysicists in really-integrated fracture reservoir studies as a result of obtaining a real picture of a fracture network in the reservoir. Later, both “forward” geological modelling approach and “inverse” techniques usually used by engineers were combined (Sabathier et al, 1998; Baker et al, 2000). A detailed study of the mechanisms involved in gravity drainage processes in scale of block to block interaction which allowed to increase the precision of predictions. This method includes the calculation of pseudo capillary potentials which give accurate flow behavior predictions (Fung, 1991).

Multiple Interacting Continua (MINC) method was first introduced in 1998 which is a generalization of double porosity technique that allows to describe the inter-porosity flow by numerical methods. Adequacy of MINC technique was proved for forecasting of the behavior of the fractured reservoirs. MINC approach requires only a slight increase in computational load whereas double porosity method requires a significant increase in computational load. Later, this method was extended for numerical simulation of unconventional low permeability reservoirs (Yu-Shu Wu et al, 1998; Farah et al, 2016).

The process of imbibition in fractures and on the boundary of contact between matrix and fracture was numerically simulated in early 2000s. Fracture were represented as a two-dimensional lattice of pores and matrix was represented as a three-dimensional network of throats. It was determined that matrix plays an important role in matrix-fracture mass transfer. (Hughes et al, 2001). A droplet detachment model to arrive at an effective water saturation in a thin boundary layer at the fracture-matrix interface was presented in 2002. It was determined that for water wet reservoirs, the increase of the fluid velocity in fractures would increase the amount of water that matrix is exposed to resulting in increase of oil recovery rate from matrix (Gautam et al, 2002).

Accurate prediction of the performance of naturally fractured reservoirs requires precise description of water transfer between matrix and fractures. A new time-dependent matrix-fracture transfer shape factor formulation and transfer functions were derived using dimensionless analysis of the experimental data. It was determined that fracture relative permeability is very sensitive to the total fluid velocity in fractures and the rate of uptake of water by the matrix. (Rangel-German et al, 2003; Rangel-German et al, 2004). Parameters required for determining matrix-fracture transfer functions from laboratory data were obtained by Civan (2005). Later, the approach was upgraded and allowed to estimate parameters that affect matrix-fracture mass transfer in naturally fractured oilfields (Civan, 2006). The same year, an upscaling procedure for construction of generalized dual porosity dual permeability systems from discrete fracture characterization was developed that gave results in close agreement with the underlying discrete fracture model (Gong al, 2006). Introduction of new transfer functions for simulation of dual porosity models of naturally fractured reservoirs helped to increase the precision of the simulation results by eliminating the assumption of orthogonal fracture distribution and pseudo-steady state flow (Sarma et al, 2006). Introduction of centrifuge tests allowed to achieve high quality predictions of matrix-fracture interaction in NFR based laboratory tests of core samples (Kyte et al, 1970).

Mathematical model allowing to account for both convection and diffusion mechanisms in naturally fractured reservoirs presented later allowed to significantly increase the precision of a dual porosity simulation. Also, it accounts for a counter flow inside the rock (Jamili, 2011; Chordia, 2010; Hoteit, 2011).

A recently developed multi-rate dual porosity numerical approach allowed to extend the use of conventional dual-porosity model and account for a wide range of mass transfer rates between matrix and fracture (Geiger, 2011). Shi Su et al. in 2013 introduced the concept of a dynamic shape factor for matrix-fracture transmissibility for improvement of the precision of dual-media simulation. It was a significant advancement that is nowadays introduced in a great number of numerical simulators. (Shi Su et al, 2013). Characterization of mass/heat transfer in naturally fractured reservoirs for extremely complex systems was conducted that allowed to simulate highly faulted systems and systems having small fracture spacing (Anna Suzuki et al, 2015). Matrix-fracture interaction for sandstones during nitrogen, methane and carbon dioxide injection was studied by Bulbul (Bulbul, 2012). Recently, a new approach was developed for simulation of dual porosity multiphase flow in naturally fractured reservoirs. It included so-called poro-elasticity theory that included stress-dependent deformation of hydrocarbon-bearing formations due to change in pressure. The governing transport equations describing fluid flow and deformation of the rock use two interactive environments that consist of continuous fracture medium and discontinuous matrix medium (Eker, 2017). With assumption that both fracture and matrix produce directly into the wellbore, a new innovative model for dual-permeability simulation was developed by Lu et al. (2013) that estimated four stages of pressure behavior in naturally fractured reservoirs.

2.5 SAGD in naturally fractured reservoirs and other EOR techniques to increase oil recovery

Steam-assisted gravity drainage is an enhanced oil recovery (EOR) technique, widely used in naturally fractured heavy oilfields. Two main goals that are principally needed to be achieved are: a) to minimize matrix residual oil saturation and b) to accelerate oil recovery process for economic efficiency (Babadagli, 2001). Study of steam-assisted gravity drainage processes in naturally fractured reservoirs has shown that SAGD can be an attractive recovery technique in many fractured reservoirs allowing to reach 80% of oil recovery in several cases (Das, 2007; Penney et al, 2005), however the location of the fractures is an extremely important parameter affecting the efficiency of the technique (Bagci, 2007). Also, in an analogous study Fatemi (2011) emphasized the effect of the presence of vertical fractures in SAGD processes. Horizontal fractures were determined to have a detrimental effect on the recovery and efficiency of the technique (Fatemi, 2011). Fluid in fractures acted as a “force” helping to displace oil from matrix. Displacement can be initiated by viscous displacement, mass transfer of capillary displacement (Babadagli, 2002). Natural fractures provide a path of high permeability for steam and oil and may increase the risk of steam breakthrough. Oil saturation, remaining after steam breakthrough is related to oil and water viscosity ratio at steam temperature (Closmann, 1983). However, high vertical fracture relative water permeability helps to establish communication between well pair in SAGD and accelerate steam chamber propagation (Akhondzadeh, 2015). If the majority of fractures are located in the upper part of the reservoir, an upward movement of steam will be initiated which can result in significant overburden heat loss and reduced oil recovery (Ali, 2012). Analogous conclusion was made by Yang et al (1992) that a faster production can be established when a higher permeability layer is present above a low permeability layer in the reservoir. Heat travels throughout the formation predominantly due to thermal conduction. Driving force contributing to the steam propagation into the formation in a temperature gradient established between steam and the formation (Shen et al, 2017). The importance of horizontal fractures in a SAGD process should not be underestimated: the increase of the density of fracture network may cause restriction against development of steam chamber. Although in case of a very developed network of vertical fractures, the negative effect of horizontal fractures can be eliminated (Fatemi, 2009). Another crucial factor affecting the efficiency of SAGD is the type of the reservoir. For instance, SAGD application in carbonates is generally less effective than in sandstones due to oil-wet nature of carbonates (Tang, 2011). However, wettability is considered to be a dynamic parameter that can change due to increase/decrease in temperature. Some carbonates were observed to express water-wet nature in regions of high temperature during steam injection (Al-Hadhrami, 2001). It was observed that combination of water flooding and a subsequent thermal stimulation is more effective in certain cases than a separate thermal recovery process (Nabipour et al, 2007). Efficiency of SAGD technology also depends on presence of underlying aquifer or overlying gas cap layers. Thereby, the presence of overlying gas cap can potentially reduce the efficiency of SAGD by up to 25%. In case of aquifer and gas cap being present simultaneously, efficiency of SAGD technology can be decreased up to 75% (Chan, 1997).

After the start of SAGD implementation, various design for injection wells was tested. However, it was determined that horizontal wells are generally much more effective and allow to inject higher volumes of heat-transfer agent (Sawhney et al, 1995; Tamer et al, 2009).

Another technology often being used for heavy oilfield development is steam flooding. Steam flooding technology found to be effective in a great number of heavy oilfields. San Miguel field in Texas in a good example of the efficiency of the technology: after pilot tests residual tar saturation was found to be 8% and the recovery factor as higher than 50% (Britton, 1983). During this EOR process, original oil saturation is an important factor that affects oil recovery (Chu, 1990).

In-situ combustion technology was also found to be effective in development of NFR. However, it requires a pre-heating of the injector well to initiate a combustion process (Schulte, 1985).

Experiments and numerical simulation conducted to access the efficiency of gas-assisted gravity drainage (GAGD) process in naturally fractured oilfields indicate, that presence of vertical natural fractures may increase the efficiency of immiscible GAGD (Mahmoud et al, 2008). Since thermal EOR may not be possible due to economic reasons, the implementation of GAGD in heavy oilfields is also possible, however in the case of YHOF, the implementation of GAGD is not feasible due to extremely high oil viscosity.

From overview of a various number of technologies, it can be concluded that steam injection is the only commercially successful method being used for development of naturally fractured heavy oilfields. Although other methods can provide a good substitution for thermal processes, steam generation is a cheaper technology than for instance surfactant production and preparation (Mollaei, 2007).

CHAPTER 3. YAREGA HEAVY OIL FIELD

Yarega oilfield is located within 18 kilometers from Ukhta, a city in Komi Republic of the Russian Federation. The oilfield is situated within the limits of large, low-angle and asymmetric Ukhta fold system. It is 36 kilometers in length and 4 to 6 kilometers in width (Fridman et al, 2011).

3.1 Geology of YHOF

Commercially attractive reserves are situated in the III formation related to mid-Devonian depositions of Givetian period. III formation is located at depths between 130 and 220 meters in the sandstones of middle Devonian directly on metamorphic shales of Riphean age and covered with mid-Devonian argillites. Above the argillites, there is a tuft-diabase layer and sand-argillite stack of the upper Devonian. The formation is represented with weakly and medium-consolidated sandstones consisting of quartz feldspar grains that are cemented with ferruginous-carbonate and clay material. Average effective thickness of the formation is 26 meters. The Yarega and Lyael oil pools are very asymmetric and have flat wings (from 1 to 3°) extended along north-eastern direction (Kalinina et al, 2013).

The Ukhta fold system is about 225 km (long axis) and 60 km (short axis).

In the arch of the fold, several local flat dome-like structures are found with lengths from 10 to 15 km. The Yarega oilfield lies in one of these domes. Dimensions of this fold is 12.5 km (along the axis) and 1.5 – 4.5 km in width. The fold is asymmetric (its north-eastern wing is almost 3 times wider than south-western) (Kalinina et al, 2013).

All rock types are fractured (to variable degree) and closed with disjunctive faults. There is a big influence of this faults on productive deposits (oil), because this faults affect the porosity and permeability of the formation. Detailed study of this disjunctive fault system, fractures in the formation and crossing/underlying rocks is conducted during the building of mine shafts and corridors and mine development techniques (Telnova, 2005).

Disjunctive disruptions of the oilfield are represented with relatively large fractures. Some of them are closed/filled, some of them open or accompanied with the fracturing. These faults and fractures cross different layers of the oilfield.

Among them, we can separate:

1) Large, but relatively faults having lengths from 1 to 3 km with offsets of 5 – 10 meters.

2) Average sized faults, having lengths of hundreds of meters with offset of 2 meters.

3) Little disjunctive fractures and faults, having lengths of tens of meters and offset of 0.5 meters.

All these fractures are easily visible inside the mine corridors and shafts. Also, sometimes the presence of these fractures is evident because of steam/water/oil breakthroughs in the neighboring wells. The network of microfractures are visible only in thin sections (Telnova, 2005).

According to mine excavation data, III formation of Yarega oilfield is fractured with steep (from 60 to 80°) fractures that break the reservoirs into multiple blocks having various shapes and sizes. Diagonal system of fractures prevails (in relation to the overall extent of the structure), however in some places north-western and south-eastern trending fractures appear more dominant. These fractures can vary in length from 10 meter to as large as 2.5 km. Fracture spacing in the upper parts of the formations 25 meters while fracture spacing in the lower formations is every 9 meters (7.6 – 12. 5 meters range) (Ruzin et al, 2015).

The reservoirs in the Yarega oilfield are composed of medium and fine grained sandstones, with some silt and clay zones/layers. The basement is massive quartzite of Riphean age above which lie graphitized shale formations. The Yarega reservoirs overlie these shale layers. The porosity and permeability distributions are shown in Figures 3-5.

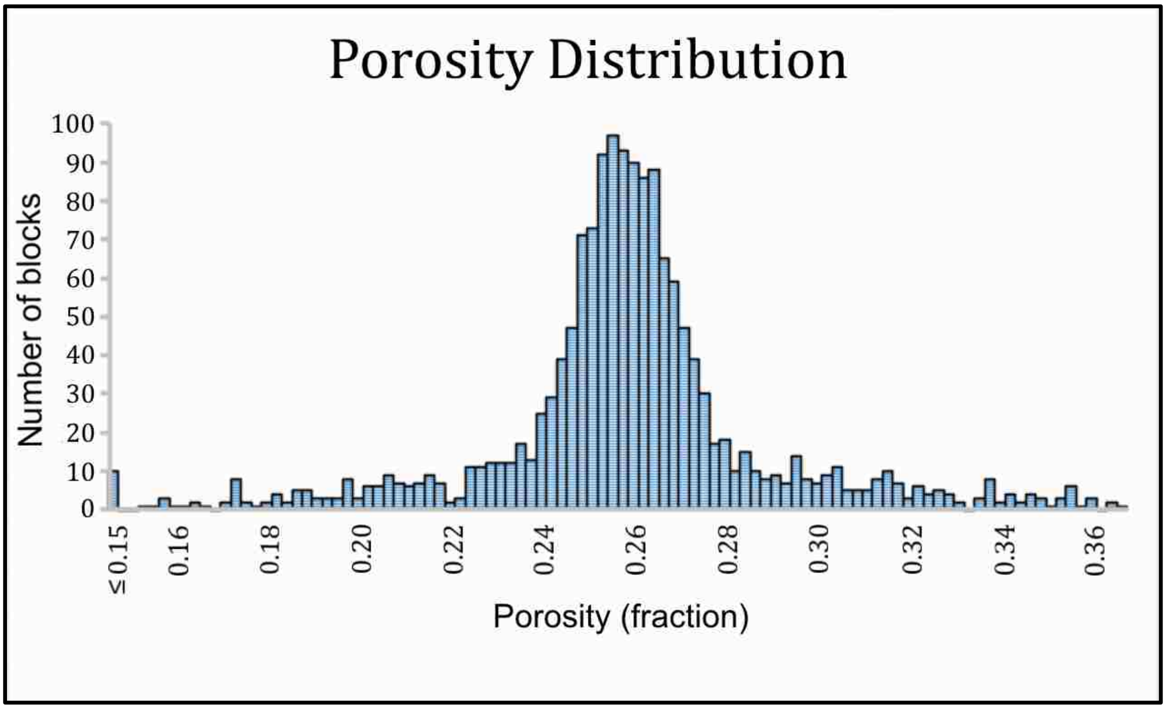

Figure 3. Porosity distribution in reservoir N (Ruzin et al, 2015)

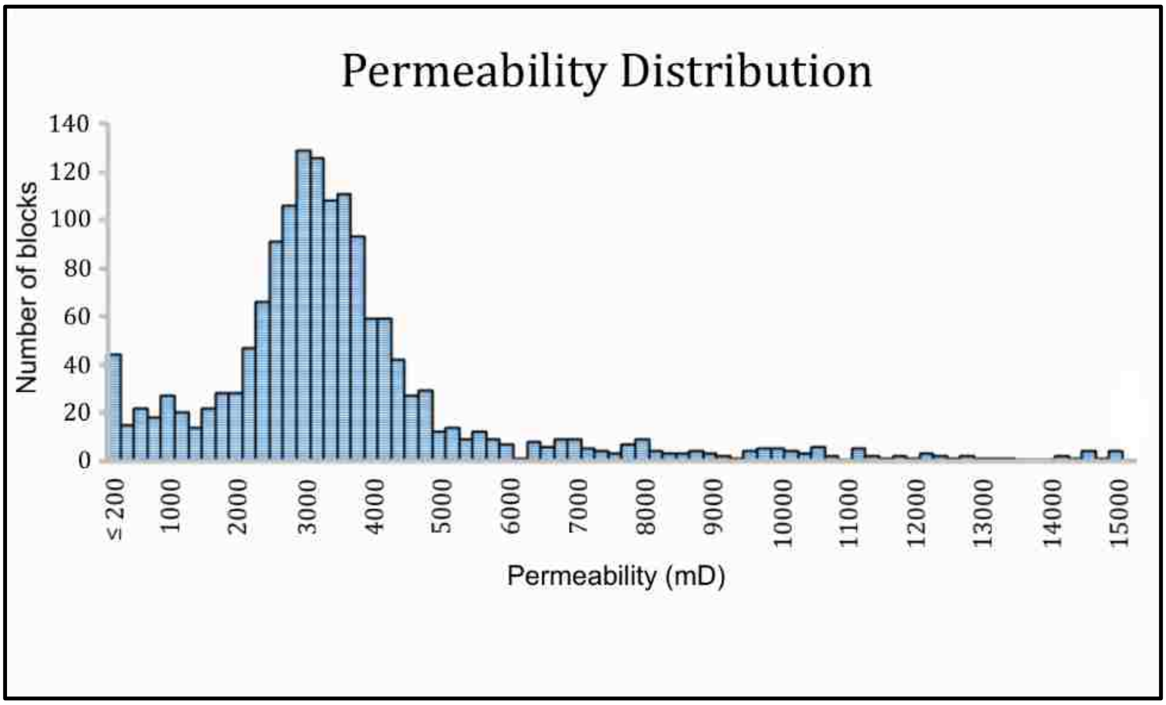

Figure 4. Permeability distribution in reservoir N (Ruzin et al, 2015)

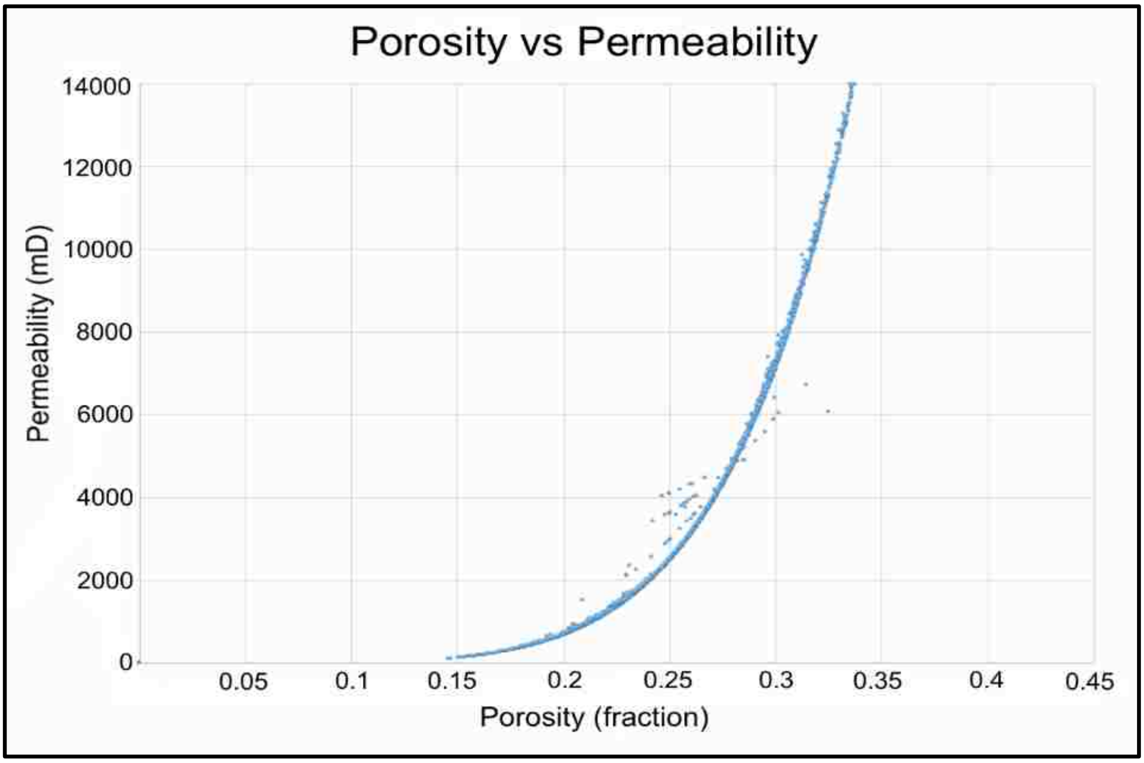

Figure 5. Porosity-permeability relationship model for numerical simulation of reservoir N (Ruzin et al, 2015)

3.2 Reservoir fluid properties

The Yarega oilfield is home to a heavy, dense, sulfurous oil with small amount of dissolved gas. Average density of oil under standard conditions (at 20°C) is 945 kg/m^3, average dynamic viscosity is 3600 centipoise, molecular weight is 379 (Nikitin et al, 2012). The properties of the heavy oil are given in Table 3.

Table 3. Physical-Chemical Properties of Degasified Oil from YHOF (Nikitin et al, 2012)

Property	Value
Density, kg/m^3	945
Viscosity, cp	3600
Molecular weight	379
Combustion temperature, °C	115-130
Freezing temperature, °C	<20
Sulfur content, %	1.15
Silica-gel tar content, %	20.6
Pyro bitumen, %	1.99
Paraffin, %	0.43
Oil viscosity composes 60 cp at 100°C	

Gas content in the Yarega oilfields can be described as follows (Nikitin et al, 2012): methane composition varies from 88.2 – 99.3 % (average – 92.5%), , carbon dioxide – from 0.3 to 9.4% (average – 2.44%), nitrogen – from 0 to 12.6% (average 1.9%). There is some gas dissolved in formation water: in brine of formation III, there is 12 – 29% of methane, 8 – 20% of nitrogen and 60% of carbon dioxide. Overall, gas composition corresponds to oil composition. Gas factor of formation oil from well #49p is equal to 1.223 m^3/ton (Ruzin, 2010).

Chemical composition of water in formation III varies greatly depending on the place of sampling. Some water has low mineralization the values of which compose from 3 to 10 g/liter, highest mineralization was found to be from 13 to 24 g/liter in some cases. Along with increase of the water sampling depth, its mineralization increases. It is determined by the influence of lower laying water in metamorphic shales that has mineralization up to 40 g/liter (Ruzin, 2010).

Table 4. Physical and chemical properties of water from formation III (Ruzin, 2010)

Viscosity at reservoir conditions, centipoise	Density at res. con., g/cc	Content, mg/liter						Overall mineralization, mg/liter	pH
		Cl^-	SO_4^{2-}	HCO_3^-	Ca^{2+}	Mg^{2+}	Na^++K^+		
1.1	1.0186	15932	2,5	292,3	1200	419,5	8309	26282	7.5

Water type: chlorum – calcic, water group: chloride, water subgroup: sodic.

Table 5. Properties and composition of formation oil from well #49p (Pform = 0.8 MPa, Tform = 8°C) (Ruzin et al, 2015)

Property	**Value**
Density kg/m^3	933
Viscosity, cp	15300
Molecular weight	372
Gas content, m^3/m^3	1.168
Gas content, m^3/ton	1.223
Coefficient of thermal expansion, %	6.3
Hydrogen sulfide	Absent

(table cont'd.)

Property	Value
Carbon dioxide	Absent
Nitrogen + other rare gases	0.0015
Methane	0.0777
Ethane	0.0003
Propane	0.0009
Isobutane	0.0002
Normal butane	0.0001
Isopentane	0.0001
Normal pentane, Heptane, Hexane	Absent
Remainder C7 + heavier	99.92

Table 6. Oil densities and viscosities with temperature – heavy oils from YHOF (Konoplev, 2005)

Temperature, ^0C	**Oil density, kg/m^3**		**Oil viscosity, (cp)**	
	formation	**degasified**	**formation**	**degasified**
8	933	962	12000	14000
20	914	955	3100	3600
50	868	933	350	390
100	846	898	49	60

3.3 History of oilfield development

Yarega Oilfield is a heavy oil field in Komi Republic of Russia, where the first strain of oil is said to have been discovered in 1664 in the waters from the Ukhta River that had oil slicks (Chertenkov et al., 2012). The first well in the region was drilled in 1937, the first in-situ oil mined in 1939, and till 1954 oil mining was the primary mechanism of recovery (Chekonin et al., 2012). Although thermal stimulation of the oil was proposed as early as 1937 by oilfield geologist, I.N. Strizhev, it was not until 1968 that the first steam operation was conducted. By 1972, commercial production of oil from thermal oil-mine recovery was established, and production from the Yarega oil rose from 4 % from the in-situ mining techniques to 33% from thermal mining (Chekonin et al., 2012; Chertenkov et al., 2012). Steam-assisted gravity drainage (SAGD) was introduced in the region in 2006 (Chertenkov et al., 2014), and annual production increased to 3.5 million metric tons (25 million barrels) (Chekonin et al., 2012) by 2011.

3 development stages can be distinguished:

1) Development with test-wells drilled from the surface
2) Development using mining-drainage techniques with the help of natural energy of the formation
3) Development using thermal-mining techniques with artificial thermal influence on the formation

Test development using surface wells began in 1935 on two sectors having area of 28.4 and 15 hectares. Wells were located using triangular pattern with 75-100 meter distance between the wells. The first sector was drilled with 48 wells, the second sector – with 21 wells. Cumulatively, from 1932 till 1945, 38500 tonns of oil was recovered. Oil recovery did not exceed 2%.

In 1937, building of the first oil mine started and beginning from 1939, development using mining-drainage techniques with the help of natural energy of the formation began. At the age of 1950, 3 mines were built in this oilfield.

From 1939 till 1974, the oilfield was developed using mining-drainage technologies. During this period, 92 thousand wells having lengths between 40 and 280 meters were built. The majority of the drilled wells worked as artificial fractures in the formation. During the second period of development using mines and natural energy of the formation, 7.4 million tons of oil was recovered. Oil recovery of several sectors composed 4-6 %.

Various scientific tests were conducted between 1968 and 1971 to determine the efficiency of thermal oil recovery. These tests led to establishment the world's first thermo-mining techniques. Beginning from 1972, thermomining development method was applied in Yarega oilfield in industrial scale. This method showed high economic efficiency. Oil recovery on certain picked sectors reached 53.2%. SOR composed 2.7 tonns of steam/ 1 tonn of oil.

3.4 Geology of reservoir N

This research is focused on studying a reservoir (henceforth called reservoir "N") in Yarega heavy oilfield (YHOF) for development strategies and production optimization. Reservoir N is a naturally fractured heavy oil reservoir and located in sector 2 of YHOF (figure 6). The formation extends 130-220 meters in the sandstones of upper and middle Devonian period. Average pay zone thickness of the formation is 26 meters, average porosity of the formation is 25%, and average matrix permeability is 2 micrometers^2.

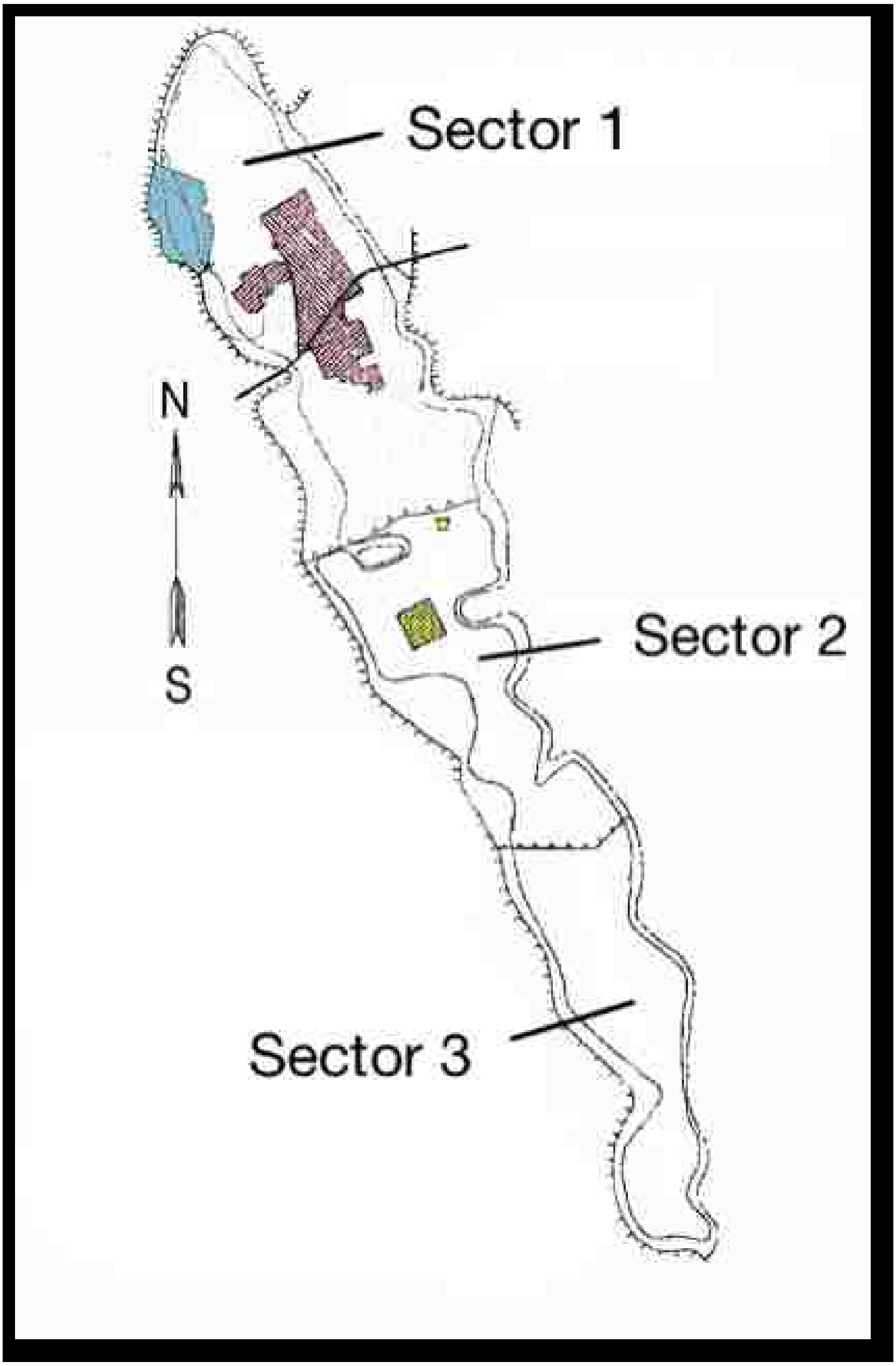
Sector 1
Sector 2
Sector 3
N
S

Figure 6. Schematic map of YHOF (scheme from YaregaRuda)

Table 7. Geological and physical characteristics of reservoir N (Ruzin et al, 2015)

Reservoir properties of a middle + upper sectors of formation III of oilfield N	
Absolute upper boundary level, m	-24 (from -62 till +16)
Absolute depth of OWC, m	-60
Type of deposition	Sheet, roof
Type of reservoir	Terrigenous, porous fractured reservoir
Payzone area, 10^3 m^2	24370
Average total thickness, m	44
Average payzone thickness, m	10.9
Average matrix permeability, 10^{-3} micrometers^2 (D)	2200 (2.23)
Average porosity, fraction	0.25
Initial oil saturation, fraction	0.86
Initial formation temperature, °C (°F)	8 (46.4)
Initial formation pressure, MPa (psi)	1,1 - 1,4 (159.54 – 203.05)
Bubble point pressure, MPa	0.45 (65.27)
Gas saturation, m^3/ton	1.2
Oil density at reservoir conditions, kg/m^3 (°API)	933 (20.02)
Oil density at surface conditions, kg/m^3 (°API)	945 (18.09)
Oil viscosity at reservoir conditions, Mpa×s (centipoise)	12000 (12000)
Oil formation volume factor	1.02
Water density at reservoir conditions, kg/m^3 (lb/ft^3)	1002 (62.55)

The reservoir is cross-crossed by fractures every 20-25 meters. Significant variation of the fracture sizes and permeabilities led to division of them into two types – macrofractures and microfractures. Both types of fractures happen to be exposed to well-formation contact. As a result, initial oil rate of some of the wells sometimes composed 5-15 metric tons/day and sometimes reached 100 metric tons/day.

Oil, occupying the porous space of the rock has abnormally high viscosity: up to 18000 cp at initial pressure of 6-8°C. Initial reservoir pressure is 1-1.3 MPa, and oil density at reservoir conditions is 933 kg/m^3 and at surface conditions – 945 kg/m^3. Oil has low content of sulphur (up to 1.1% of total oil mass) and paraffin (up to 0.5 of total oil mass). More detailed description is show in table 7. Matrix is tight, whereas the fractures act as high permeability pathways (dual porosity reservoir).

Main factors that impede the effective development of the oilfield are abnormally high oil viscosity and dual porosity system (figure 7).

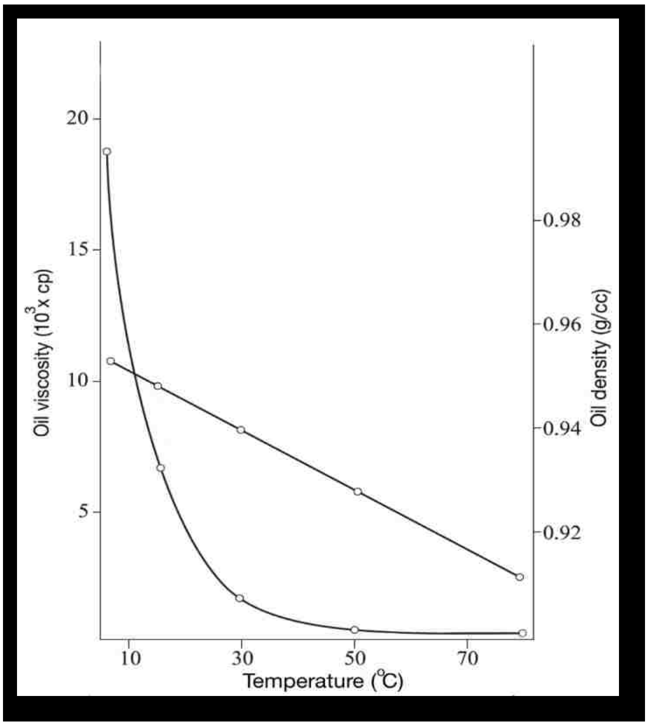

Figure 7. Oil density and viscosity with temperature – fluids from reservoir N (Ruzin et al, 2015)

Schematic Geologic Cross-Section of Formation III

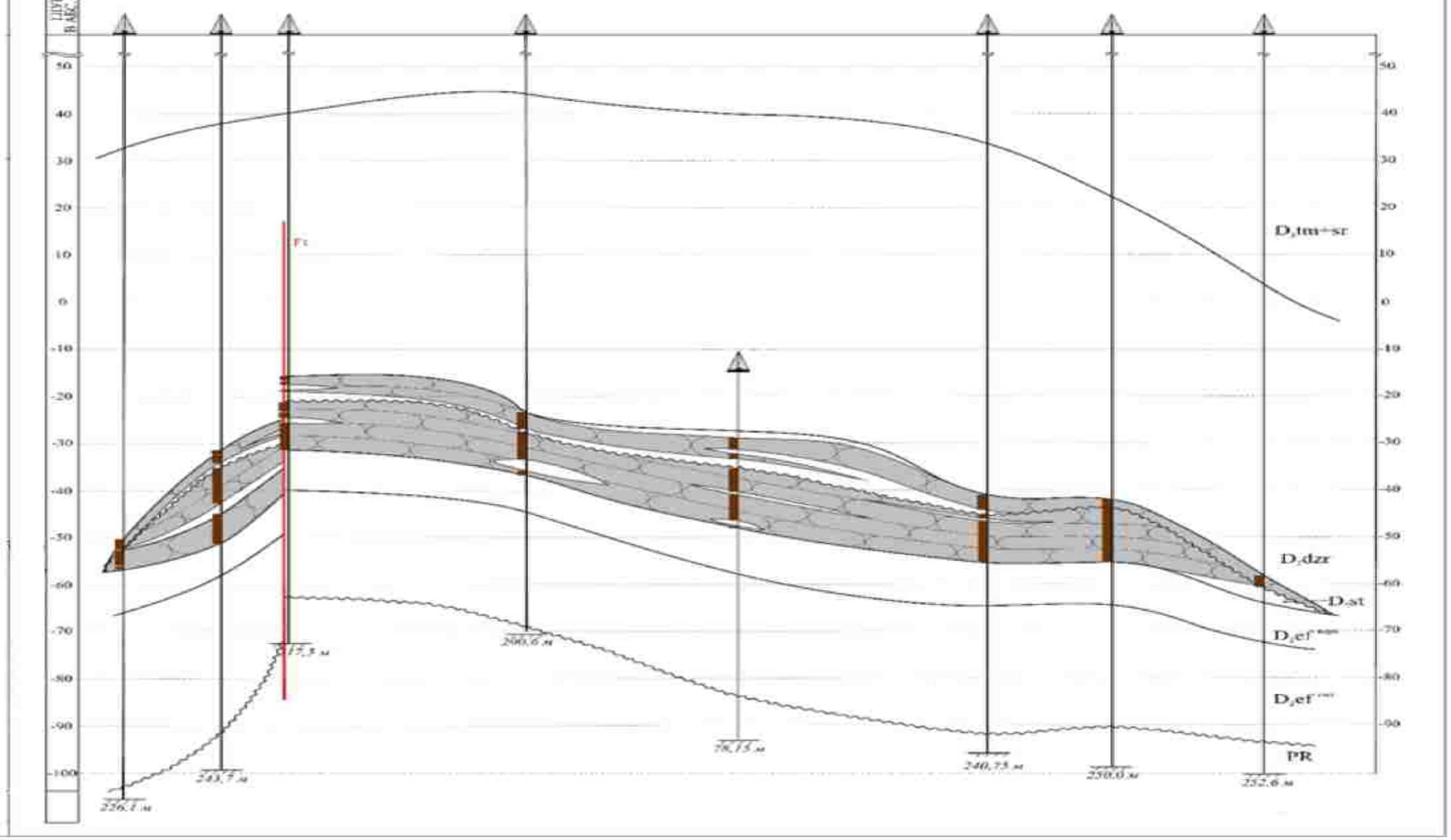
ГЛУБИНА В АБС. ОТМ., м
50
40
30
20
10
0
-10
-20
-30
-40
-50
-60
-70
-80
-90
-100
F1
226,1 м
243,7 м
217,5 м
200,6 м
78,15 м
240,75 м
250,0 м
252,6 м
D_3tm+sr
D_3dzr
D_2st
D_2ef
D_2ef
PR

[redacted]

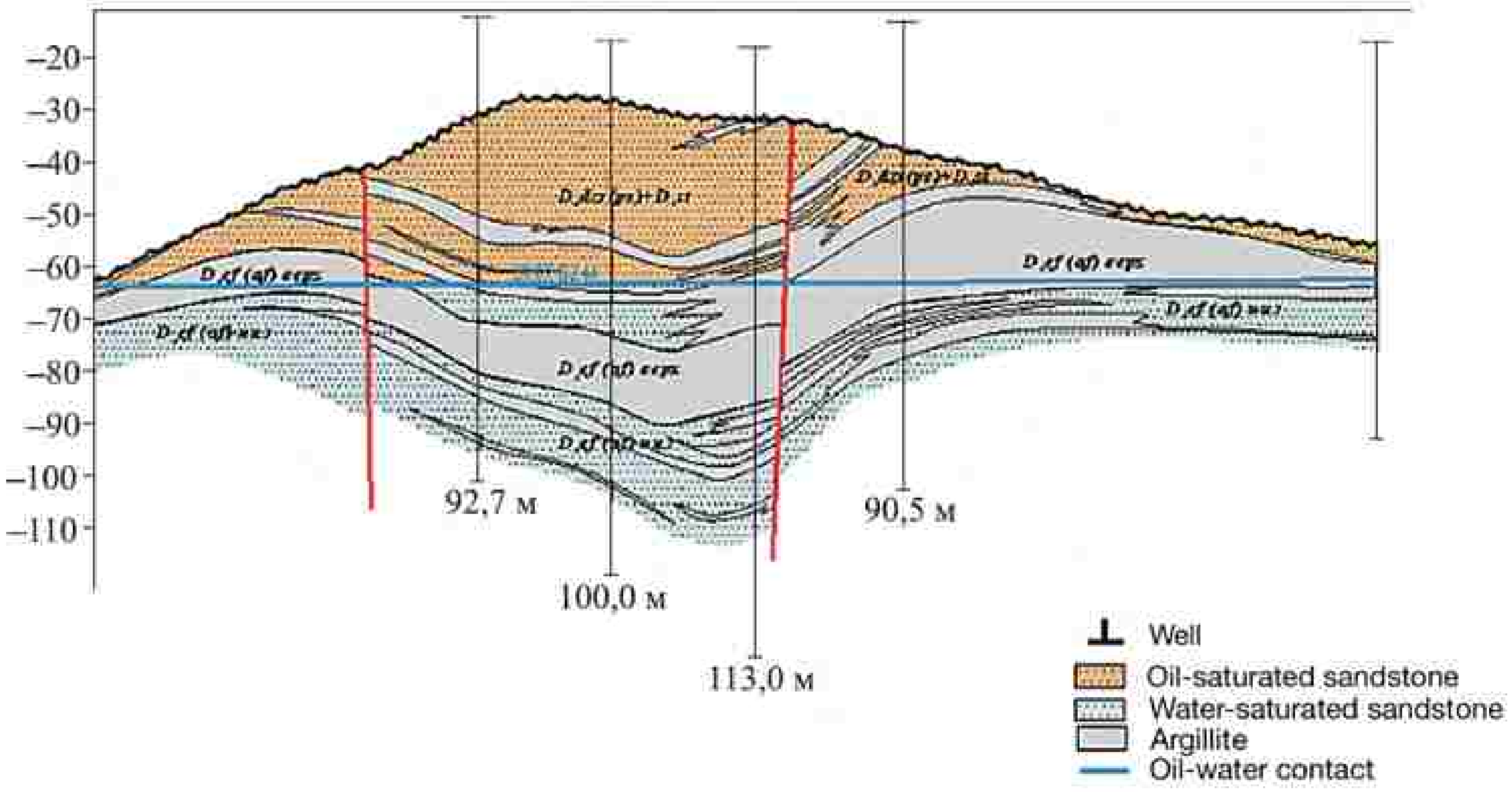
–20
–30
–40
–50
–60
–70
–80
–90
–100
–110
92,7 м
100,0 м
113,0 м
90,5 м
Well
Oil-saturated sandstone
Water-saturated sandstone
Argillite
Oil-water contact

[redacted]

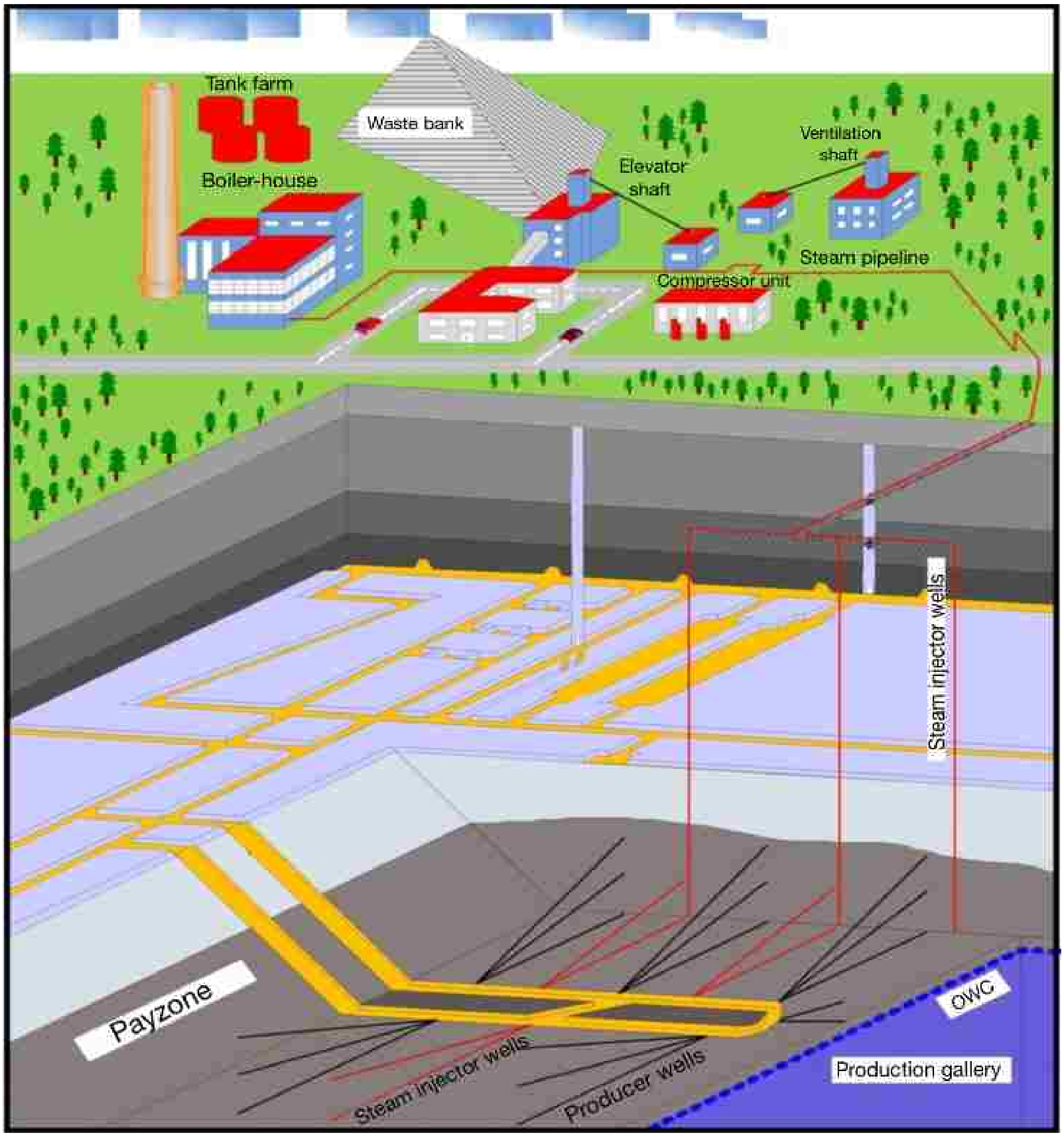
Tank farm
Waste bank
Boiler-house
Elevator shaft
Ventilation shaft
Steam pipeline
Compressor unit
Steam injector wells
Payzone
OWC
Production gallery
Steam injector wells
Producer wells

Figure 10. Modern thermomining methods currently being used in YHOF (Chertenkov et al, 2012)

CHAPTER 4. RESEARCH GOALS AND OBJECTIVES

This research is focused on studying a reservoir “N” in Yarega heavy oilfield (YHOF) for development strategies and production optimization. YHOF in a naturally fractured heavy oil field where only very recently SAGD technology has been introduced. This study explores numerically different static and dynamic reservoir characterization models (single porosity versus dual porosity systems), and subsequent pressure-production history matched reservoir simulation for understanding heat and mass transfer mechanisms. Thereafter, different drilling and production scenarios are tested for candidate selection for the highest recovery and production optimization.

It is to be noted that the most recent methods of SAGD production from this region uses the drilling technology of opposing injectors and producers. In fact, the world’s first opposing SAGD horizontal drilling was performed in this oilfield in 2011-2012 (Chertenkov et al., 2014). The uniqueness of this research is that:

a) it is the first dual porosity reservoir simulation of this area to quantify and understand the impact of the different SAGD methods currently employed in this area, and that

b) it goes beyond current SAGD technology to propose and recommend a new method of drilling and production in the region (the SAGD fishtail) using results from a dual porosity/dual permeability reservoir model and history-matched simulation runs.

The primary goal of this research is thus to determine development strategies for reservoir N located in a naturally fractured, heavy oilfield using single, dual porosity and dual permeability models (computational expenses permitting).

The objectives of this research are thus to:

1) Understand heat and mass transfer in the densely fractured heavy oil reservoir N in the YHOF.

2) Develop numerical strategies to simulate SAGD processes in the reservoir using single porosity, and dual porosity / dual permeability reservoir simulation techniques.

3) Recommend development strategy or strategies based on simulation, and pressure-production history-matched results and forecasting results.

CHAPTER 5. METHODOLOGY

In this study coupled fluid and heat flow is simulated using a variety of porosity models to capture the reservoir characterization. The non-isothermal multiphase fluid flow that is simulated here is fundamentally governed by mass and energy balance, Darcy's Law and diffusivity equation (Table 8). Heat transfer is governed by Carslaw and Jaeger (1959) equation and thus both conduction and convection are simulated (Table 8).

The reservoir models are tested with both single porosity and dual porosity systems. In the single porosity model, zones having low density of fracture network are considered to be matrix and zones with high density of fracture network are considered as fractures (figure 11). However, this method has limitations associated with the assumption that fractures are presented only in particular layers in the reservoir and smaller fractures in the low-permeability matrix are neglected. Additionally, accuracy of this approach is questionable due to "unrealistic" rectangular representation of fractures. Despite the above, this approach is widely used in the industry. The second way for representing naturally fractured reservoirs is the use of dual porosity/dual permeability models. This approach is considered to be more accurate than single porosity approach for forecasting of parameters related to flow of fluid in naturally fractured reservoirs, however, they are computational expensive. Two different modes for simulation of dual media are possible: dual porosity simulation and dual permeability simulation (figure 12).

[redacted]

Darcy's equation:

$$u_x = -\frac{k}{\mu}\frac{dp}{dx}$$

Diffusivity equations:

$$\frac{\partial^2 p}{\partial r^2} + \frac{1}{r}\frac{\partial p}{\partial r} = \frac{\phi \mu c_t}{k}\frac{\partial p}{\partial t}$$

Continuity equation

$$\frac{\partial \rho}{\partial t} + \nabla \cdot (\rho u) = 0$$

Equation for Fluid flow:

$$\frac{\partial}{\partial t}(\phi^* \rho_f) - \nabla \cdot \left(\rho_f \frac{k}{\mu} \cdot [\nabla p - \rho_f g]\right) - Q_f = 0$$

Equation for Heat Flow

$$\frac{\partial}{\partial t}[\phi^* \rho_f U_f + (1-\phi^*)\rho_\gamma U_\gamma] - \nabla \cdot \left(\rho_f \frac{k}{\mu} \cdot [\nabla p - \rho_f g] H_f\right) + \nabla \cdot (k \Delta t) - Q_h = 0$$

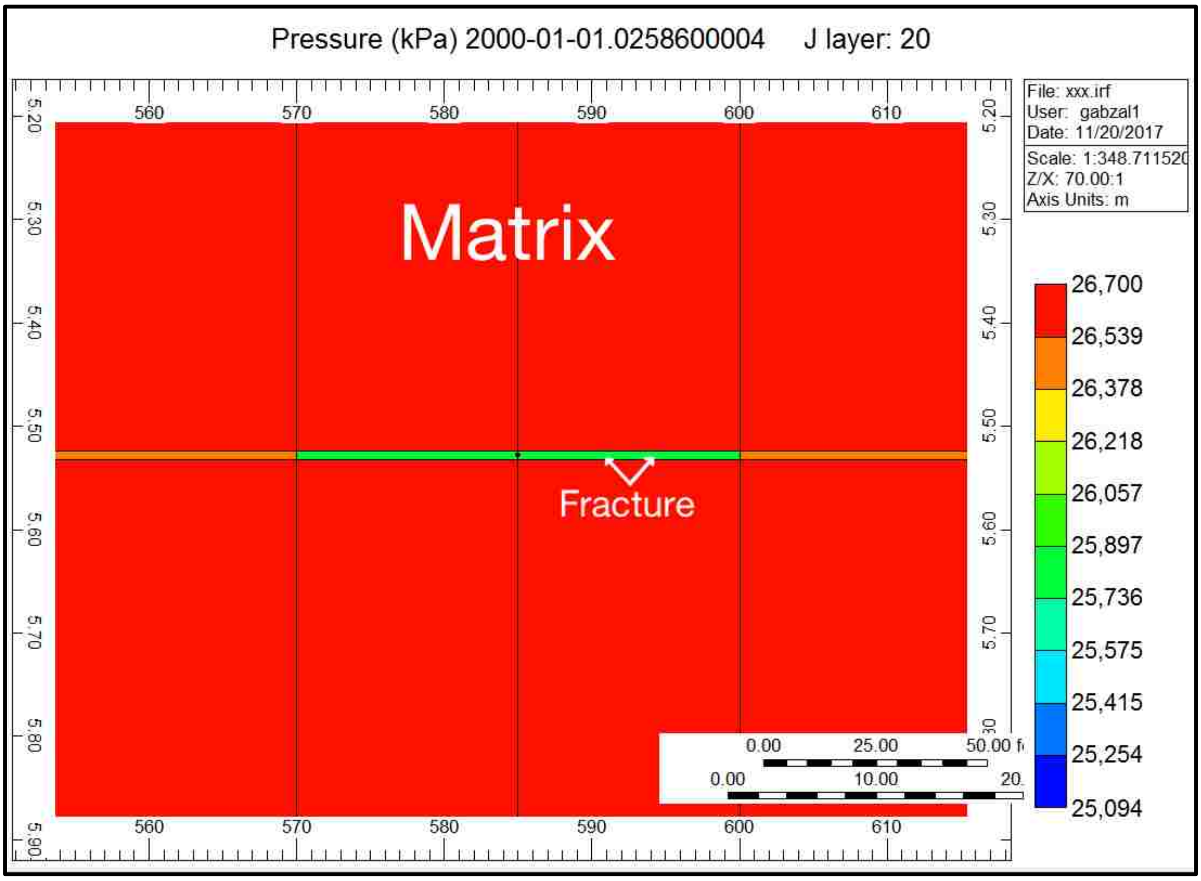

Figure 11. Single porosity approach for numerical simulation of naturally fractured reservoirs

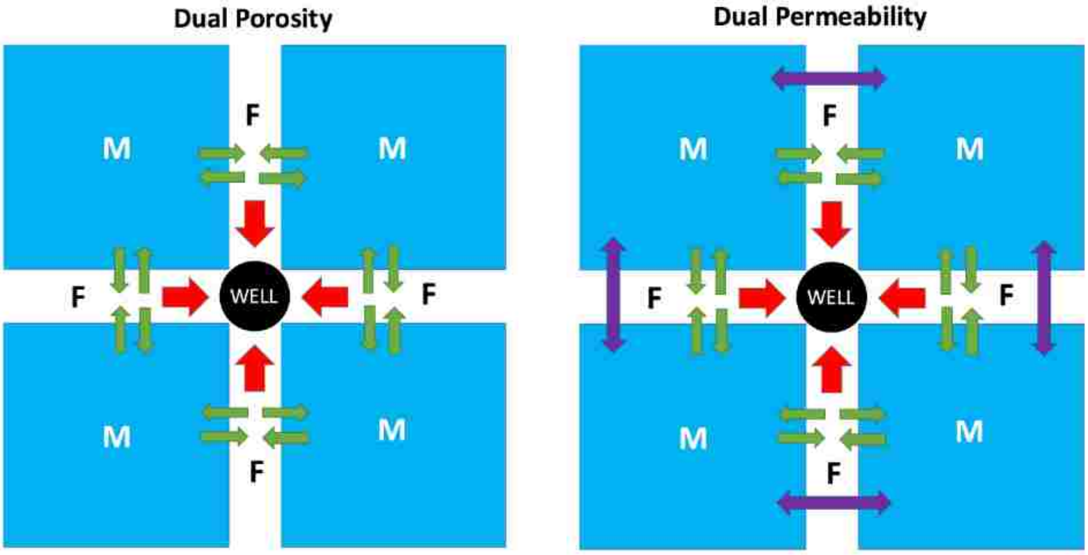
Dual Porosity
Dual Permeability
M
F
WELL

Figure 12. Schematic representation of flow in dual porosity and dual permeability media

The dual permeability model is an extension of the porosity model that additionally accounts for the flow between matrix blocks. For certain types of reservoirs, very small amounts of fluid are transferred between matrix block due to high pressure differential between matrix and fracture (thus movement along matrix blocks is not preferred) and therefore, dual permeability model can be neglected. On the other hand, certain reservoirs may have significant permeability of the matrix zone and therefore, numerical simulation of such reservoirs is complicated due to difficulty achieving convergence. Accounting for fluid transfer between matrix blocks in dual permeability models makes the model more complicated and more computational power and time are required.

The third way for numerical simulation of naturally fractured reservoirs is the Multiple Interacting Continua (MINC) approach. This approach is even more complicated than dual porosity/dual permeability simulations. In the MINC approach, each matrix block in the model is further subdivided into a series of sub-continua and fluid flow regime/flow path is individually determined for each sub-continua according to its properties. This approach has not yet found a wide use in the industry due to enormous computational requirements. The use of this method often (if not always) requires the application of a supercomputer with parallel processing capabilities due to a high number of heat flow/mass transfer equations being computed simultaneously. Full scale reservoir simulation models generally have not used the MINC approach due to the computational requirements.

In this research, the first set of simulations included the study of matrix/fracture interaction using single porosity approach for computational efficiency and ability to run a large number of multiple models within a certain timeframe. In the first model created, zone of low and high density of fracture network were represented as horizontal adjacent layers connecting injector of heat-transfer agent and producer. Model consisted of 200 single porosity blocks and could be numerically calculated within a very small period of time (less than 10 minutes using high performance computing (HPC). This is a computationally simple 2-dimentional numerical simulation of dual media (figure 13). In order to study the effect of gravity, simulations were run for the cases when highly fractured zone is located above and below the zone having small number of fractures. Each set of simulations included a preliminary grid block size sensitivity analysis.

However, spatial dimensions of fractures are different than of porous matrix zones and distance between injector and producer is typically more than 100 meters as in the first model run. Therefore, the initially created 2-dimentional model was increased up to a 20 thousand grid block single porosity model (figure 14). Besides the size, the model had different relative thicknesses of matrix and fracture zones. Similar to the previous set of simulations, the effect of gravity was considered by arranging highly fractured zone above and below the porous matrix zone.

The next step included simulation of various steam injection modes (figure 15). The simulations included separate steam injection into one of the zones for a certain period of time and subsequent injection into both matrix and fracture zones.

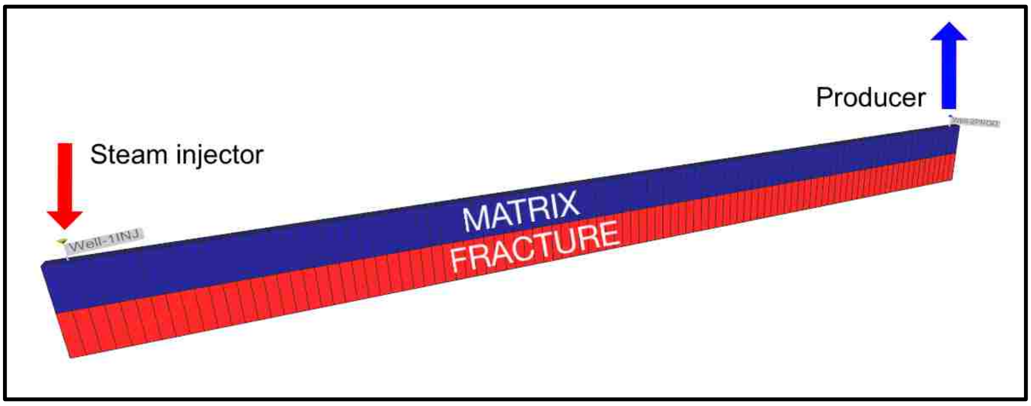
Producer
Steam injector
Well-1INJ
MATRIX
FRACTURE

Figure 13. Simple 2-layer 2-dimentional representation of dual media distribution

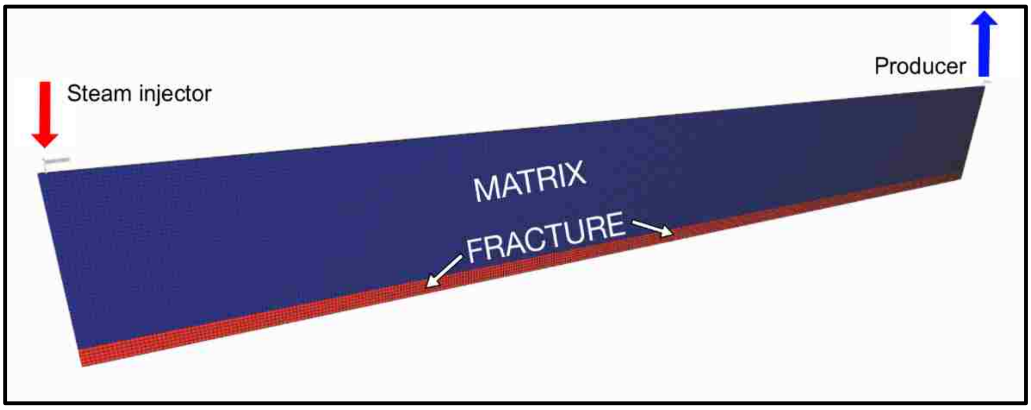
Producer
Steam injector
MATRIX
FRACTURE

Figure 14. 20-thousand 2-dimentional single porosity model

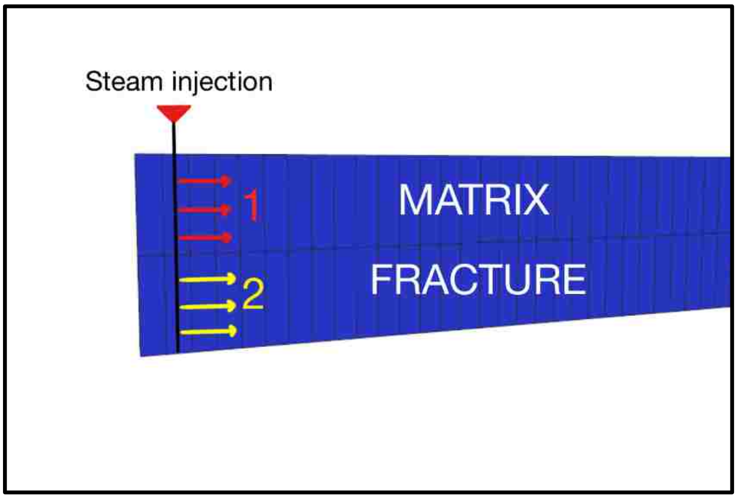
Steam injection
1
MATRIX
2
FRACTURE

Figure 15. Testing of various steam-injection modes

The next stage of the research included the study of the effect of thermogel application. In our case, thermogel is a fluid capable of plugging certain zones in the reservoir by decreasing their permeability and therefore enhancing oil recovery by increasing matrix sweep efficiency. This helps to decrease the possibility of water or steam breakthroughs (figure 16). Assuming that thermogel injection into zones with high density of fracture network separately is possible, the effect of preliminary thermogel injection plugging the fractures in the wellbore surrounding area on the development of matrix zone was studied (figure 17). Analogous study was conducted for producer well with its wellbore surrounding area with fractures being plugged. Certain results and conclusions were obtained.

After single porosity simulations, a dual porosity dual permeability numerical simulation of an inverted 5-point model with injector in the middle and four producers in the corners was tested (figure 18). This simulation included the study of the effect of various values of fracture spacing. Fracture spacing is the distance between the fracture in horizontal (X or Y) or vertical direction (Z). Results regarding dependency between matrix-fracture mass transfer and permeability of fractures together with their spacing were obtained.

The second part of the thesis included various numerical simulation tests on a sector of a real heavy oilfield N located in Russia (figure 19). Based on the geologic data provided, a sector model for oilfield N was built in CMG STARS software. The accuracy of the data allowed to build a model with grid blocks having extent in horizontal directions of 10 meters and vertical 0.5 meters.

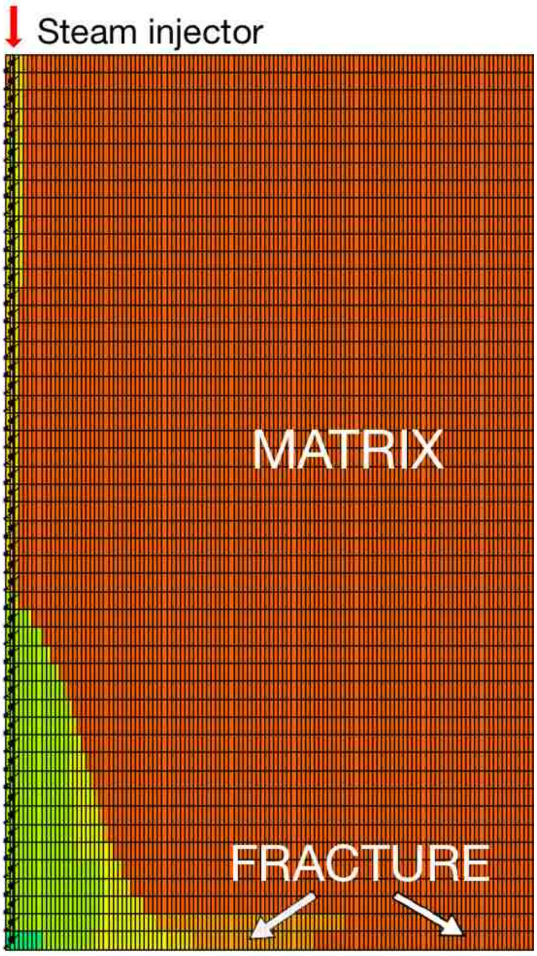
Steam injector
MATRIX
FRACTURE

Figure 16. Visual representation of initiation of early water/steam breakthrough

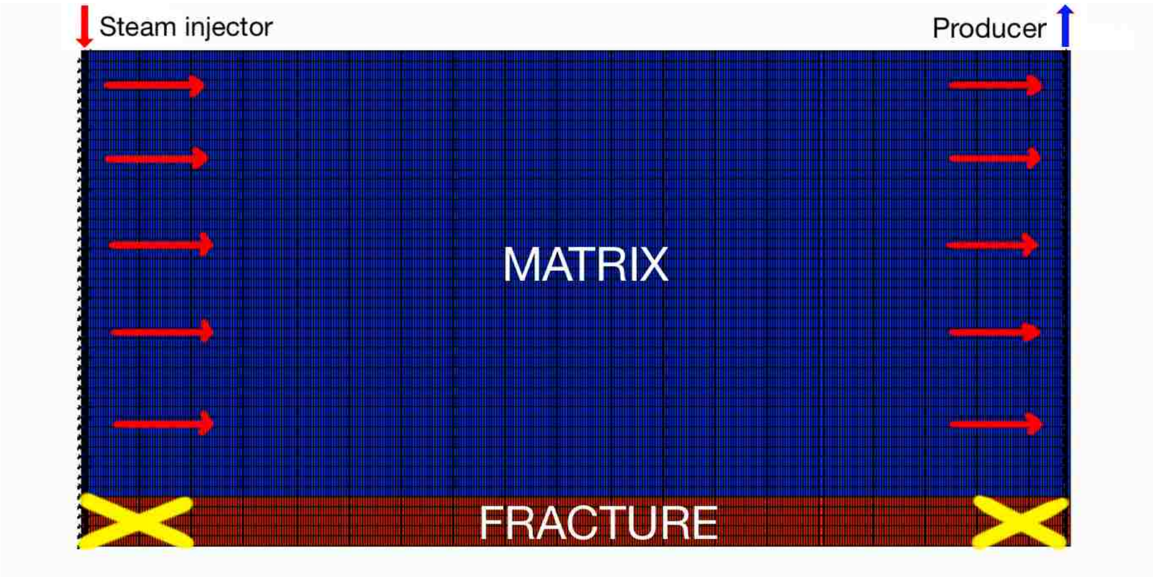
Steam injector
Producer
MATRIX
FRACTURE

Figure 17. Testing of a preliminary thermogel injection technique

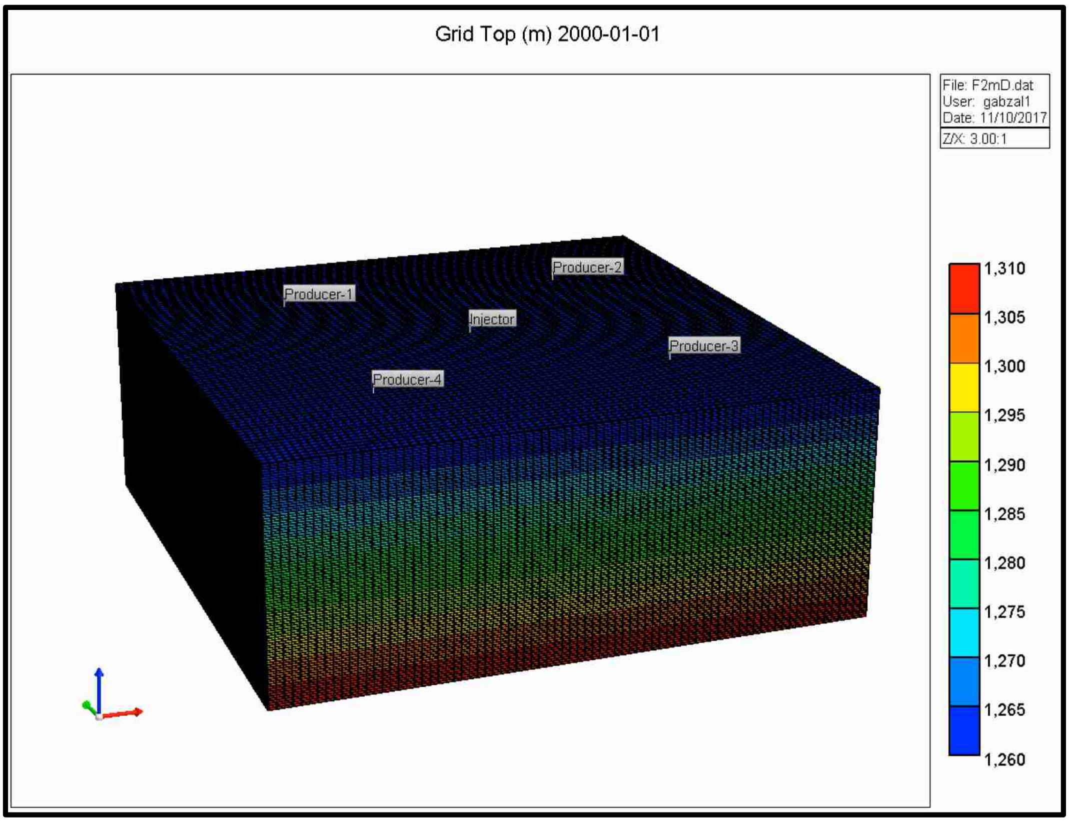
Grid Top (m) 2000-01-01
File: F2mD.dat
User: gabzal1
Date: 11/10/2017
Z/X: 3.00:1
Producer-1
Producer-2
Injector
Producer-3
Producer-4
1,310
1,305
1,300
1,295
1,290
1,285
1,280
1,275
1,270
1,265
1,260

Figure 18. Inverted 5-point dual porosity dual permeability development model

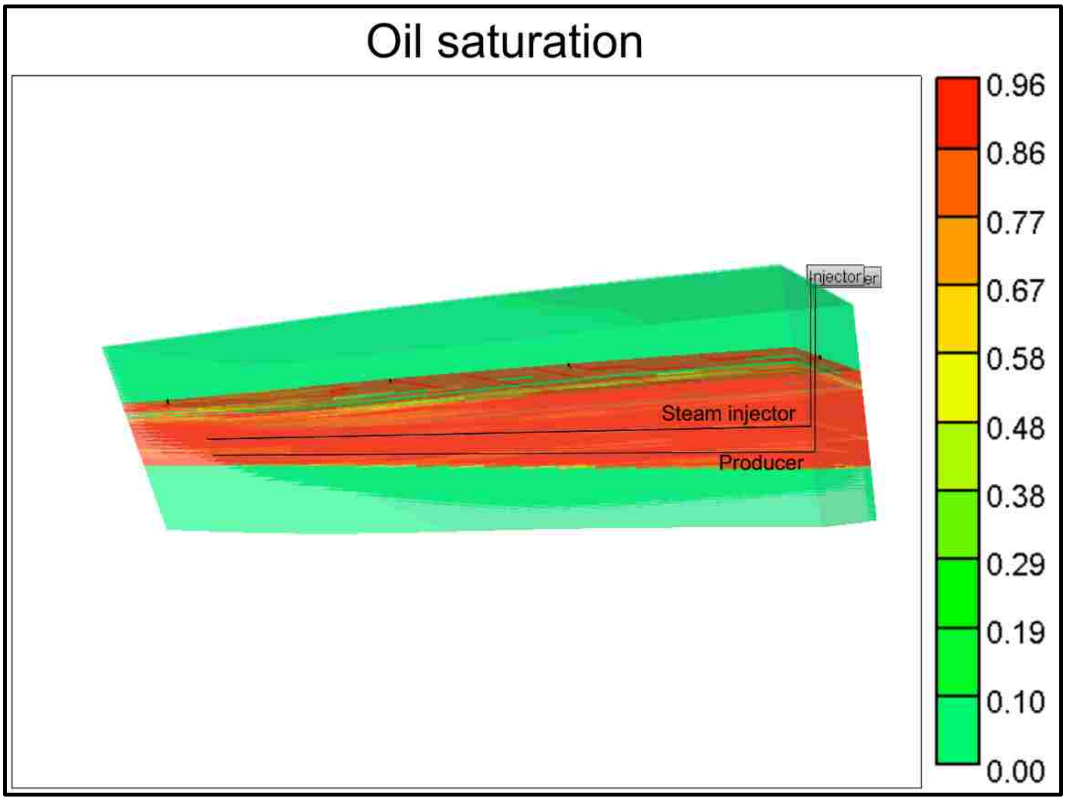
Oil saturation
Injector
Steam injector
Producer
0.96
0.86
0.77
0.67
0.58
0.48
0.38
0.29
0.19
0.10
0.00

Figure 19. Initial oil saturation of sector from reservoir N

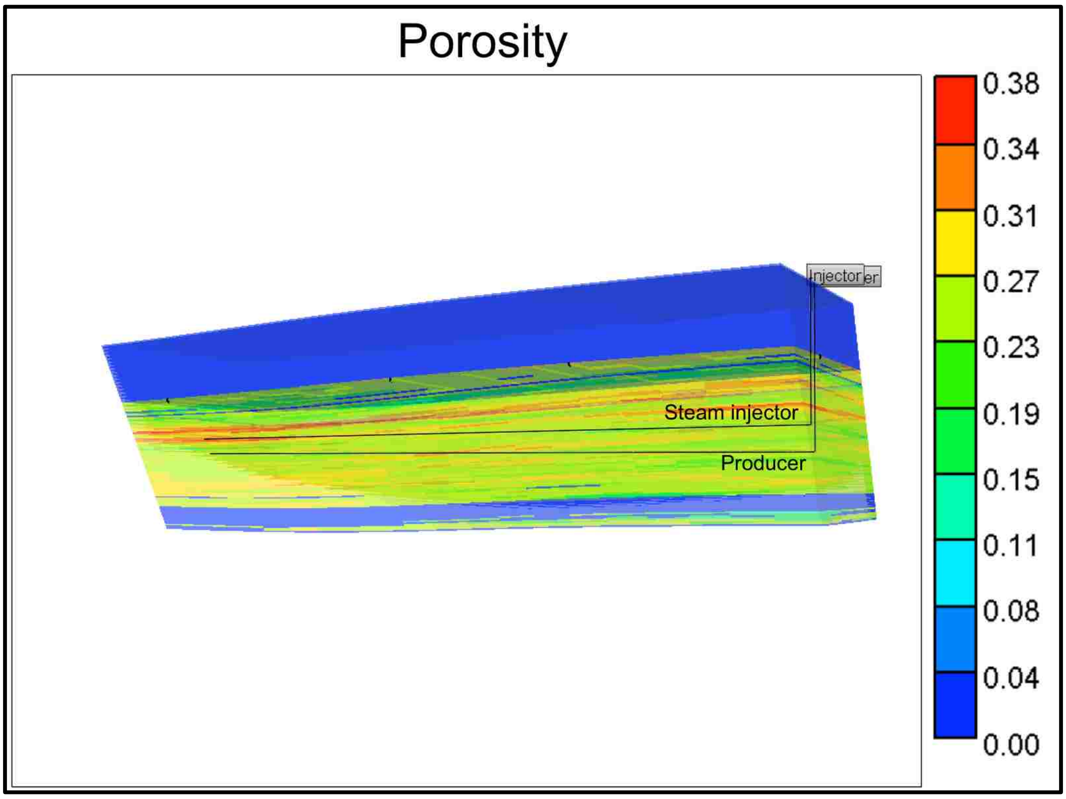
Porosity
Injector
er
Steam injector
Producer
0.38
0.34
0.31
0.27
0.23
0.19
0.15
0.11
0.08
0.04
0.00

Figure 20. Porosity distribution of a sector from reservoir N

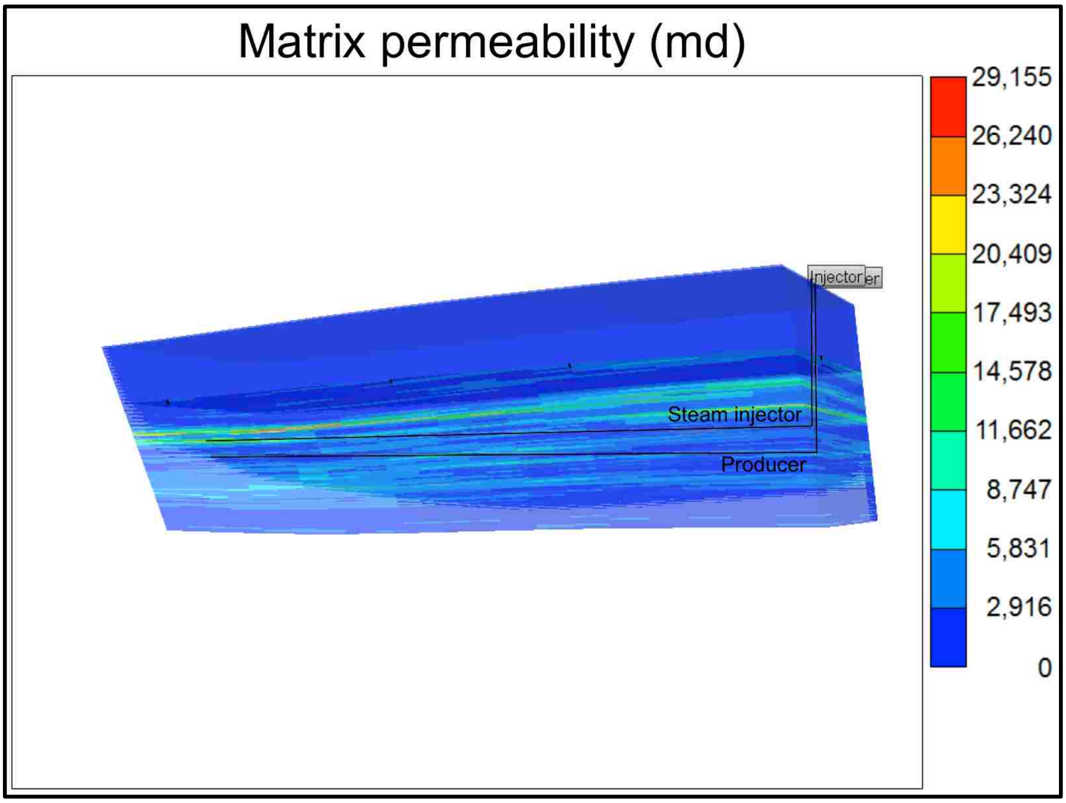
Matrix permeability (md)
Injector
er
Steam injector
Producer
29,155
26,240
23,324
20,409
17,493
14,578
11,662
8,747
5,831
2,916
0

Figure 21. Permeability distribution of sector from oilfield N

As for all other simulations, the first step of numerical simulation for the sector model for oilfield N included a grid block size sensitivity analysis. Four different grid block sizes were considered in X and Y direction: 10 x 10 m, 5 x 5 m, 2 x 2 m, 1 x 1 m. The size of grid block in Z direction was fixed and constrained to 0.5 m.

Reservoir N is currently under SAGD production with well spacing of 5 meters. However, according to results of the simulations described in "Results and Discussion" chapter, current SAGD methods do not permit high recovery fdue to a high and near-immediate water cut. The first volumes of produced oil have about 80% of water cut which soon reaches 100% due to water and steam breakthroughs. When we implement vertical fractures, the problem of steam breakthrough appear almost immediately.

In order to assess the efficiency and importance of SAGD, a comparative analysis of various injection agents were conducted: cold water injection (10°C), hot water injection (90°C), steam injection (224°C at 2500 kPa) and primary depletion without any injection. A parametric analysis for various fracture permeabilities, fracture spacing and injection pressures was also performed. Thermogel injection was also tested. The hypothesis tested was that the zone of decreased permeability next to injector or producer would help contain water and steam breakthroughs and, as a result increase recovery.

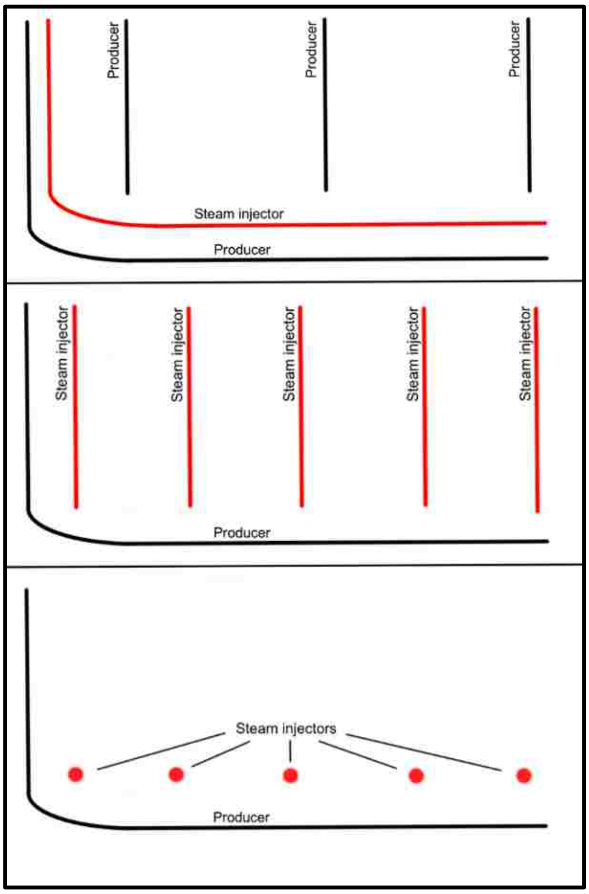
Producer
Producer
Producer
Steam injector
Producer
Steam injector
Steam injector
Steam injector
Steam injector
Steam injector
Producer
Steam injectors
Producer

Figure 22. Tested development models for the sector of oilfield N

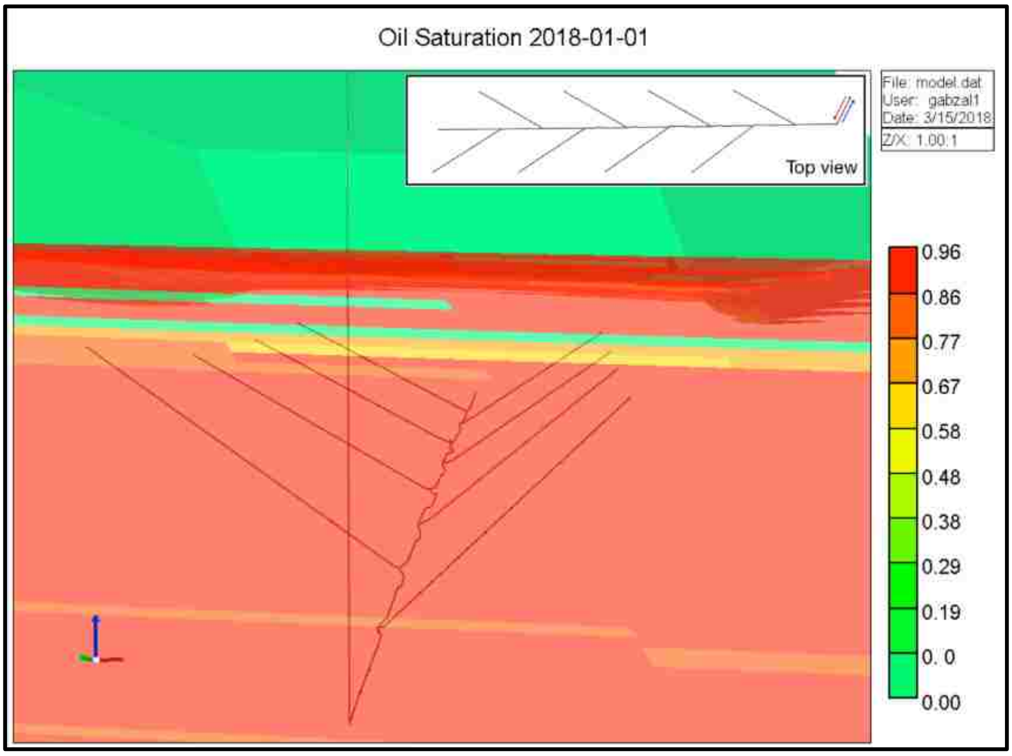
Oil Saturation 2018-01-01
File: model.dat
User: gabzal1
Date: 3/15/2018
Z/X: 1.00:1
Top view
0.96
0.86
0.77
0.67
0.58
0.48
0.38
0.29
0.19
0. 0
0.00

Figure 23. Fishtail well design for cyclic steaming

Besides conventional SAGD, 3 different scenarios were tested (figure 22, 23) – conventional SAGD, cyclic steam injection and fishtail wellbore design with cyclic steam injection (figure 23). In the fishtail arrangement, the well works as injector and as producer interchangeably.

Figure 24. SuperMike-II supercomputer at LSU

All simulations were run at Louisiana State University's high performance computing (HPC) system using Mike II supercomputer (Figure 24).

CHAPTER 6. RESULTS AND DISCUSSION

Numerical simulations of mass and heat transfer in dual porosity, dual permeability systems are computationally expensive. Therefore, the very first step of the numerical simulation included the determination of the limitations associated with the size and complexity of the models. First, a 2.7 million grid block Steam-Assisted Gravity Drainage (SAGD) single-porosity model was built (figure 25). For SuperMike-II it required 46 hours to calculate the results for 10 years of numerical simulation. This result gave a quick assessment of the performance capabilities at HPC, LSU and determine computational limitations associated with size and complexity of the models. Every model run included a grid block size sensitivity analysis, the example of which can be seen on figure 26. In this particular case, 1 x 1 x 1 meter grid block size was determined to be the most optimum with 4.8% of maximum error and 1.8% average error according to cumulative oil production of 0.5 x 0.5 x 0.5 meter reference model.

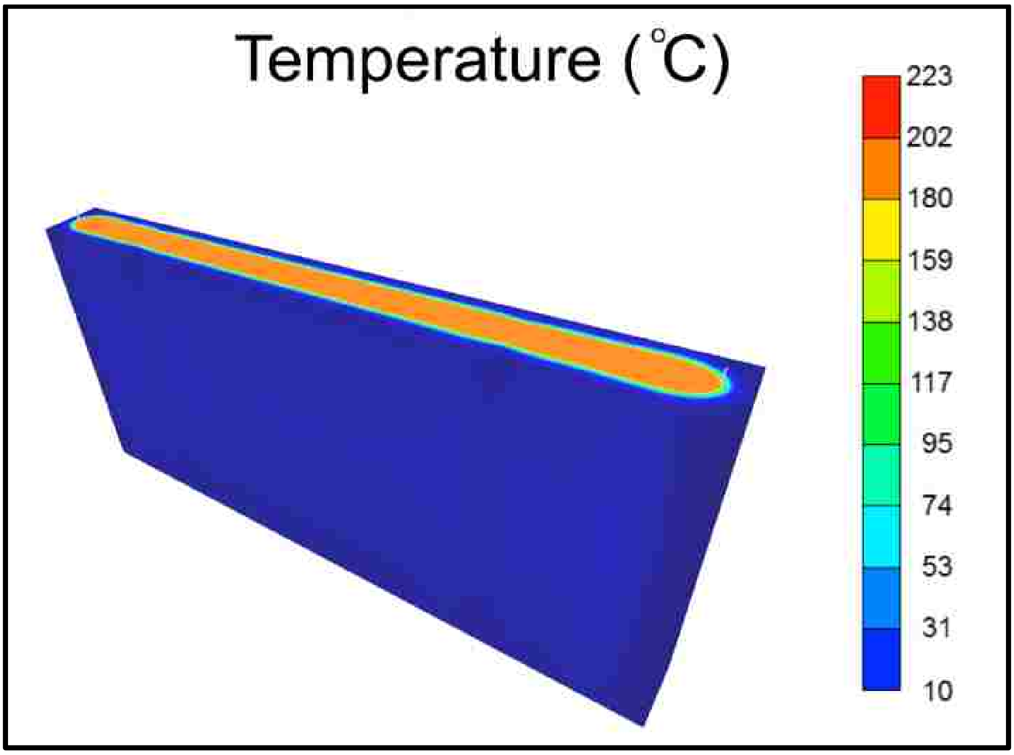

Figure 25. Temperature distribution in a test 2.7 million SAGD model

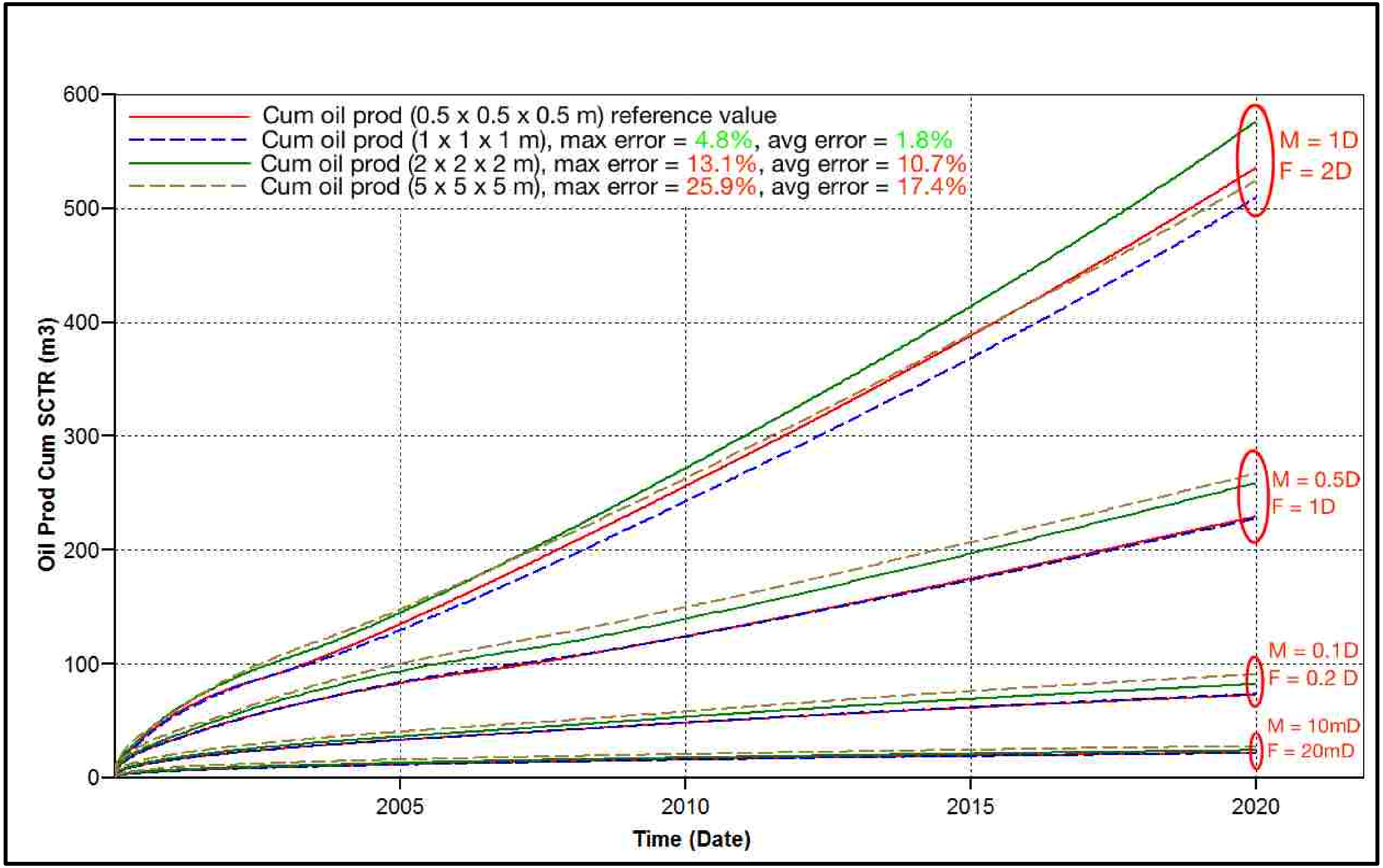
600
500
400
300
200
100
0
Oil Prod Cum SCTR (m3)
2005
2010
2015
2020
Time (Date)
Cum oil prod (0.5 x 0.5 x 0.5 m) reference value
Cum oil prod (1 x 1 x 1 m), max error = 4.8%, avg error = 1.8%
Cum oil prod (2 x 2 x 2 m), max error = 13.1%, avg error = 10.7%
Cum oil prod (5 x 5 x 5 m), max error = 25.9%, avg error = 17.4%
M = 1D
F = 2D
M = 0.5D
F = 1D
M = 0.1D
F = 0.2 D
M = 10mD
F = 20mD

[redacted]

6.1 Simulation results from 2-dimensional model

Results from a single porosity 2 dimensional representation of reservoir N demonstrated the complex relation between fractures and matrices in terms of sweep efficiency and recovery factors. The single porosity system was replicated using a layer of low density micro fractures (matrix), followed by a layer of high permeability (fractures). No direct correlation was observed when a range of fracture and matrix permeability scenarios were tested (all within field observations/data) (figure 27). In addition to the absence of a straight line direct correlation, increase in fracture permeability was observed to contribute both to enhancing and worsening matrix oil recovery depending on the matrix permeability (blue and green curves, figure 27). For relatively high matrix permeability, the model gave higher recovery in these cases, heated oil from matrix, migrated downward due to gravity effects into the permeable fractured zone and then were produced. Therefore, it can be recommended to perforate matrix layers adjacent (and above) fractured zones. Injecting steam along the entire thickness of the reservoir (matrix and fracture) versus the schemes of “matrix first”, and “fracture first” before injecting the entire thickness were tested to see if the recovery differed by heating up the reservoir differentially in the latter scheme (figure 28). Results indicate (figure 28) that steam injection into both the matrix and fractured layers simultaneously was the most effective as the highest amount of heat could be transmitted when the contact between steam and the reservoir rock was the longest. This test was conducted for a varying range of matrix and fracture permeability values and in all cases tested, highest recovery occurred when the steam was injected into the entire length of perforation (matrix and fracture included).

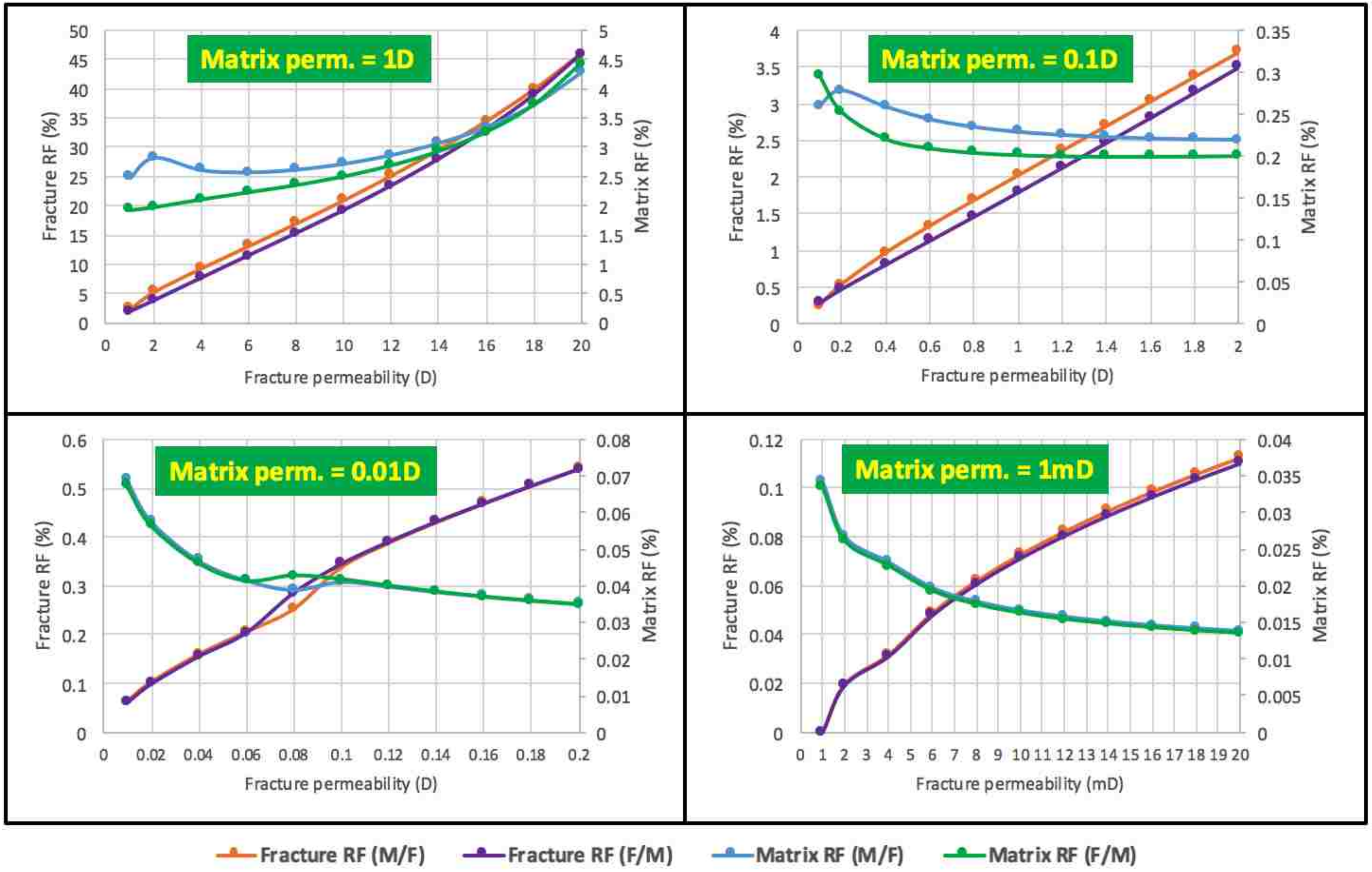
Matrix perm. = 1D
Fracture RF (%)
50
45
40
35
30
25
20
15
10
5
0
Matrix RF (%)
5
4.5
4
3.5
3
2.5
2
1.5
1
0.5
0
0
2
4
6
8
10
12
14
16
18
20
Fracture permeability (D)
Matrix perm. = 0.1D
Fracture RF (%)
4
3.5
3
2.5
2
1.5
1
0.5
0
Matrix RF (%)
0.35
0.3
0.25
0.2
0.15
0.1
0.05
0
0
0.2
0.4
0.6
0.8
1
1.2
1.4
1.6
1.8
2
Fracture permeability (D)
Matrix perm. = 0.01D
Fracture RF (%)
0.6
0.5
0.4
0.3
0.2
0.1
0
Matrix RF (%)
0.08
0.07
0.06
0.05
0.04
0.03
0.02
0.01
0
0
0.02
0.04
0.06
0.08
0.1
0.12
0.14
0.16
0.18
0.2
Fracture permeability (D)
Matrix perm. = 1mD
Fracture RF (%)
0.12
0.1
0.08
0.06
0.04
0.02
0
Matrix RF (%)
0.04
0.035
0.03
0.025
0.02
0.015
0.01
0.005
0
0 1 2 3 4 5 6 7 8 9 10 11 12 13 14 15 16 17 18 19 20
Fracture permeability (mD)
Fracture RF (M/F)
Fracture RF (F/M)
Matrix RF (M/F)
Matrix RF (F/M)

[redacted]

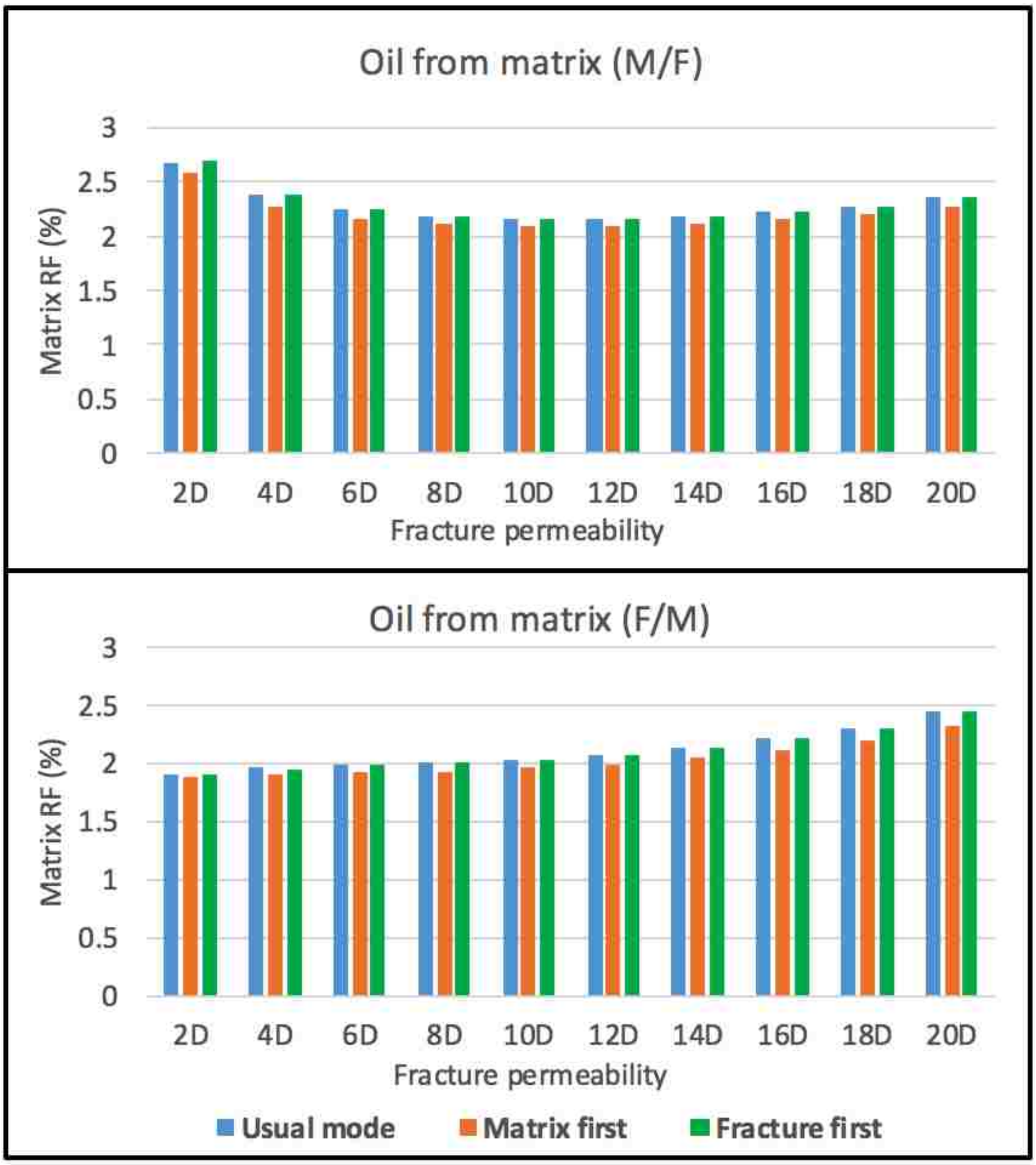

Figure 28. Results of various steam injection modes simulation

Next, the simulation was upscaled to a 20-thousand grid block model (figure 29). Increase in fracture permeability resulted in decrease of matrix recovery factor because the fractures acted as permeability super highways within the reservoir. For high-viscosity systems, however, conductive fractures help distribute a heat-transfer agent throughout the reservoir, and thus the mechanism of matrix recovery is complicated and “ideal” facture permeability is a subjective value, depending on various factors.

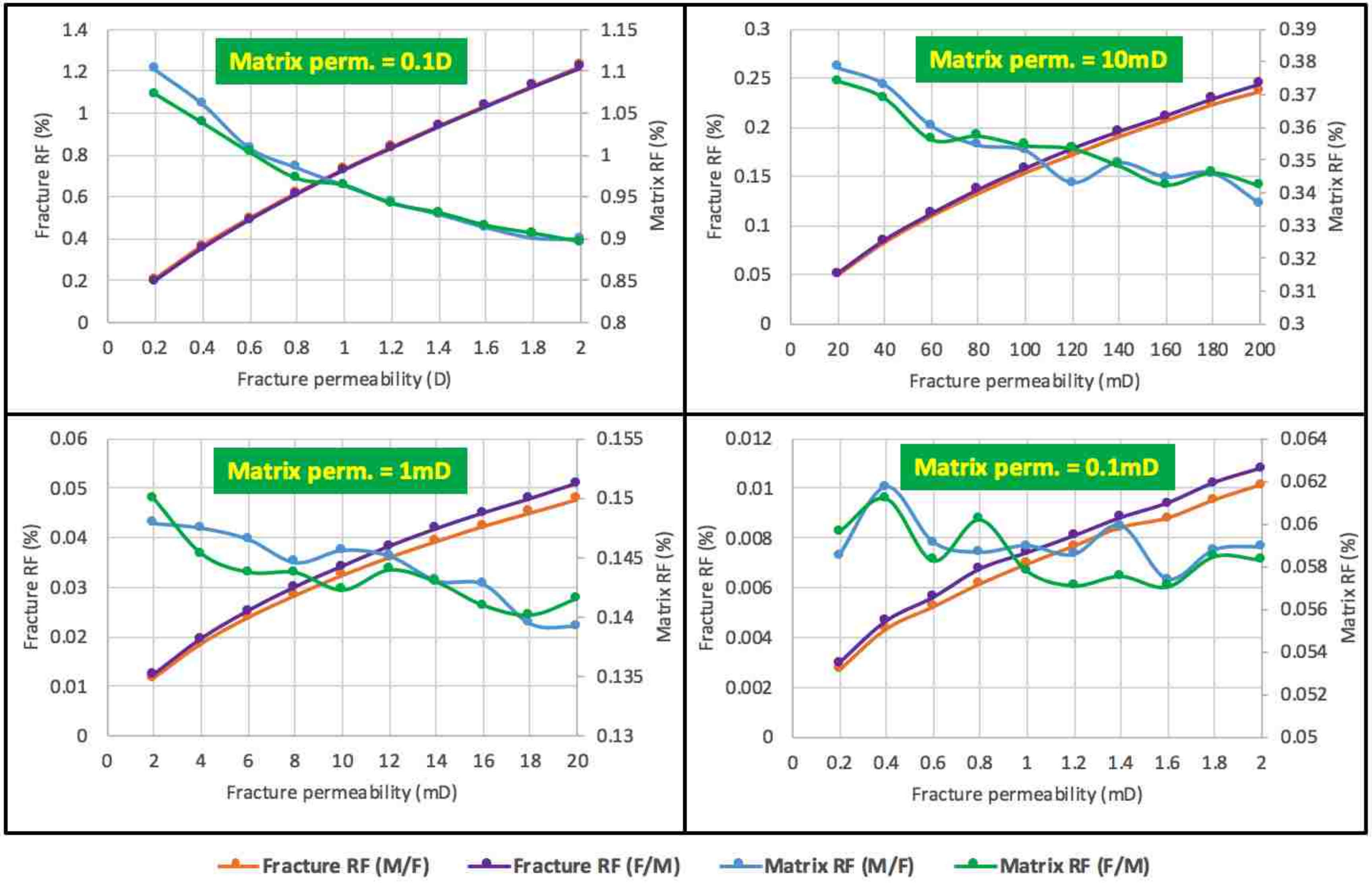
Matrix perm. = 0.1D
Fracture RF (%)
Matrix RF (%)
Fracture permeability (D)
1.4
1.2
1
0.8
0.6
0.4
0.2
0
0.2
0.4
0.6
0.8
1
1.2
1.4
1.6
1.8
2
1.15
1.1
1.05
1
0.95
0.9
0.85
0.8
Matrix perm. = 10mD
Fracture RF (%)
Matrix RF (%)
Fracture permeability (mD)
0.3
0.25
0.2
0.15
0.1
0.05
0
20
40
60
80
100
120
140
160
180
200
0.39
0.38
0.37
0.36
0.35
0.34
0.33
0.32
0.31
0.3
Matrix perm. = 1mD
Fracture RF (%)
Matrix RF (%)
Fracture permeability (mD)
0.06
0.05
0.04
0.03
0.02
0.01
0
2
4
6
8
10
12
14
16
18
20
0.155
0.15
0.145
0.14
0.135
0.13
Matrix perm. = 0.1mD
Fracture RF (%)
Matrix RF (%)
Fracture permeability (mD)
0.012
0.01
0.008
0.006
0.004
0.002
0
0.2
0.4
0.6
0.8
1
1.2
1.4
1.6
1.8
2
0.064
0.062
0.06
0.058
0.056
0.054
0.052
0.05
Fracture RF (M/F)
Fracture RF (F/M)
Matrix RF (M/F)
Matrix RF (F/M)

[redacted]

Results from thermogel injection prior to steam flooding indicate that injection of thermogel into highly fractured zone next to an injector constrained the propagation of steam (figure 30) throughout the reservoir which negatively impacted recovery from the matrix zone. This pertained to various permeabilities of matrix zone (0.1 mD – 0.1 D). The steam routed through the matrix zone till above the point where the fractured was plugged with the thermogel, but jumped into the fracture as soon as the plug zone ended. Interestingly, however, thermogel injection into fractured zone next to producer resulted in increased matrix recovery along the producer. Magnitude of this increase varied with matrix permeability (figure 31). Thermogel injection into a fractured zone next to a producer increase sweep efficiency of the adjacent matrix zone since steam breakthrough directly through the fractures was restricted in this case. Thus if thermogel is used in layered fractured and matrix reservoirs, injecting it next to producers could potentially restrict steam breakthrough and help sweep matrix nearby.

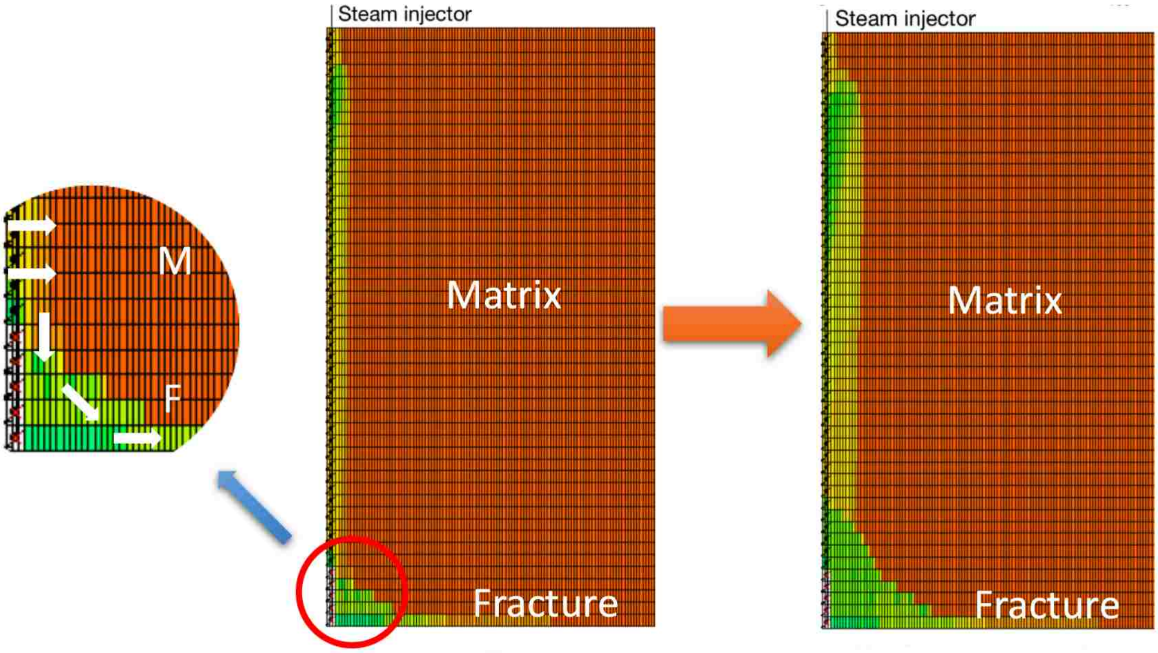

Figure 30. Visual representation of preliminary thermogel plugging a fractured zone next to an injector well

While running inverted 5 – point dual porosity dual permeability model, it was observed that increase of the permeability of fractures contributed to higher recovery (figure 32). For the case of a higher matrix permeability (upper left figure) increase of fracture permeability resulted in a decrease of total recovery factor. This is related to early steam/water breakthrough. Also it was observed that fracture spacing has considerable effect for systems with low matrix permeability. For biggest fracture spacing (50 m), recovery factor is the lowest since the number of factures is reduced in comparison with fracture spacing 5 m example.

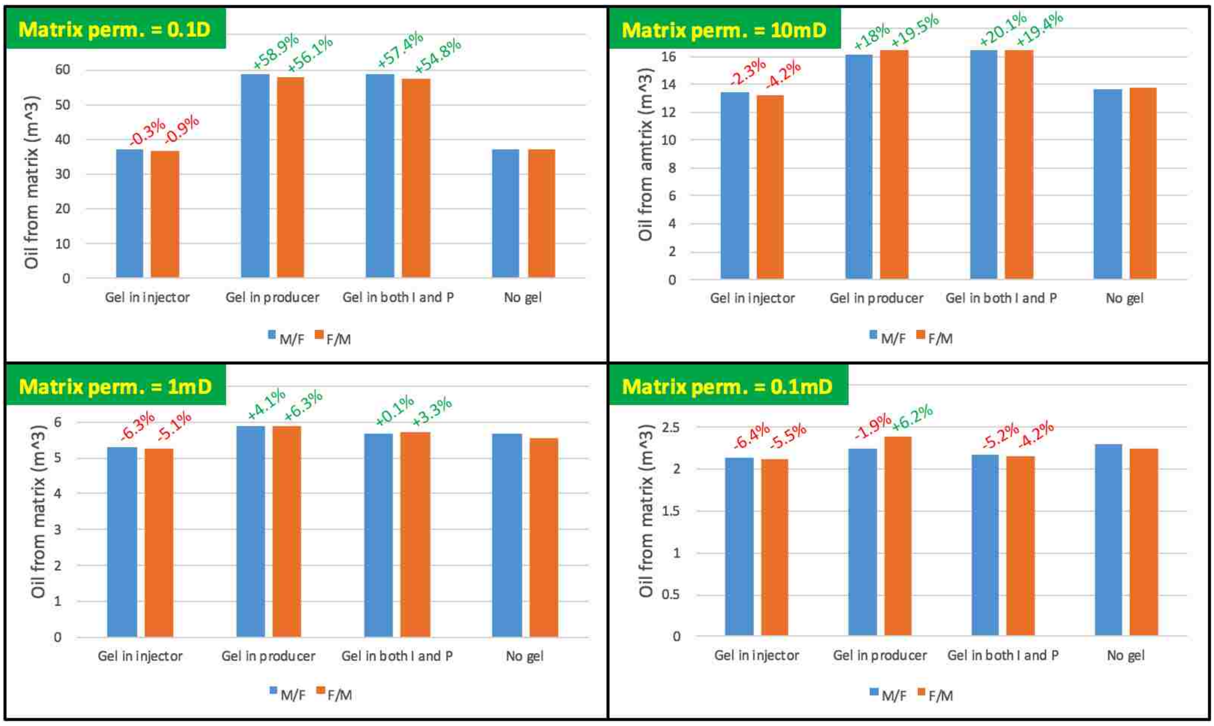

Figure 31. Results of preliminary thermogel injection in a 2-dimentional model

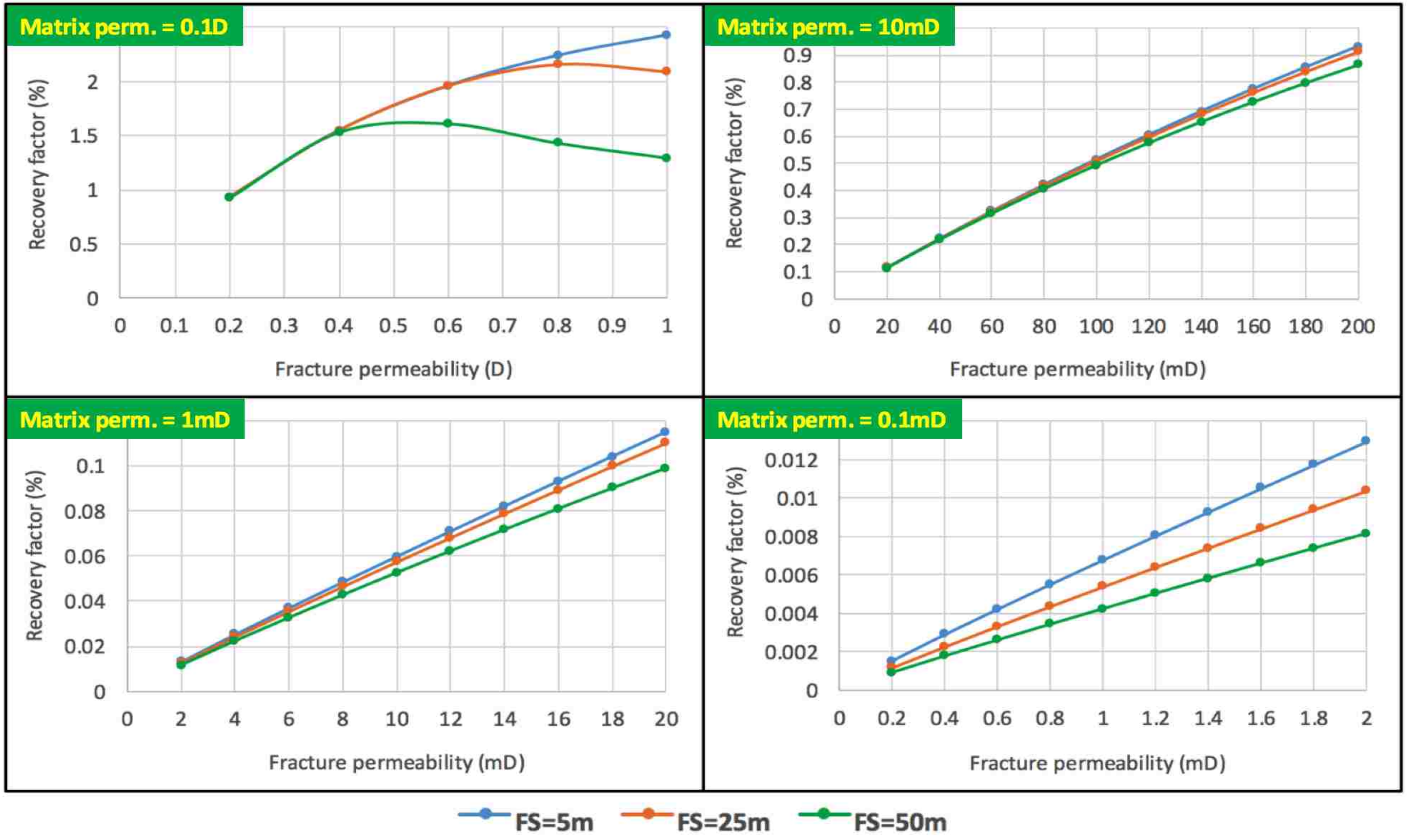
Matrix perm. = 0.1D
Recovery factor (%)
0
0.5
1
1.5
2
0
0.1
0.2
0.3
0.4
0.5
0.6
0.7
0.8
0.9
1
Fracture permeability (D)
Matrix perm. = 10mD
Recovery factor (%)
0
0.1
0.2
0.3
0.4
0.5
0.6
0.7
0.8
0.9
0
20
40
60
80
100
120
140
160
180
200
Fracture permeability (mD)
Matrix perm. = 1mD
Recovery factor (%)
0
0.02
0.04
0.06
0.08
0.1
0
2
4
6
8
10
12
14
16
18
20
Fracture permeability (mD)
Matrix perm. = 0.1mD
Recovery factor (%)
0
0.002
0.004
0.006
0.008
0.01
0.012
0
0.2
0.4
0.6
0.8
1
1.2
1.4
1.6
1.8
2
Fracture permeability (mD)
FS=5m
FS=25m
FS=50m

[redacted]

6.2 Numerical simulations for sector N of YHOF oilfield

Once the conceptual tests were run using the simpler two dimensional model, a 3 dimensional sector model for reservoir N was constructed. The static model was populated with field data mostly from well logging, and special core analysis. Once the static model was built and quality checked, an initial run was made to determine the volume in place to compare with static estimates (volumetric). Once the initial hydrocarbon volume was reconciled with volumetric estimates, a dynamic simulation was initiated for history matching with pressure-production-injection data. After the iterative history matching process was completed, a grid block size sensitivity analysis was conducted. Initially, the size of a grid block in the model composed 10 meters in length and width and 0.5 meters in thickness. In order to conduct a grid block size sensitivity analysis, the length and width of grid blocks was decreased by 2, 5 and 10 times and composed 5, 2 and 1 meters respectively. Thickness of grid block initially was small and therefore it was decided not to increase it in order to keep the precision of the simulation at a high level, since the SAGD system was implemented which is typically very sensitive to thickness of grid blocks. Analysis was conducted for single porosity model. The time of calculation ranged depending on the number of grid blocks. For smaller grid block sizes (i.e. bigger number of blocks in the system) time required to simulate 10 years of development was considerably longer. Thereby, 1 hours and 13 minutes were required to simulate 10 years of development for a model having 10 x 10 x 0.5 m grid block size, 4 hours and 17 minutes for the model with grid blocks of 5 x 5 x 0.5 m, 62 hours and 57 minutes for the model with grid blocks of 2 x 2 x Z m. Model with grid blocks of 1 x 1 x Z meters was not calculated within the allotted 72-hour period (only 27 days of the simulation were calculated) and therefore the results of the simulation with 1 x 1 x 0.5 m grid block size is not depicted.

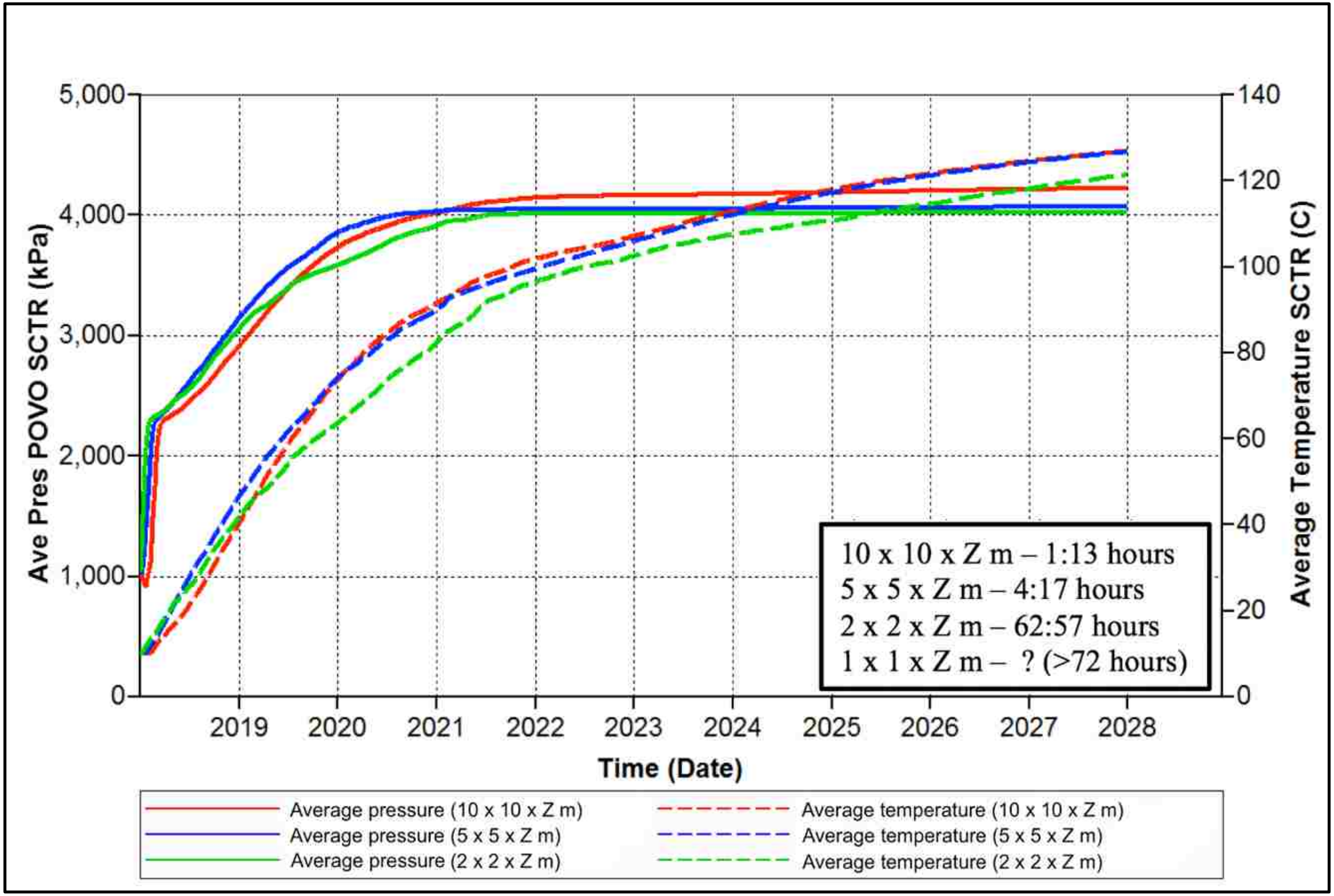
5,000
4,000
3,000
2,000
1,000
0
Ave Pres POVO SCTR (kPa)
140
120
100
80
60
40
20
0
Average Temperature SCTR (C)
2019
2020
2021
2022
2023
2024
2025
2026
2027
2028
Time (Date)
10 x 10 x Z m – 1:13 hours
5 x 5 x Z m – 4:17 hours
2 x 2 x Z m – 62:57 hours
1 x 1 x Z m – ? (>72 hours)
Average pressure (10 x 10 x Z m)
Average pressure (5 x 5 x Z m)
Average pressure (2 x 2 x Z m)
Average temperature (10 x 10 x Z m)
Average temperature (5 x 5 x Z m)
Average temperature (2 x 2 x Z m)

[redacted]

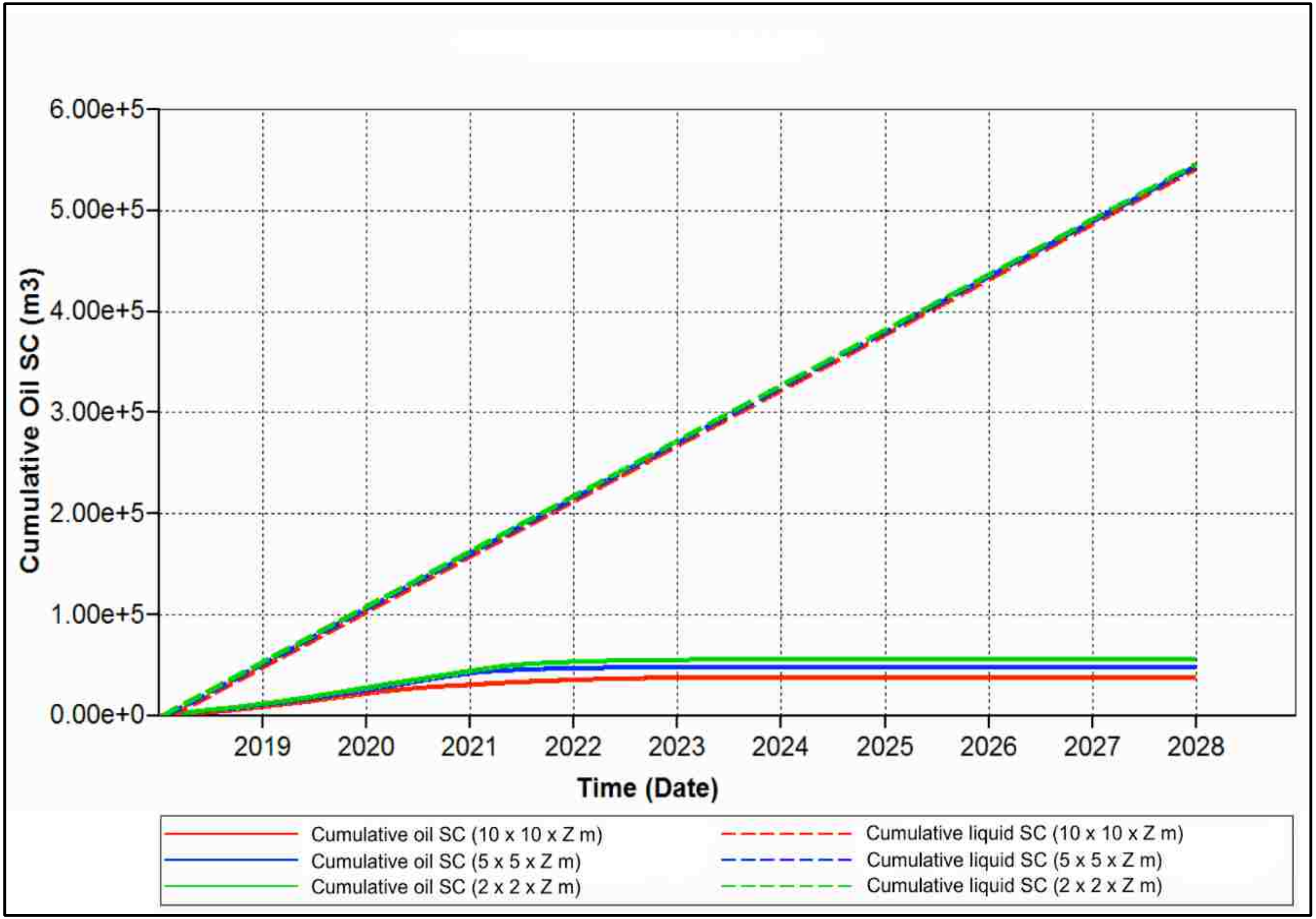
6.00e+5
5.00e+5
4.00e+5
3.00e+5
2.00e+5
1.00e+5
0.00e+0
Cumulative Oil SC (m3)
2019
2020
2021
2022
2023
2024
2025
2026
2027
2028
Time (Date)
Cumulative oil SC (10 x 10 x Z m)
Cumulative oil SC (5 x 5 x Z m)
Cumulative oil SC (2 x 2 x Z m)
Cumulative liquid SC (10 x 10 x Z m)
Cumulative liquid SC (5 x 5 x Z m)
Cumulative liquid SC (2 x 2 x Z m)

[redacted]

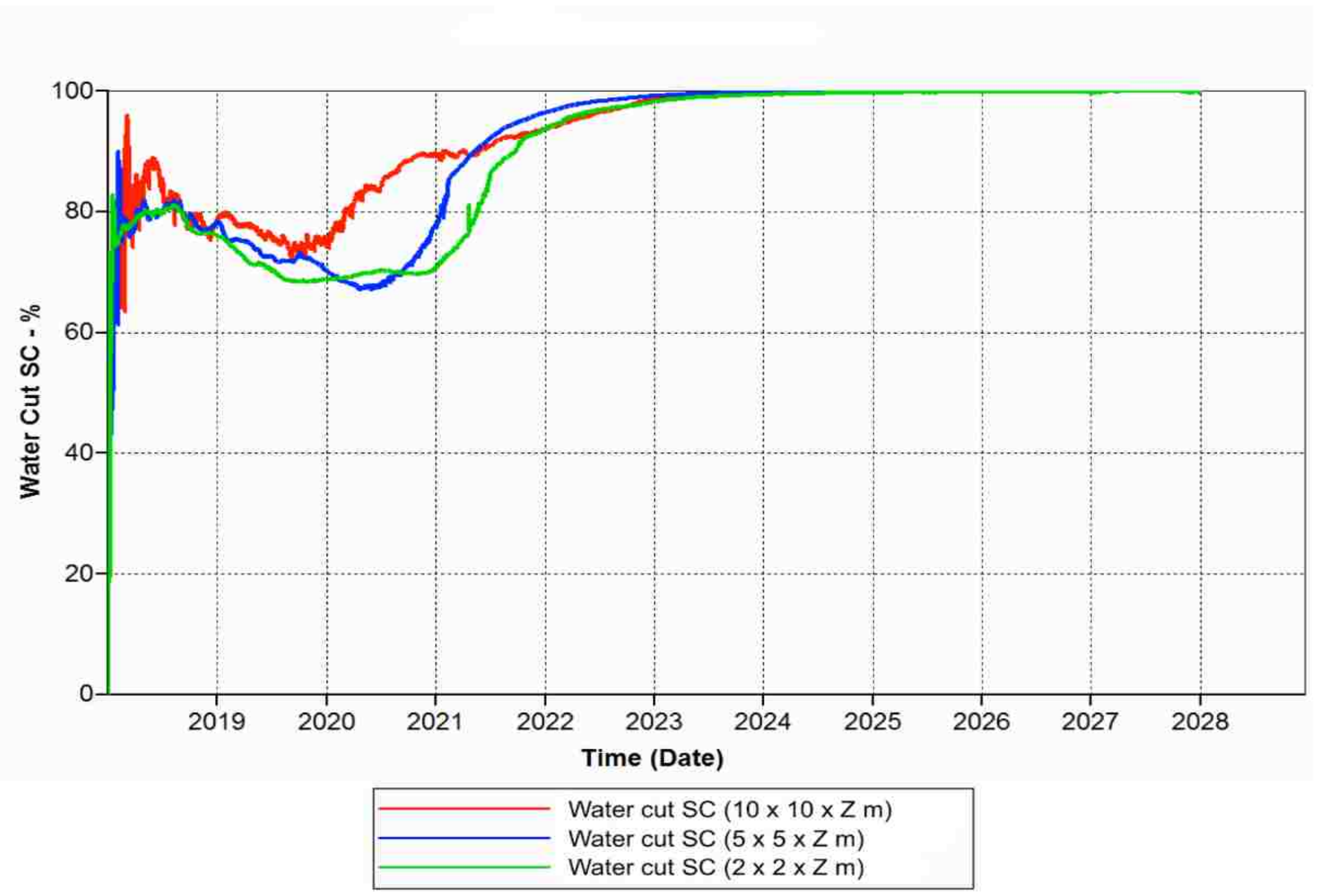
Water Cut SC - %
100
80
60
40
20
0
2019
2020
2021
2022
2023
2024
2025
2026
2027
2028
Time (Date)
Water cut SC (10 x 10 x Z m)
Water cut SC (5 x 5 x Z m)
Water cut SC (2 x 2 x Z m)

[redacted]

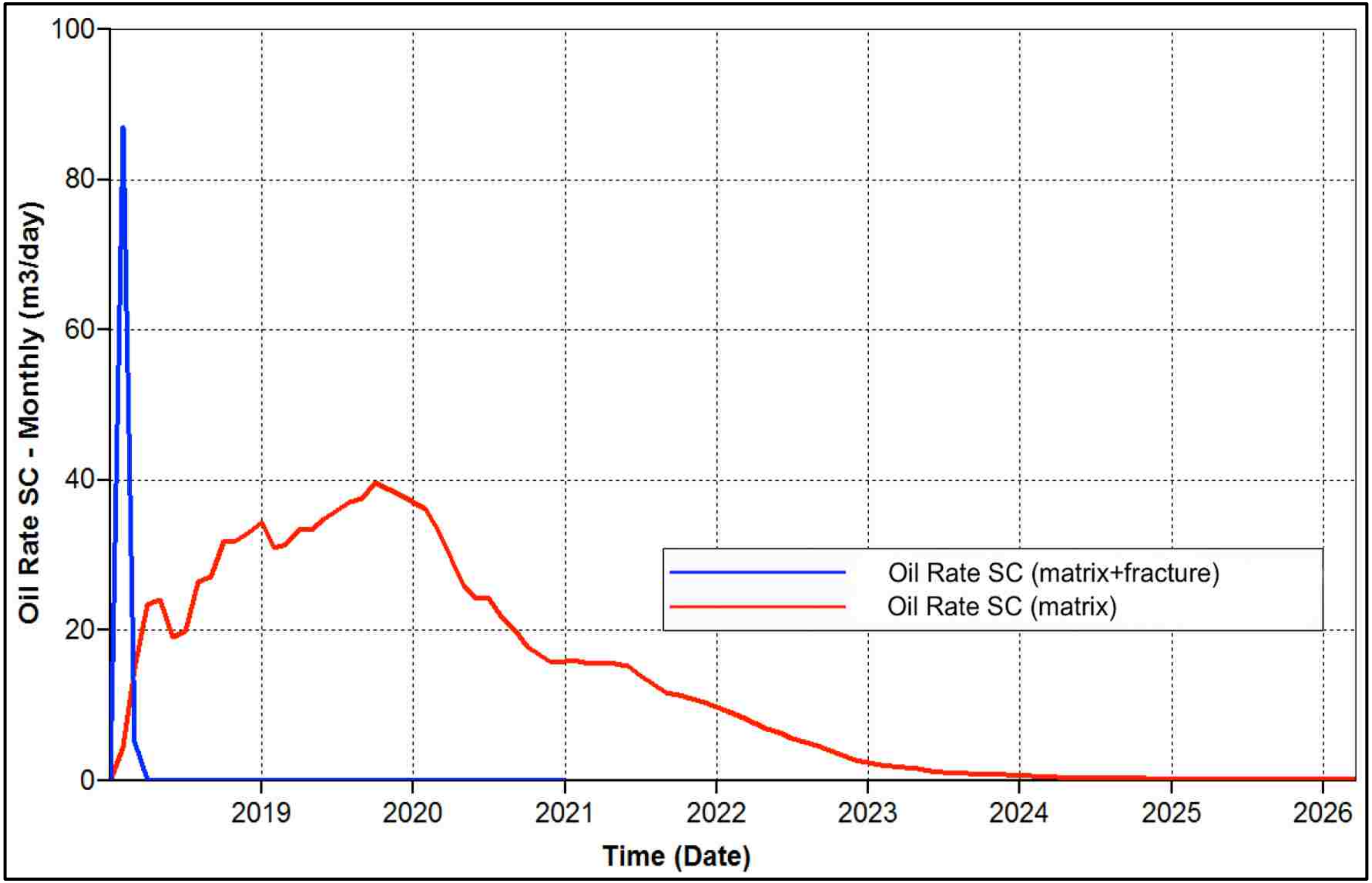
Oil Rate SC - Monthly (m3/day)
100
80
60
40
20
0
2019
2020
2021
2022
2023
2024
2025
2026
Time (Date)
Oil Rate SC (matrix+fracture)
Oil Rate SC (matrix)

[redacted]

As already mentioned, the considered sector (reservoir N) of the oilfield is currently developed using SAGD technology. However, in order to understand the importance and necessity of applied development techniques, we observed the behavior of production parameters during primary depletion (no injection), cold (10°C) and hot (90°C) water injection. As can be clearly noticed, the importance of heat injection into the reservoir can be hardly overestimated (figure 37). Therefore, effective development technologies should be based on thermal methods of oil recovery. However, while comparing hot water injection with currently applied steam injection, the superiority of steam is clear. (figure 38).

Sensitivity tests were run to understand the impact of fracture permeability, fracture spacing and pressure of steam injection on cumulative oil production. The optimum fracture permeability that increased recovery without resulting in early steam breakthrough was determined to be about 35D for the fractures in this reservoir (figure 39).

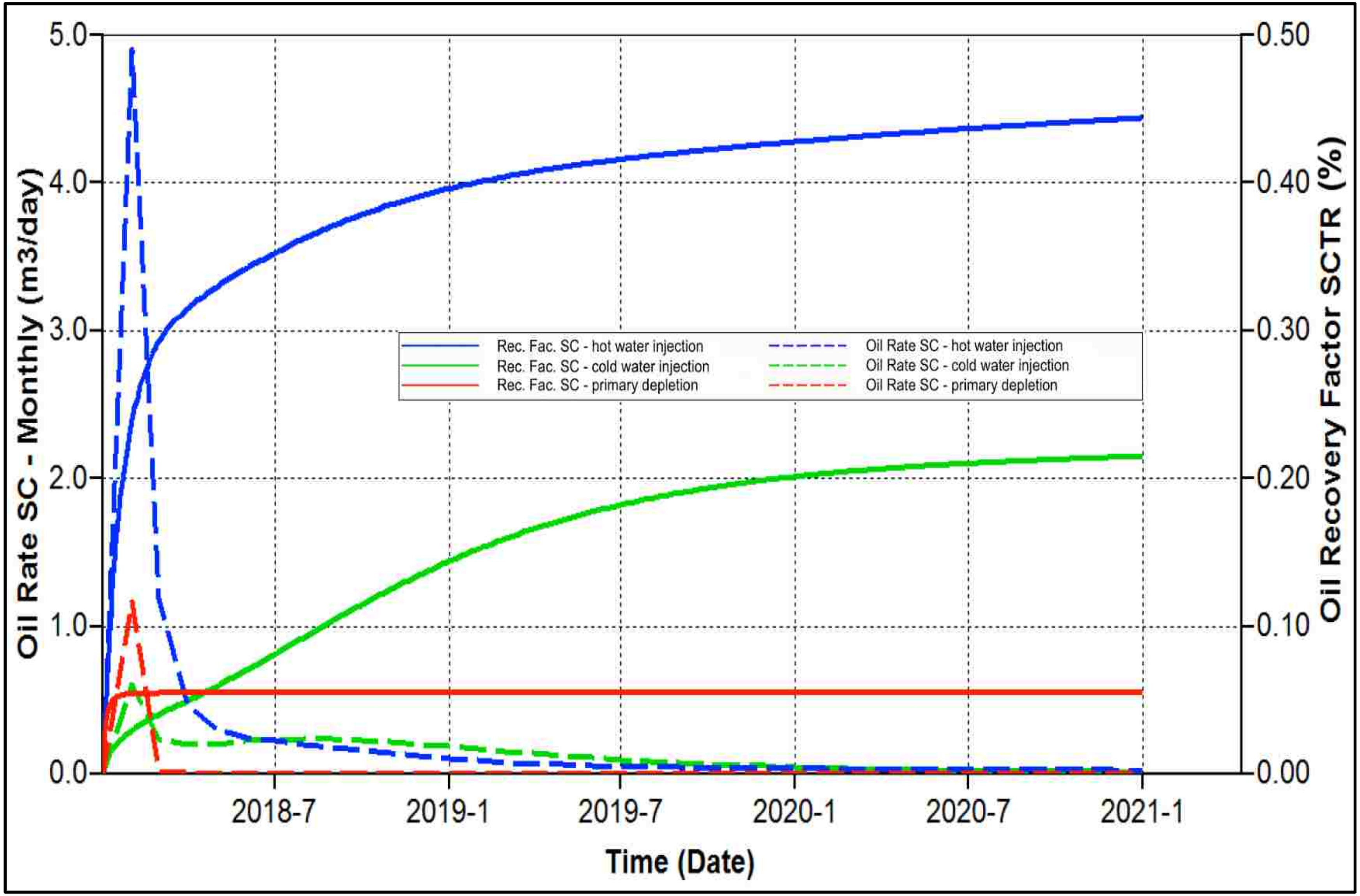

5.0
4.0
3.0
2.0
1.0
0.0
Oil Rate SC - Monthly (m3/day)
0.50
0.40
0.30
0.20
0.10
0.00
Oil Recovery Factor SCTR (%)
2018-7
2019-1
2019-7
2020-1
2020-7
2021-1
Time (Date)
Rec. Fac. SC - hot water injection
Rec. Fac. SC - cold water injection
Rec. Fac. SC - primary depletion
Oil Rate SC - hot water injection
Oil Rate SC - cold water injection
Oil Rate SC - primary depletion

[redacted]

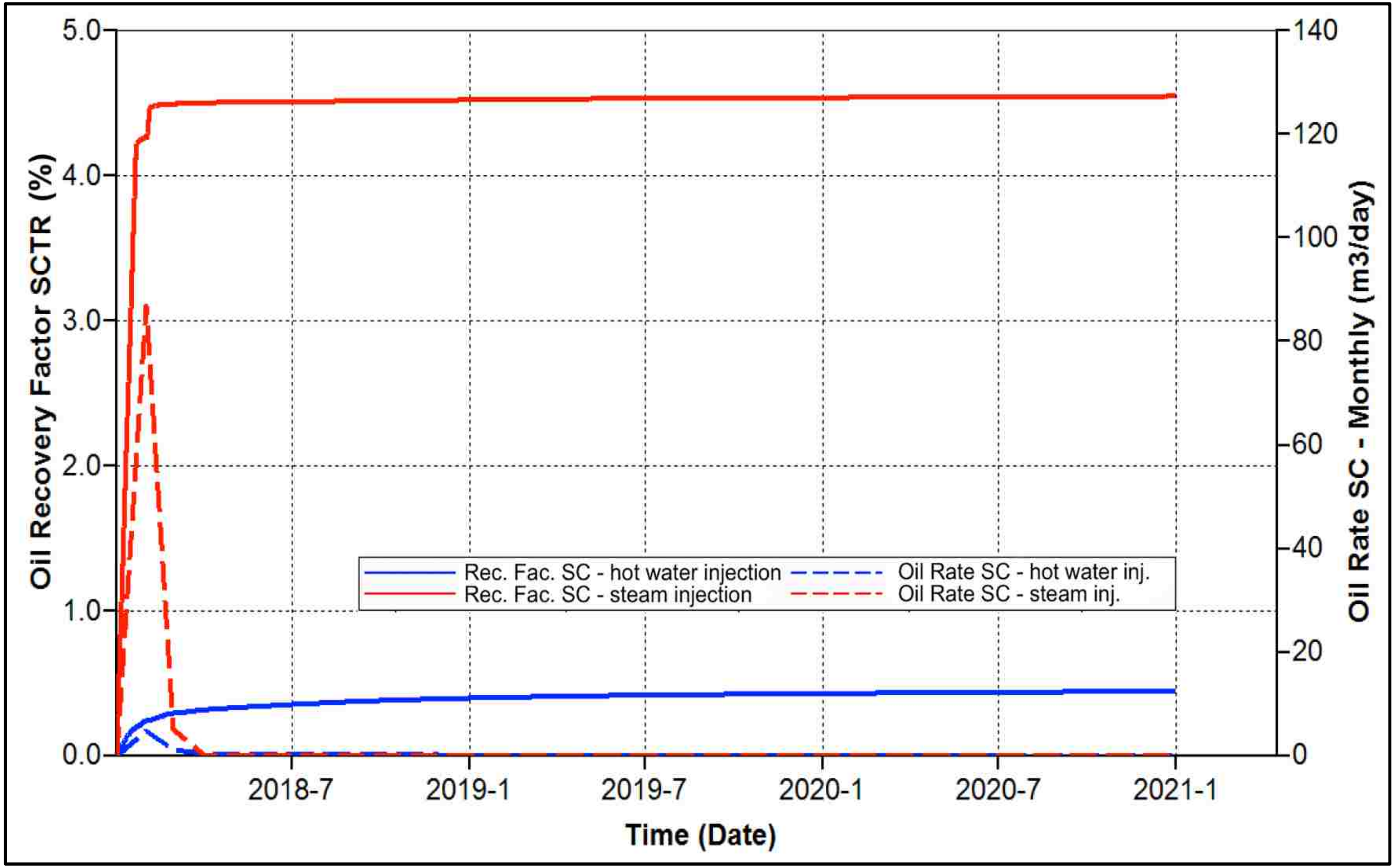
5.0
4.0
3.0
2.0
1.0
0.0
Oil Recovery Factor SCTR (%)
140
120
100
80
60
40
20
0
Oil Rate SC - Monthly (m3/day)
2018-7
2019-1
2019-7
2020-1
2020-7
2021-1
Time (Date)
Rec. Fac. SC - hot water injection
Rec. Fac. SC - steam injection
Oil Rate SC - hot water inj.
Oil Rate SC - steam inj.

[redacted]

Analysis of the second parameter, fracture spacing shows that recovery was highest when the average spacing was 20 – 30 m for the fracture spacing in reservoir N. Effective steam propagation due to the high number of highly permeable channels (fractures) and a lower steam breakthrough due to lower fracture number resulted in optimal recovery (figure 40).

Among tested pressures of steam injection (1500, 2000, 2500, 3000 and 3500 kPa), it was determined that along with the highest pressures of steam injection, recovery factor is the highest due to higher temperature of injection (figure 41). Higher pressures of steam injection than 3500 kPa were not considered due to a low pressure required to artificially fracture the formation (around 3000 – 3500 kPa).

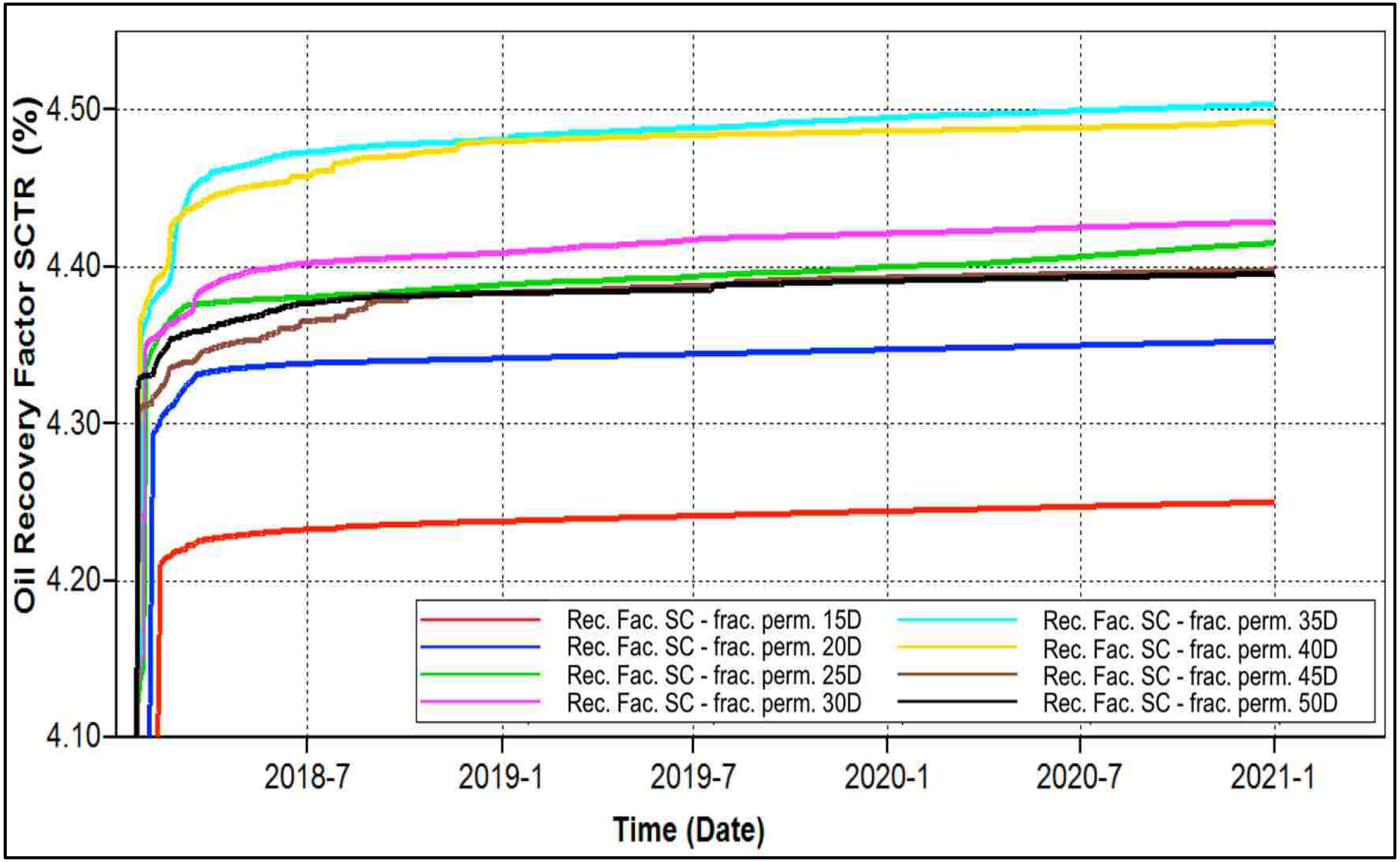
Oil Recovery Factor SCTR (%)
4.50
4.40
4.30
4.20
4.10
2018-7
2019-1
2019-7
2020-1
2020-7
2021-1
Time (Date)
Rec. Fac. SC - frac. perm. 15D
Rec. Fac. SC - frac. perm. 20D
Rec. Fac. SC - frac. perm. 25D
Rec. Fac. SC - frac. perm. 30D
Rec. Fac. SC - frac. perm. 35D
Rec. Fac. SC - frac. perm. 40D
Rec. Fac. SC - frac. perm. 45D
Rec. Fac. SC - frac. perm. 50D

[redacted]

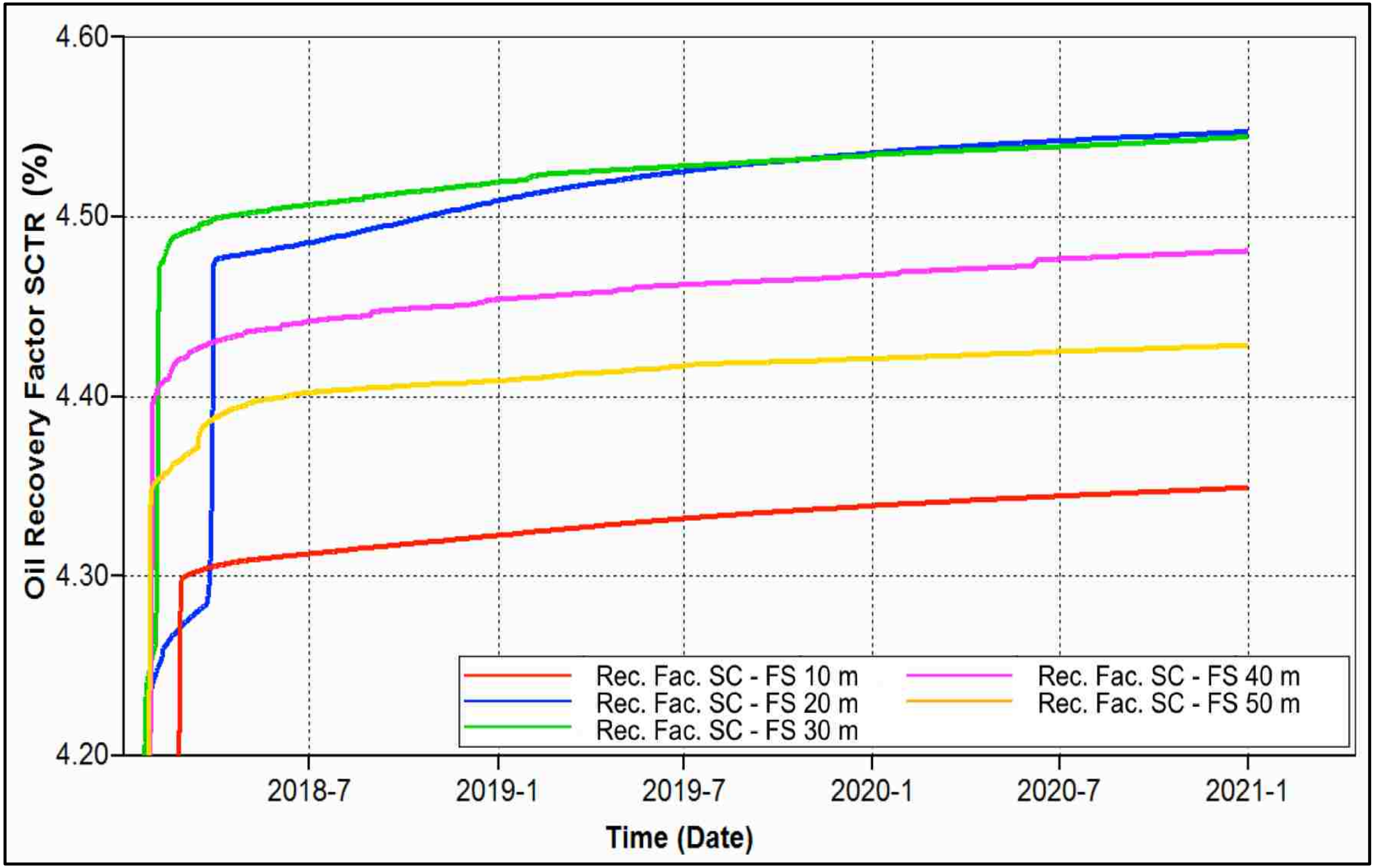
Oil Recovery Factor SCTR (%)
4.60
4.50
4.40
4.30
4.20
2018-7
2019-1
2019-7
2020-1
2020-7
2021-1
Time (Date)
Rec. Fac. SC - FS 10 m
Rec. Fac. SC - FS 20 m
Rec. Fac. SC - FS 30 m
Rec. Fac. SC - FS 40 m
Rec. Fac. SC - FS 50 m

[redacted]

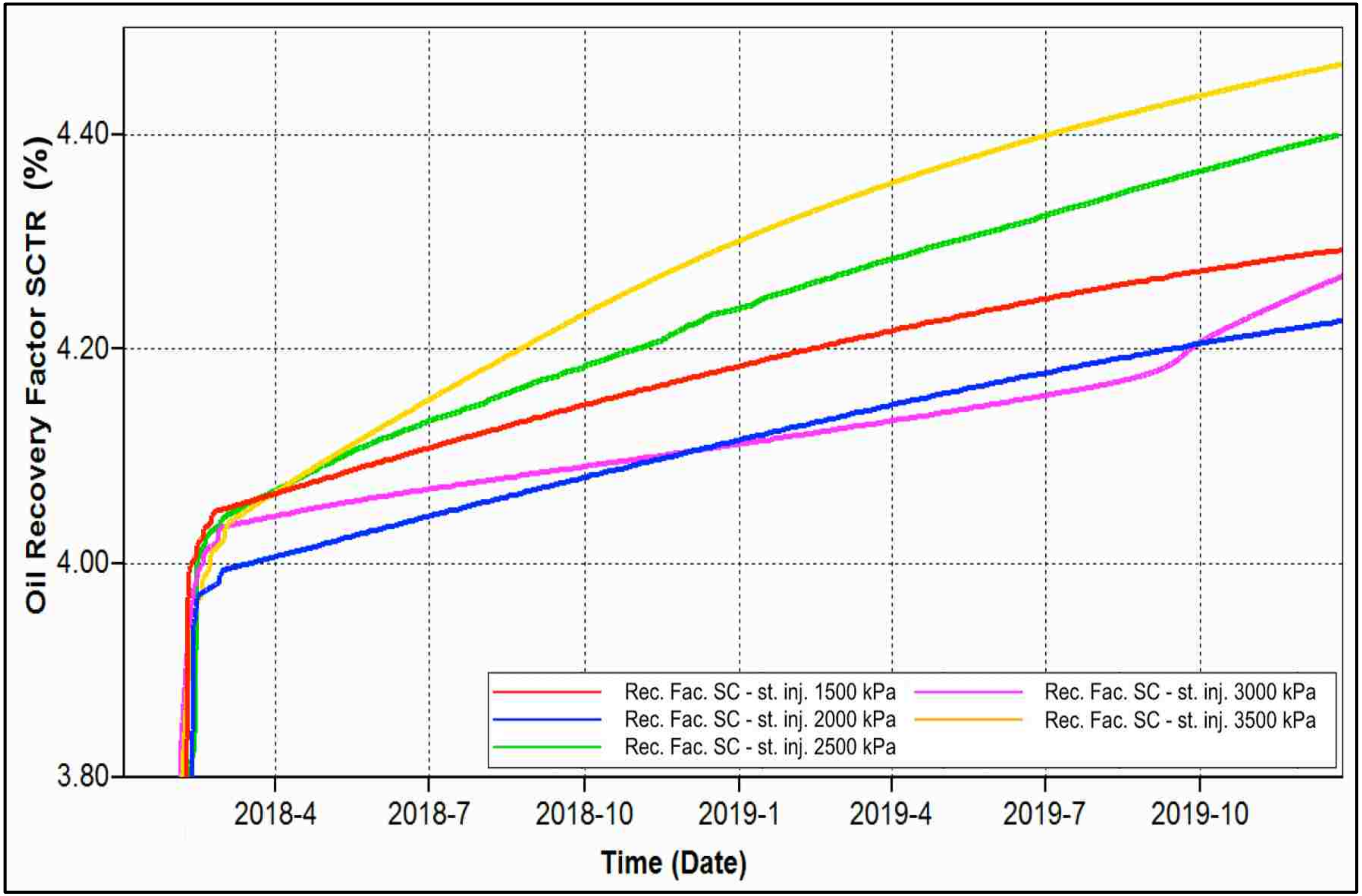
Oil Recovery Factor SCTR (%)
4.40
4.20
4.00
3.80
2018-4
2018-7
2018-10
2019-1
2019-4
2019-7
2019-10
Time (Date)
Rec. Fac. SC - st. inj. 1500 kPa
Rec. Fac. SC - st. inj. 2000 kPa
Rec. Fac. SC - st. inj. 2500 kPa
Rec. Fac. SC - st. inj. 3000 kPa
Rec. Fac. SC - st. inj. 3500 kPa

[redacted]

Since conventional SAGD technology is not resulting in satisfactory oil recovery and avoidance of steam breakthrough, the efficiency of thermogel was assessed as a development strategy for reservoir N. The idea behind this approach is to decrease the risk of early steam breakthrough and therefore, enhance the recovery of the model by preventing the risk of steam breakthrough (figures 42 and 43). In order to represent various thermogel injection configurations, decrease of the permeability due to presence of thermogel was assigned as a skin factor. Thereby, 3 various skin factors for each well was chosen: 5, 10 and 15. However, it was observed that as soon as steam passes the low permeability zone, it jumps into highly conductive vertical fracture next to it (figure 43). Thermogel plugging the zone next to producer did not permit higher recovery factor either. Additional difficulty that thermogel introduces, it that it constrains the steam propagation below the injector which also affects recovery factor. Therefore, thermogel application is not a recommended strategy for reservoir N (figure 44).

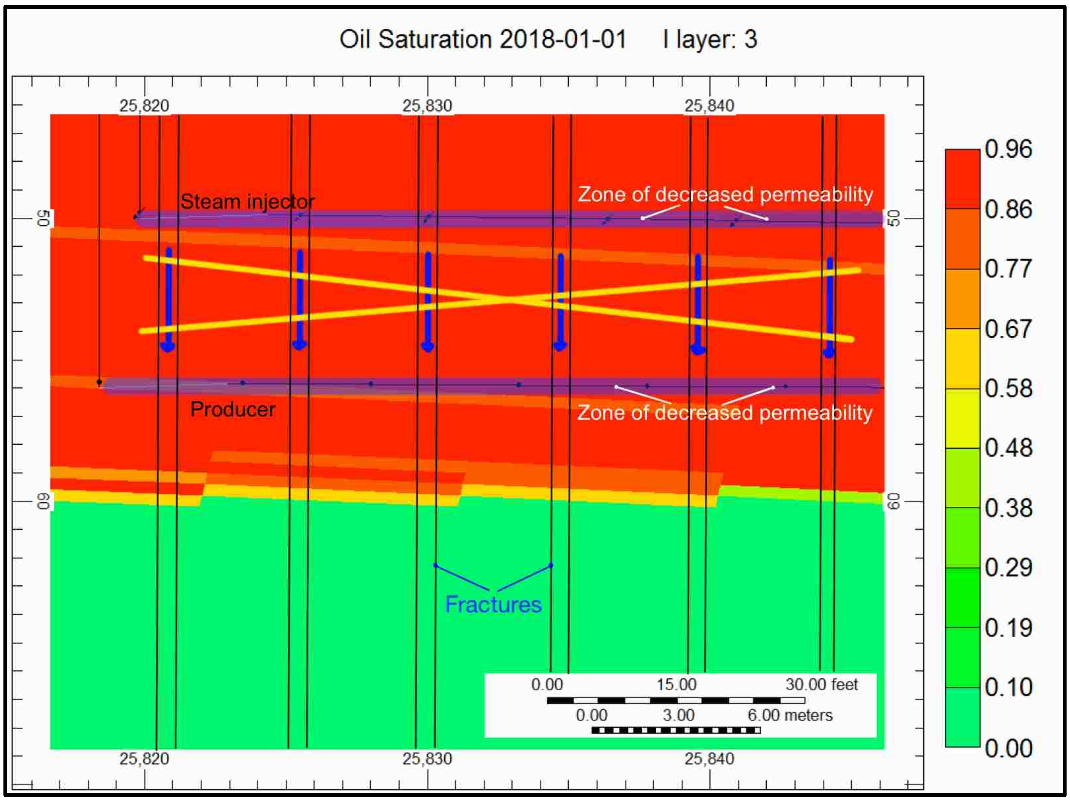
Oil Saturation 2018-01-01 I layer: 3
25,820
25,830
25,840
50
60
Steam injector
Zone of decreased permeability
Producer
Zone of decreased permeability
Fractures
0.00
15.00
30.00 feet
0.00
3.00
6.00 meters
0.96
0.86
0.77
0.67
0.58
0.48
0.38
0.29
0.19
0.10
0.00

Figure 42. Thermogel injection into injector and producer well surrounding area to enhance oil recovery

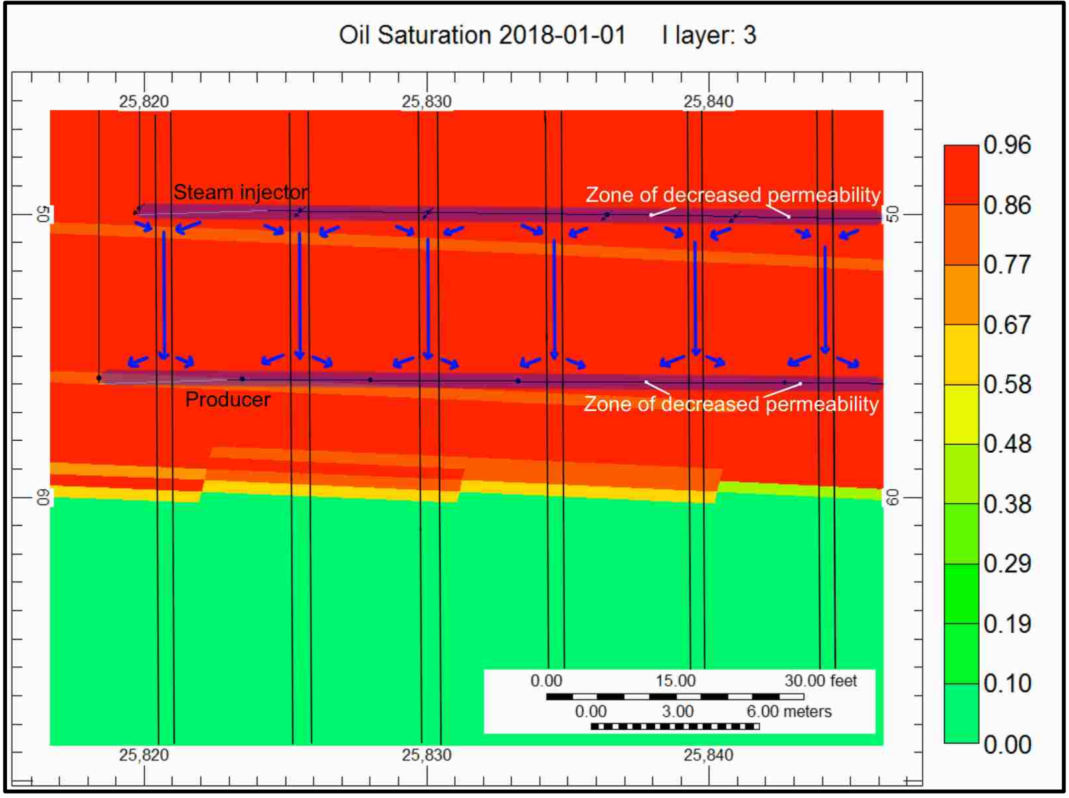
Oil Saturation 2018-01-01 I layer: 3
25,820
25,830
25,840
50
60
Steam injector
Zone of decreased permeability
Producer
Zone of decreased permeability
0.00
15.00
30.00 feet
0.00
3.00
6.00 meters
0.96
0.86
0.77
0.67
0.58
0.48
0.38
0.29
0.19
0.10
0.00

Figure 43. Steam/water movement in a fractured reservoir from thermogel injection

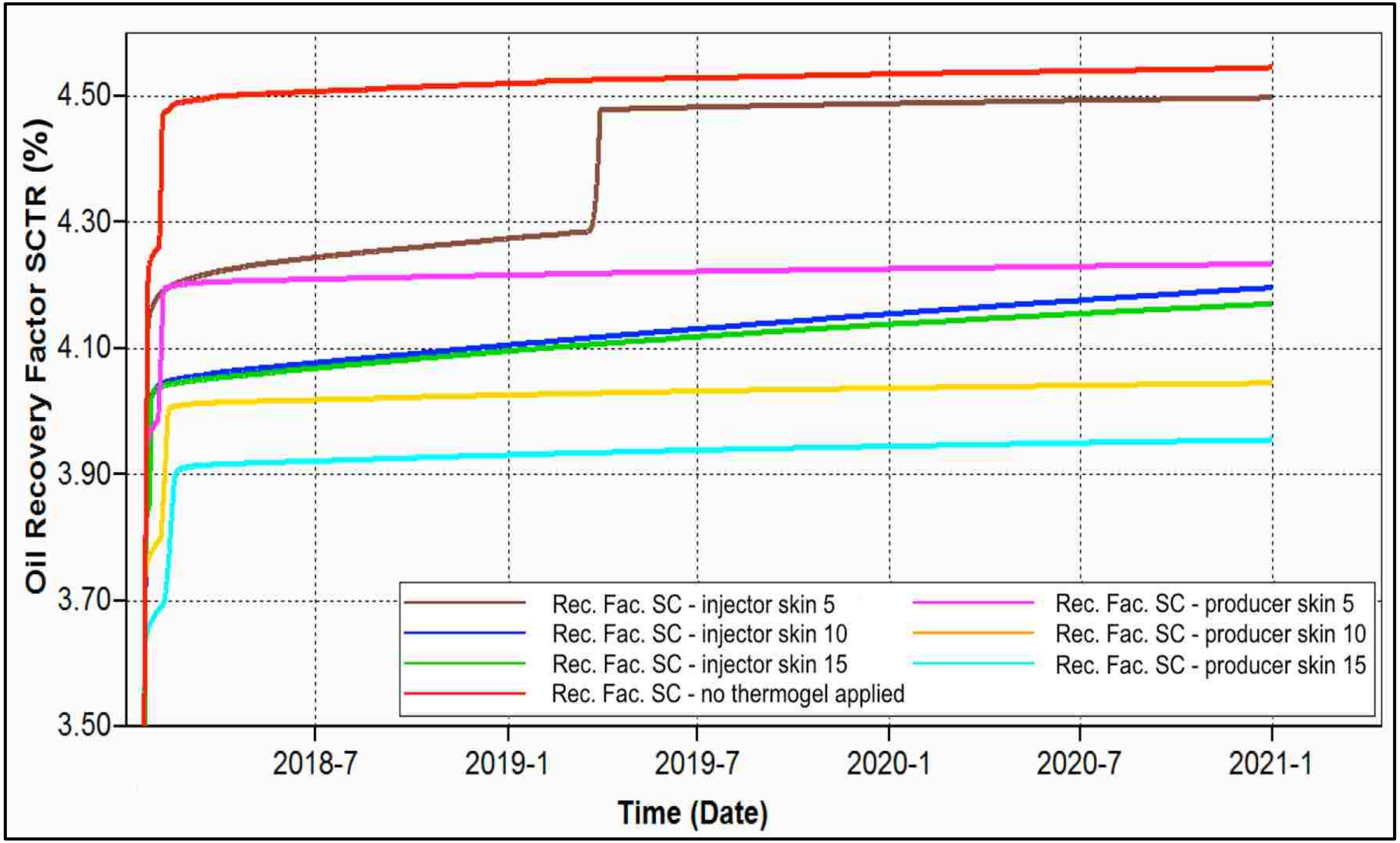
Oil Recovery Factor SCTR (%)
4.50
4.30
4.10
3.90
3.70
3.50
2018-7
2019-1
2019-7
2020-1
2020-7
2021-1
Time (Date)
Rec. Fac. SC - injector skin 5
Rec. Fac. SC - injector skin 10
Rec. Fac. SC - injector skin 15
Rec. Fac. SC - no thermogel applied
Rec. Fac. SC - producer skin 5
Rec. Fac. SC - producer skin 10
Rec. Fac. SC - producer skin 15

[redacted]

Since thermogel injection into the zone next to injector or producer does not allow to avoid the risk of steam breakthrough, the next test included the assessment of thermogel injection occupying the entire zone of between the wells in SAGD pair (figure 45). For this test, the permeability of the zone occupied by thermogel was set to be 10 times smaller (for both matrix and fractures). It was observed that thermogel did not allow to avoid steam breakthrough but considerable impeded steam propagation throughout the reservoir, which resulted in lower recovery when thermogel was applied.

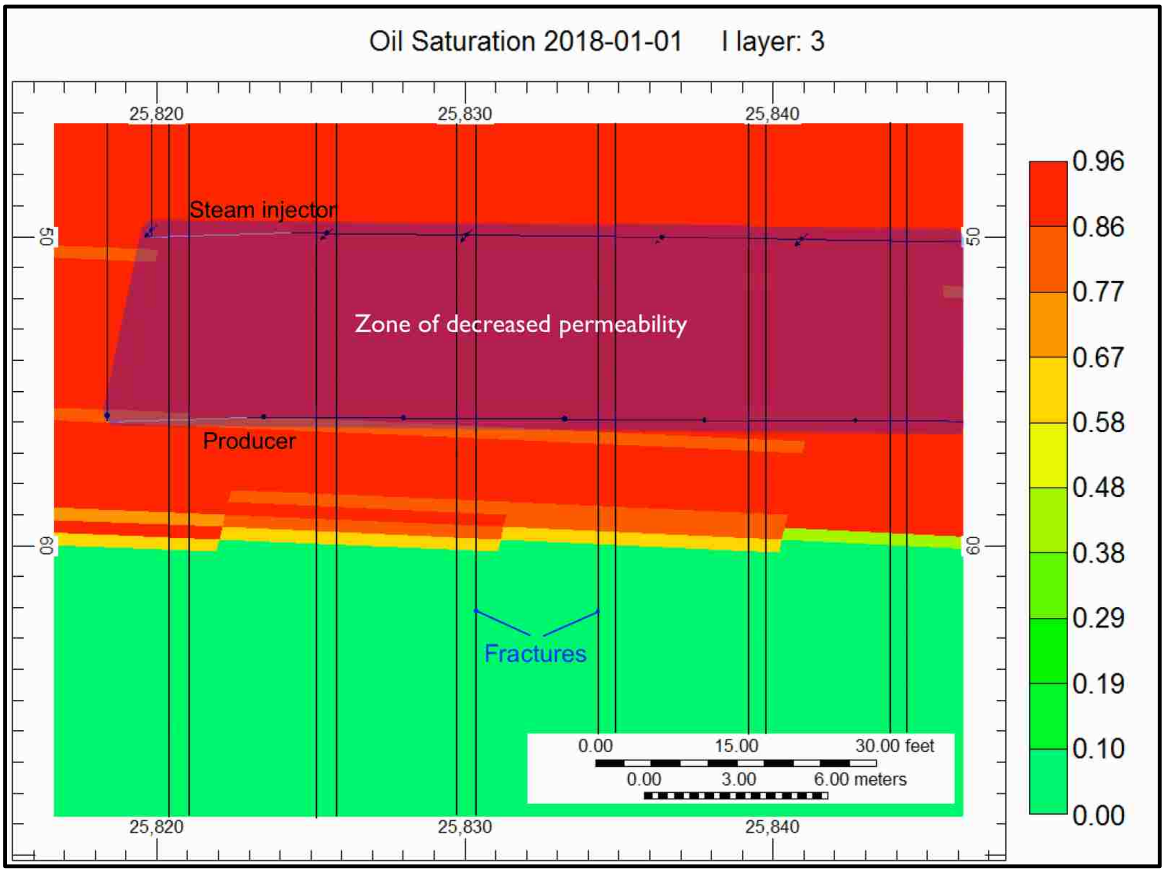

Figure 45. Visual representation of thermogel injection into the entire zone between wells in SAGD pair

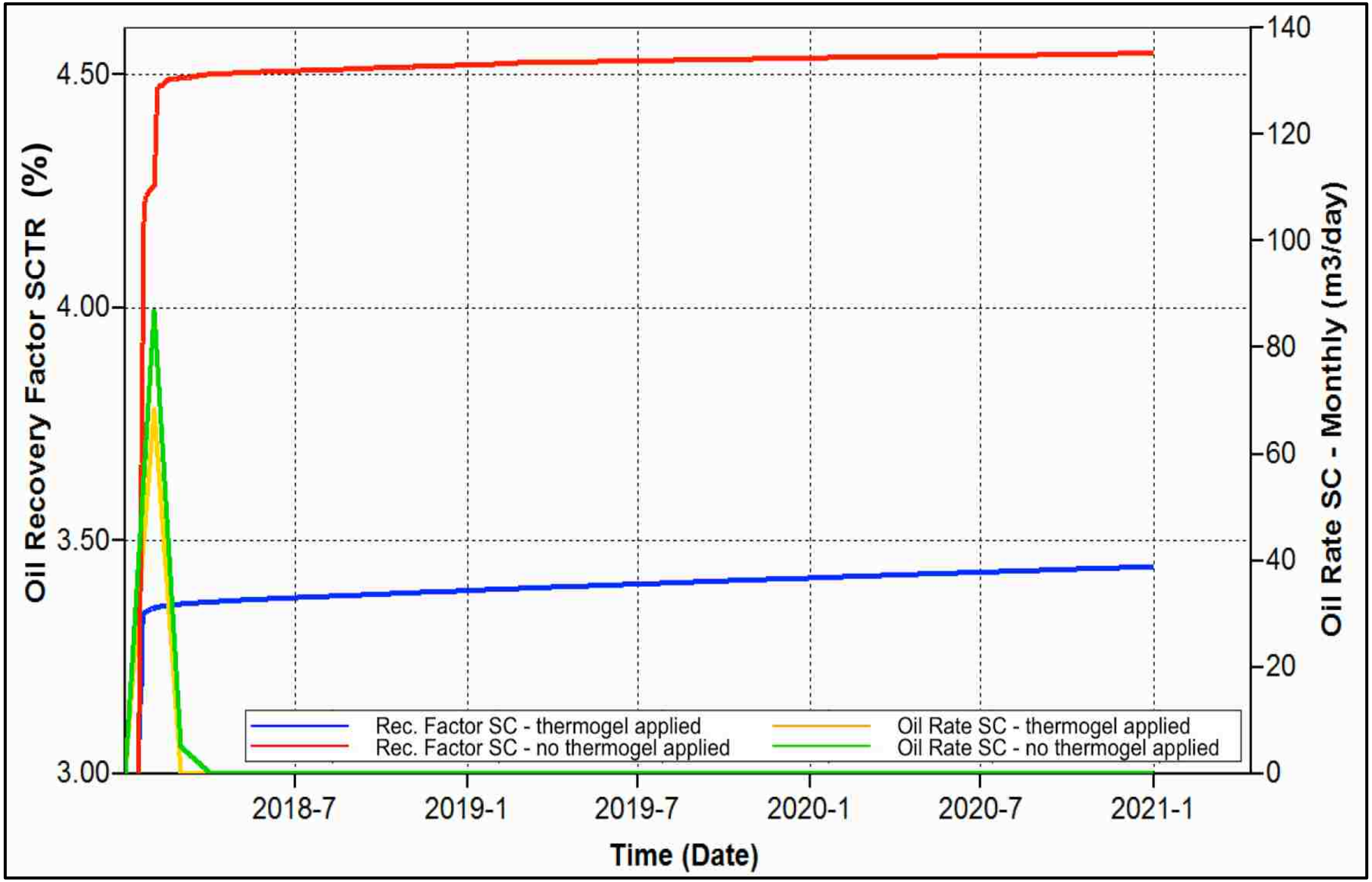
Oil Recovery Factor SCTR (%)
4.50
4.00
3.50
3.00
Oil Rate SC - Monthly (m3/day)
140
120
100
80
60
40
20
0
2018-7
2019-1
2019-7
2020-1
2020-7
2021-1
Time (Date)
Rec. Factor SC - thermogel applied
Rec. Factor SC - no thermogel applied
Oil Rate SC - thermogel applied
Oil Rate SC - no thermogel applied

[redacted]

Once the reservoir simulation was validated, different development scenarios were tested.

We considered the effect of three additional producers above the injector (figure 47). It was observed that oil flow into three upper injectors was not considerable in comparison with the lower SAGD well. Though with the presence of additional producers delayed the steam breakthrough (recovery factor curve for the tested model has a higher gradient), they did not contribute to enhancing of oil recovery.

The use of 5 vertical injectors as a different strategy led to immediate steam breakthrough which resulted in poor recovery (figure 48).

Additionally, instead of 5 vertical injectors, 5 horizontal injectors were tested (figure 49). The result was similar to the previous test – immediate steam breakthrough and correspondingly low oil recovery.

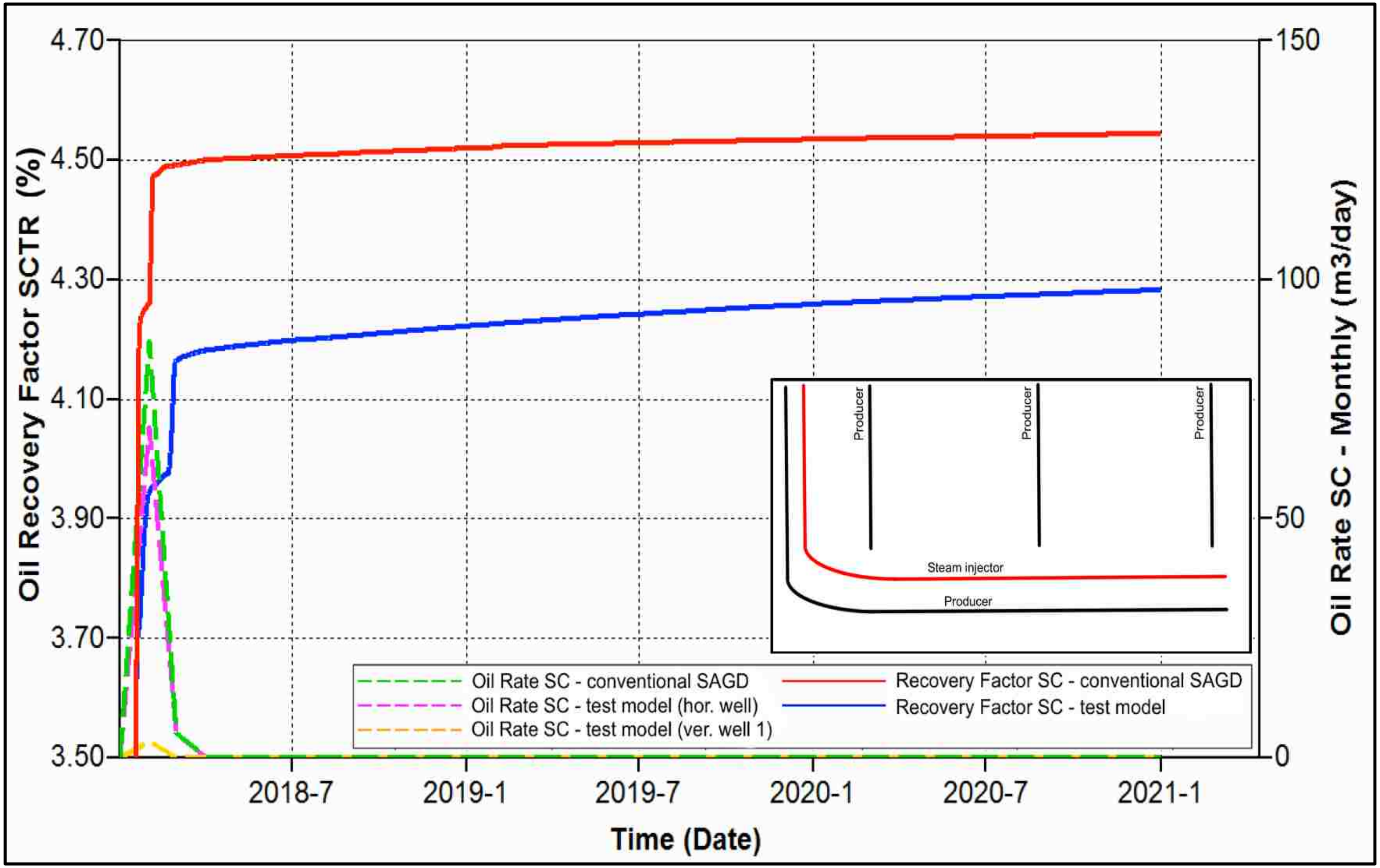
Oil Recovery Factor SCTR (%)
4.70
4.50
4.30
4.10
3.90
3.70
3.50
Oil Rate SC - Monthly (m3/day)
150
100
50
0
2018-7
2019-1
2019-7
2020-1
2020-7
2021-1
Time (Date)
Producer
Producer
Producer
Steam injector
Producer
Oil Rate SC - conventional SAGD
Oil Rate SC - test model (hor. well)
Oil Rate SC - test model (ver. well 1)
Recovery Factor SC - conventional SAGD
Recovery Factor SC - test model

[redacted]

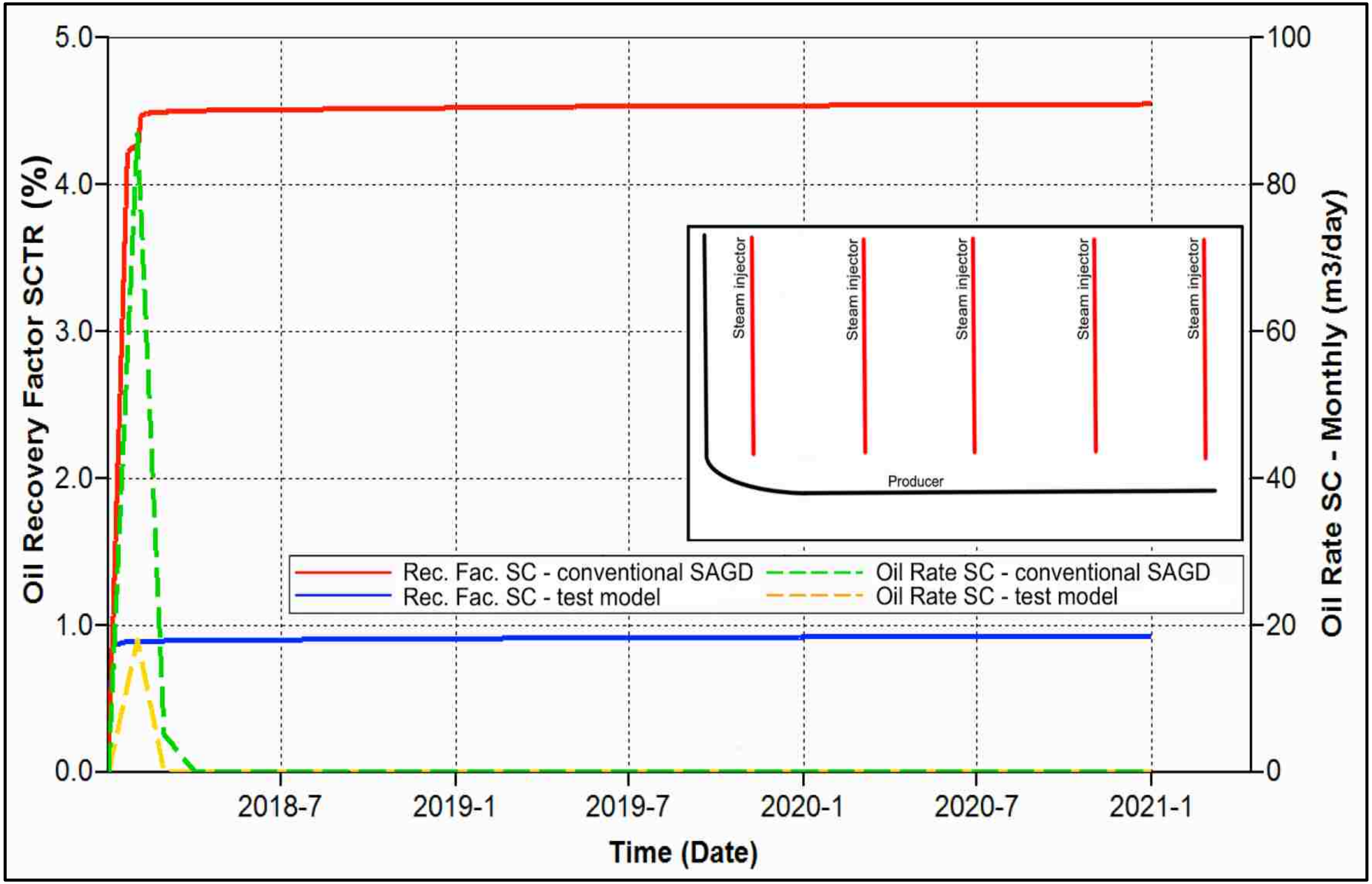
5.0
4.0
3.0
2.0
1.0
0.0
Oil Recovery Factor SCTR (%)
100
80
60
40
20
0
Oil Rate SC - Monthly (m3/day)
2018-7
2019-1
2019-7
2020-1
2020-7
2021-1
Time (Date)
Steam injector
Steam injector
Steam injector
Steam injector
Steam injector
Producer
Rec. Fac. SC - conventional SAGD
Rec. Fac. SC - test model
Oil Rate SC - conventional SAGD
Oil Rate SC - test model

[redacted]

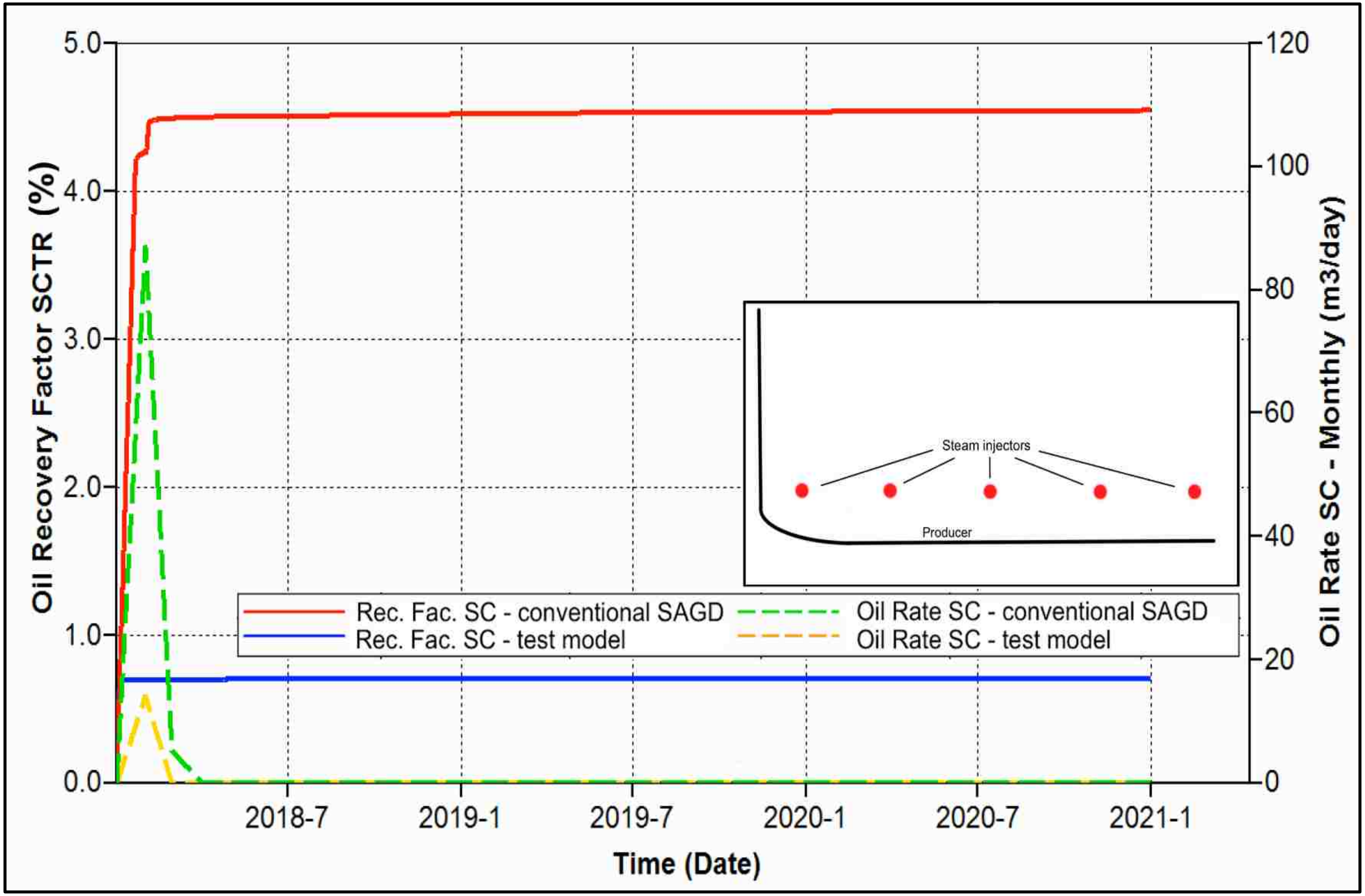
Oil Recovery Factor SCTR (%)
5.0
4.0
3.0
2.0
1.0
0.0
Oil Rate SC - Monthly (m3/day)
120
100
80
60
40
20
0
2018-7
2019-1
2019-7
2020-1
2020-7
2021-1
Time (Date)
Steam injectors
Producer
Rec. Fac. SC - conventional SAGD
Rec. Fac. SC - test model
Oil Rate SC - conventional SAGD
Oil Rate SC - test model

[redacted]

Irrespective of the different SAGD configurations tested, we were unable to increase recovery because in reservoir N, the fractures generated early steam breakthrough in all cases. Therefore, cyclic steam injection was considered next using however existing paid of SAGD wells.

The length of steam injection, soaking and production was varied from 20, 10 and 30 days respectively. However, in comparison with usual continuous steam injection, results from CSS did not indicate enhanced oil recovery. After 6 cycles, oil recovery was only 0.95% (figure 50).

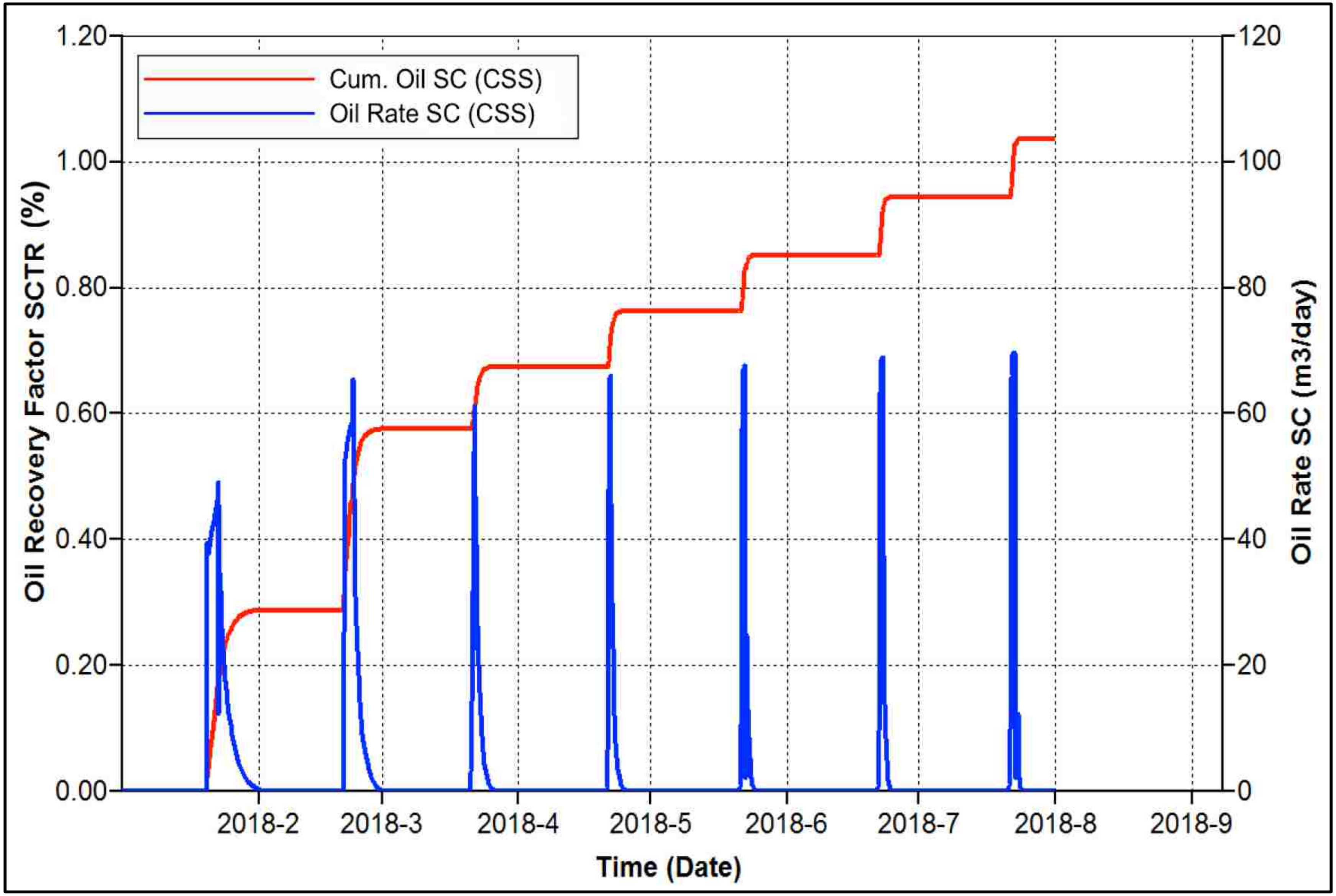
Cum. Oil SC (CSS)
Oil Rate SC (CSS)
Oil Recovery Factor SCTR (%)
1.20
1.00
0.80
0.60
0.40
0.20
0.00
Oil Rate SC (m3/day)
120
100
80
60
40
20
0
2018-2
2018-3
2018-4
2018-5
2018-6
2018-7
2018-8
2018-9
Time (Date)

[redacted]

Interestingly however, despite low oil recovery, CSS did not contribute to early steam breakthroughs as in continuous steam injection where the producer needed to be abandoned as a result, and new wells drilled. CSS will give low recovery, but over longer term can add to high volumes, and the cost and expenses associated with new wells will not need to be considered.

It is important to recall, that other part (sector 1) of Yarega oilfield is developed using thermomining techniques. From the mine corridors, the producer and injector wells are drilled into the formation with bottomholes being generally higher than wellheads in order to use the gravity to enhance oil recovery. Based on previously conducted numerical simulations, these techniques allowed to reach high oil recovery factors (up to 45% within 4 years). It is fair to assume that the same technique would efficiently work in reservoir N. However, building mine shafts and corridors is economically unattractive and can hardly be done nowadays.

We then tested a fishtail wellbore design for cyclic steam stimulation to see if that would increase recovery due to intersecting steam chambers, and increased sweep. The building of a fishtail well has two stages: (1) drilling a horizontal well in the lower part of the reservoir that will work as conduit that will transmit the fluid from the branches to the surface, (2) drilling fishtail branches at the elevated angles from the horizontal well to allow the use of gravitational forces. The branches are suggested to be drilled interchangeably to the left and right from the horizontal well under acute angles to penetrate and sweep the maximum possible volume of the formation. Once the fishtail well is drilled, a widely-known cyclic steam stimulation should be implemented to use the main well.

We ran 5 different fishtail scenarios for 3-year forecasting simulation runs with various lengths of injection, soaking and production periods (figure 51). The highest recovery was obtained in the case of 10-day long steam injection, 10-day long soaking period and 10-day long production period. After 3 years of development, it resulted in 7% recovery. In comparison we had only 4.5% from continuous steam injection using SAGD wells that is currently implemented in the reservoir N. The fish-tailed well scheme also avoided steam breakthrough as seen from simulation results (figure 51). After 3 years of CSS, cumulative steam/oil ratio (SOR) was 8 m^3/m^3, however after 3 years, the values of cumulative SOR started to decrease (figure 52). The decrease in cumulative SOR started along with increase of steam chamber volume. Since the initial temperature of the reservoir is very low (8 °C), during the first years of injection, all the steam was immediately condensed which did not allow the steam chamber to be generated. After 3 years, the average temperature of the reservoir reached 30 °C which permitted generation of a large steam chamber. Once the steam chamber appeared and started growing, we can observe a significant increase of the trend of recovery factor (red line). The last simulation was conducted for 4.5 years and could not be run for a longer time due to computational limits.

Based on all the different development scenarios tested, results from this research indicates that the use of a fishtail well design to the current development of reservoir N in the YHOF may improve recovery and cumulative oil production. However, an economic analysis will be needed to determine if this scheme can be implemented in a pilot study (as in sector model in reservoir N) prior to full field implementation.

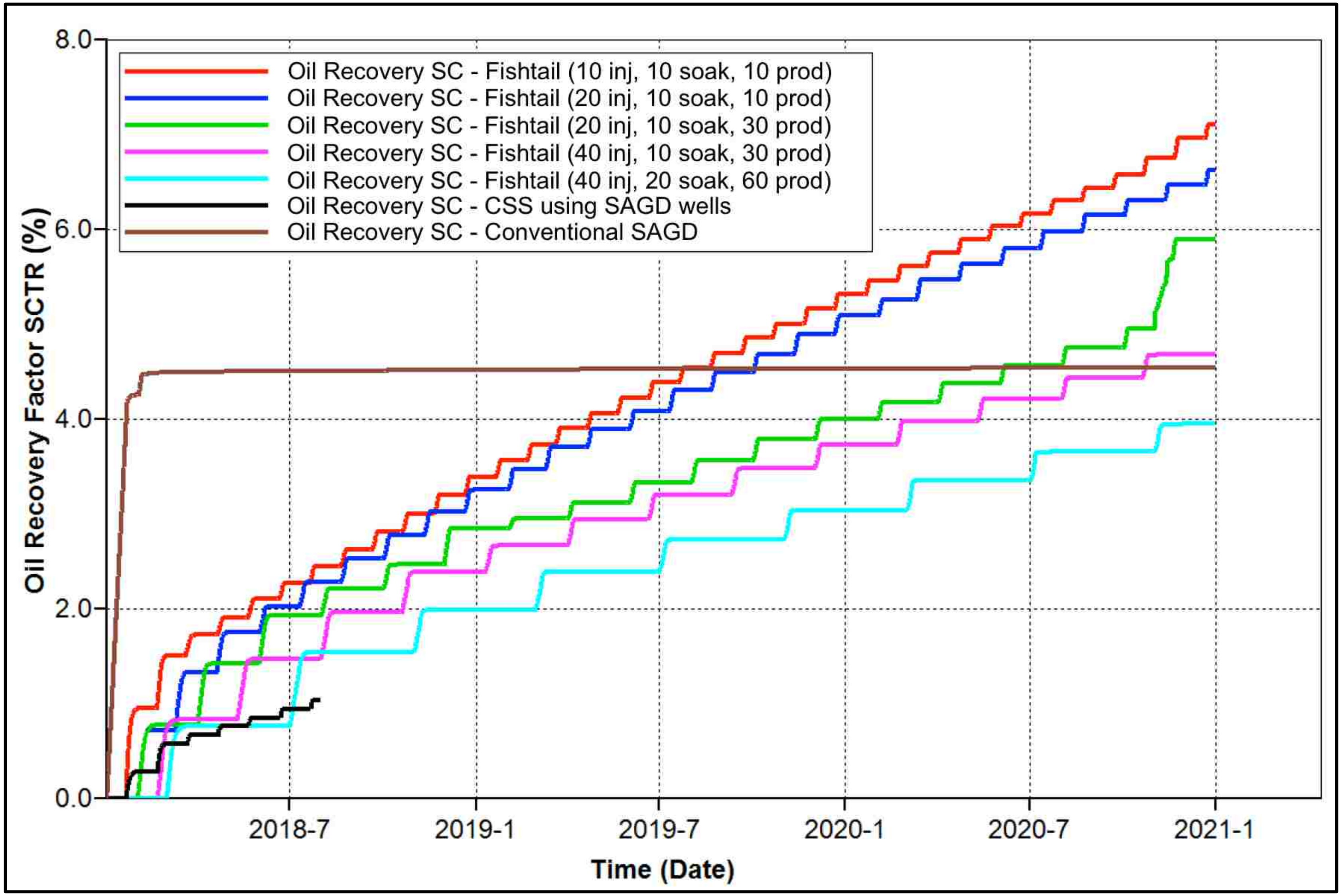
Oil Recovery SC - Fishtail (10 inj, 10 soak, 10 prod)
Oil Recovery SC - Fishtail (20 inj, 10 soak, 10 prod)
Oil Recovery SC - Fishtail (20 inj, 10 soak, 30 prod)
Oil Recovery SC - Fishtail (40 inj, 10 soak, 30 prod)
Oil Recovery SC - Fishtail (40 inj, 20 soak, 60 prod)
Oil Recovery SC - CSS using SAGD wells
Oil Recovery SC - Conventional SAGD
Oil Recovery Factor SCTR (%)
8.0
6.0
4.0
2.0
0.0
2018-7
2019-1
2019-7
2020-1
2020-7
2021-1
Time (Date)

[redacted]

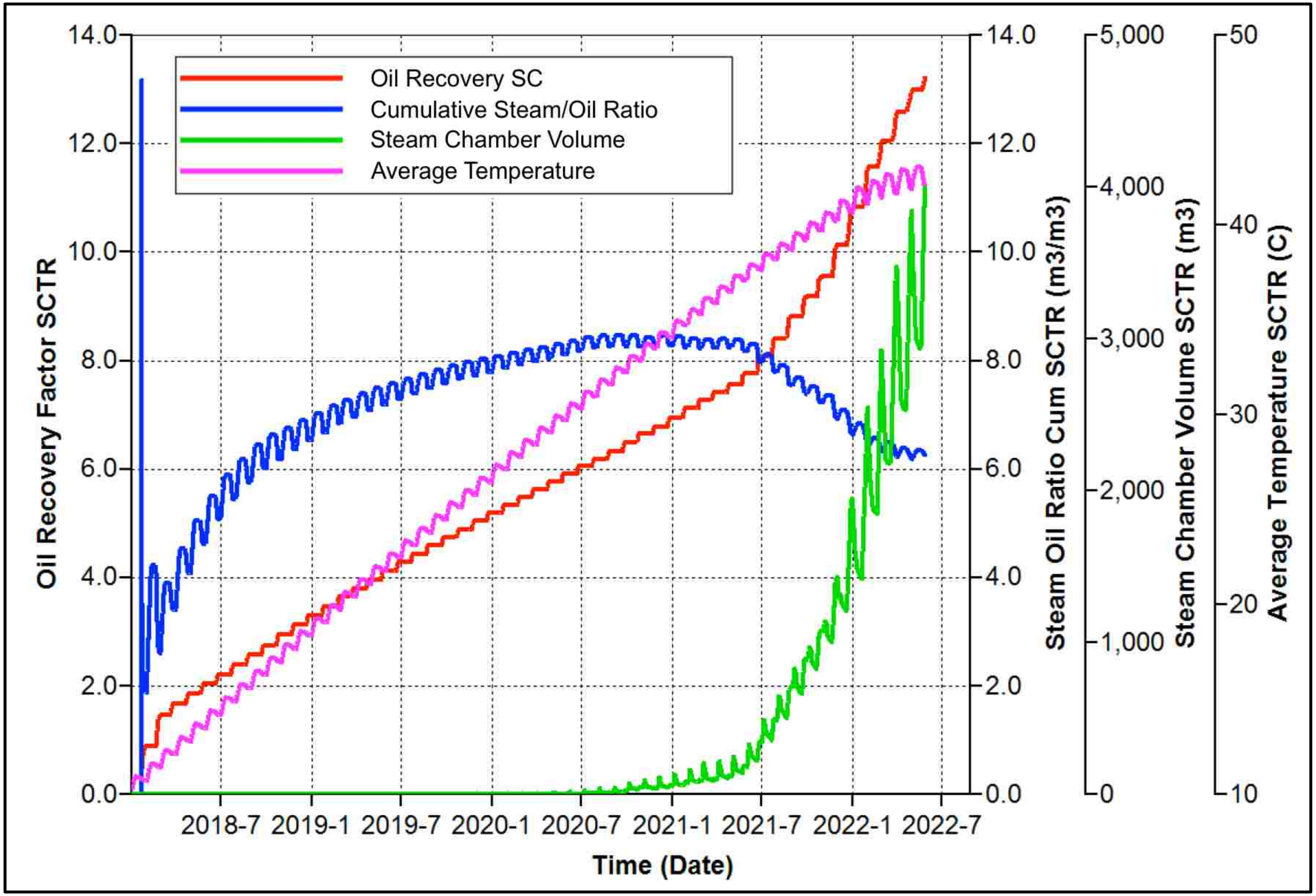
Oil Recovery Factor SCTR
14.0
12.0
10.0
8.0
6.0
4.0
2.0
0.0
Oil Recovery SC
Cumulative Steam/Oil Ratio
Steam Chamber Volume
Average Temperature
2018-7
2019-1
2019-7
2020-1
2020-7
2021-1
2021-7
2022-1
2022-7
Time (Date)
Steam Oil Ratio Cum SCTR (m3/m3)
Steam Chamber Volume SCTR (m3)
5,000
4,000
3,000
2,000
1,000
0
Average Temperature SCTR (C)
50
40
30
20
10

[redacted]

CHAPTER 7: EFFICIENCY VALIDATION OF FISHTAIL WELL DESIGN BASED ON HISTORY MATCHED DATA

The purpose of this chapter is to conduct an additional validation of “fishtail” well design efficiency based on history matched data. We used a real sector X of YHOF with a pair of real SAGD wells located in this sector (figures 53-55). SAGD wells in sector X are drilled from different locations and create so-called “opposing SAGD” well arrangement. Distance between the wells in vertical direction varies from 6 to 10 meters. Also, there is a fault that crosses the sector in diagonal direction. Distance between up-thrown and downthrown parts vary from 5 to 15 meters. The sector includes additional upper and lower shale layers to account for additional heat losses during thermal development. Length of the sector is approximately 1200 meters and width is 300 meters respectively. Sector is broken into 212256 blocks having dimensions 20 x 20 x 0.5 meters. For each block, oil saturation, porosity and permeability parameters were provided. PVT parameters of oil were identical to the oil located in this reservoir and were obtained during drilling of the SAGD pair. This sector contained geologic parameters related only to the first media (matrix) whereas parameters for secondary media (fractures) were unknown and required determination during history matching.

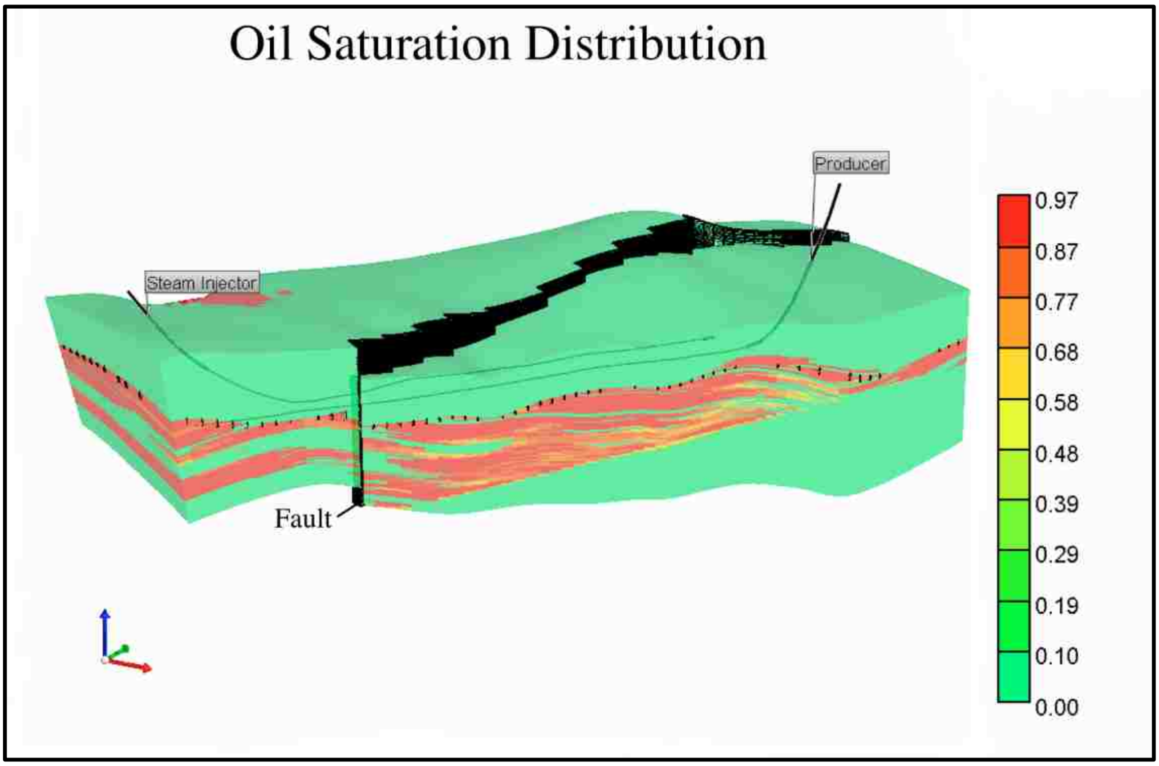
Oil Saturation Distribution
Producer
Steam Injector
Fault
0.97
0.87
0.77
0.68
0.58
0.48
0.39
0.29
0.19
0.10
0.00

Figure 53. Oil saturation distribution of sector X of YHOF

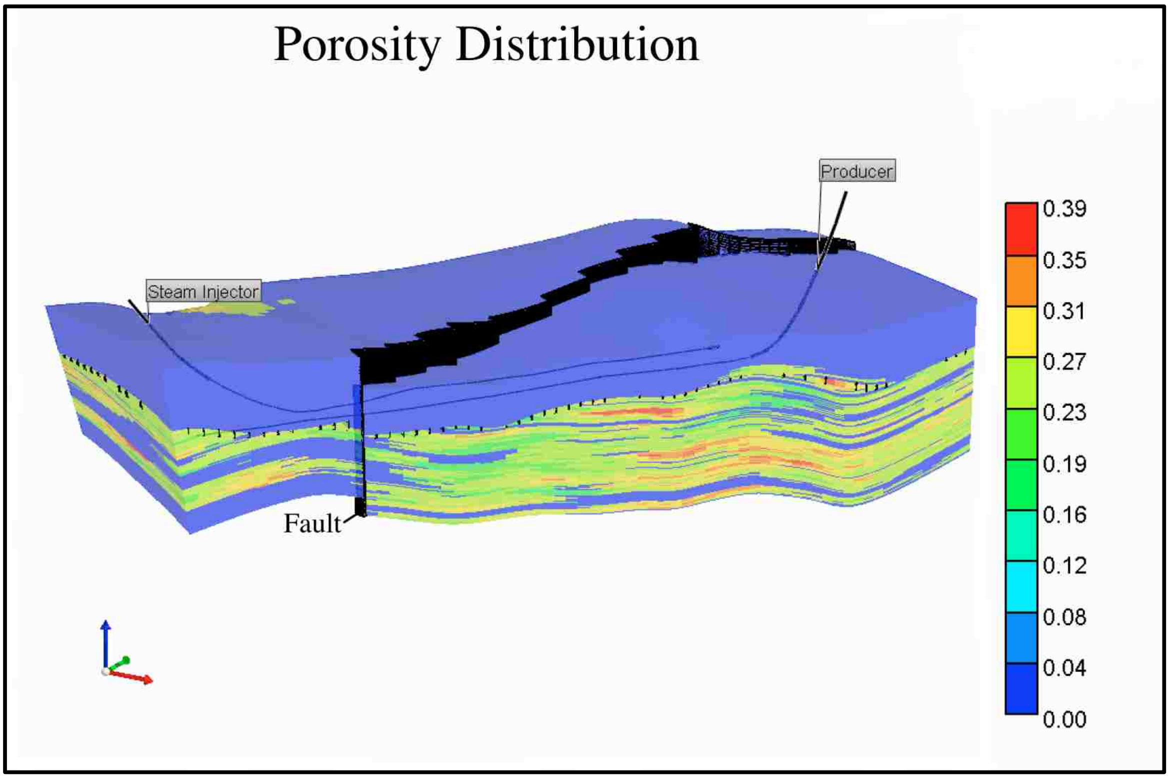
Porosity Distribution
Producer
Steam Injector
Fault
0.39
0.35
0.31
0.27
0.23
0.19
0.16
0.12
0.08
0.04
0.00

Figure 54. Porosity distribution of sector X of YHOF

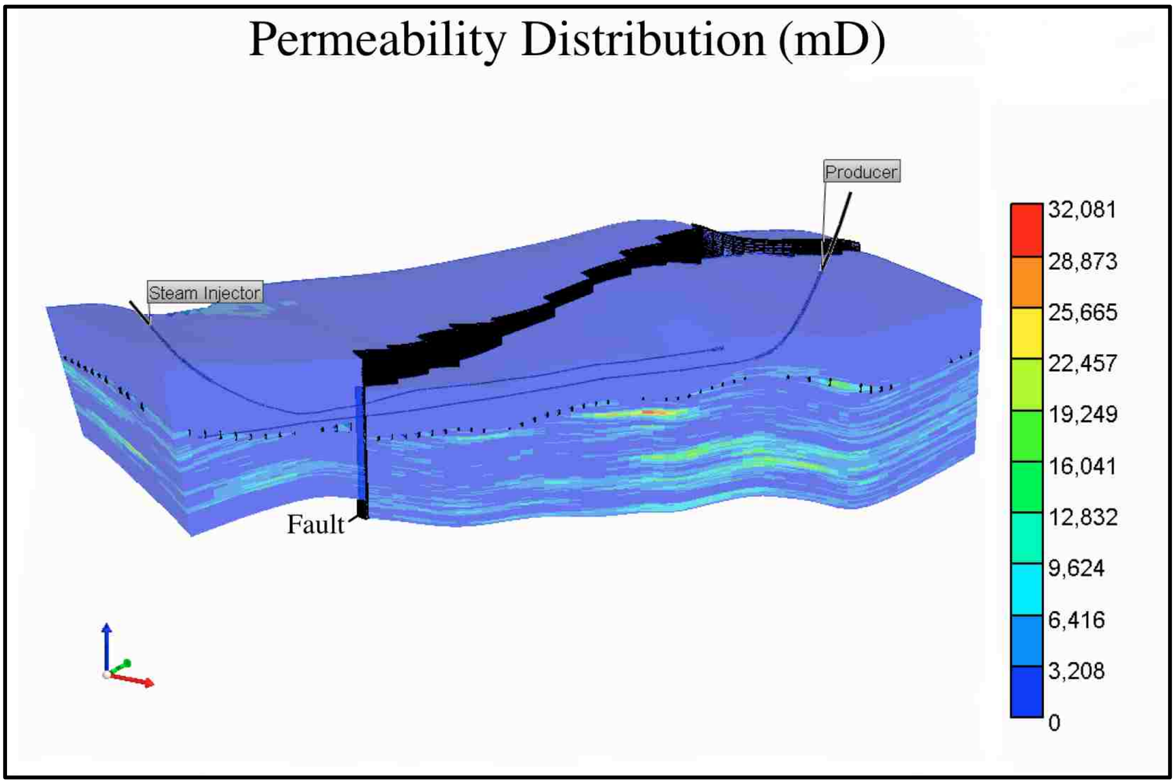
Permeability Distribution (mD)
Producer
Steam Injector
Fault
32,081
28,873
25,665
22,457
19,249
16,041
12,832
9,624
6,416
3,208
0

Figure 55. Permeability distribution of sector X of YHOF

7.1 History matching procedure

To history match the data, we used well history data that included event history for injector and producer wells in SAGD pair. For injector well we used such parameters as steam quality, pressure and temperature of steam injection and average monthly water rate used for steam generation. For producer well we used cumulative oil and water monthly production history and constraints related to minimum bottom-hole pressure and maximum daily liquid rate. Please note that none of the figures showing real history technological parameters have volume specification and show only parameter profile due to confidentiality of the data (figures 56-59).

Injector well history data was specified as an input parameter in the simulator, however necessary injectivity of the model required for providing injection volumes of water in the form of steam was obtained only after introducing secondary media in the simulator (dual porosity) with relatively high fracture permeabilities (figure 56).

Presence of highly permeable fractures in the considered sector was proved by tracer tests conducted after drilling of the SAGD pair.

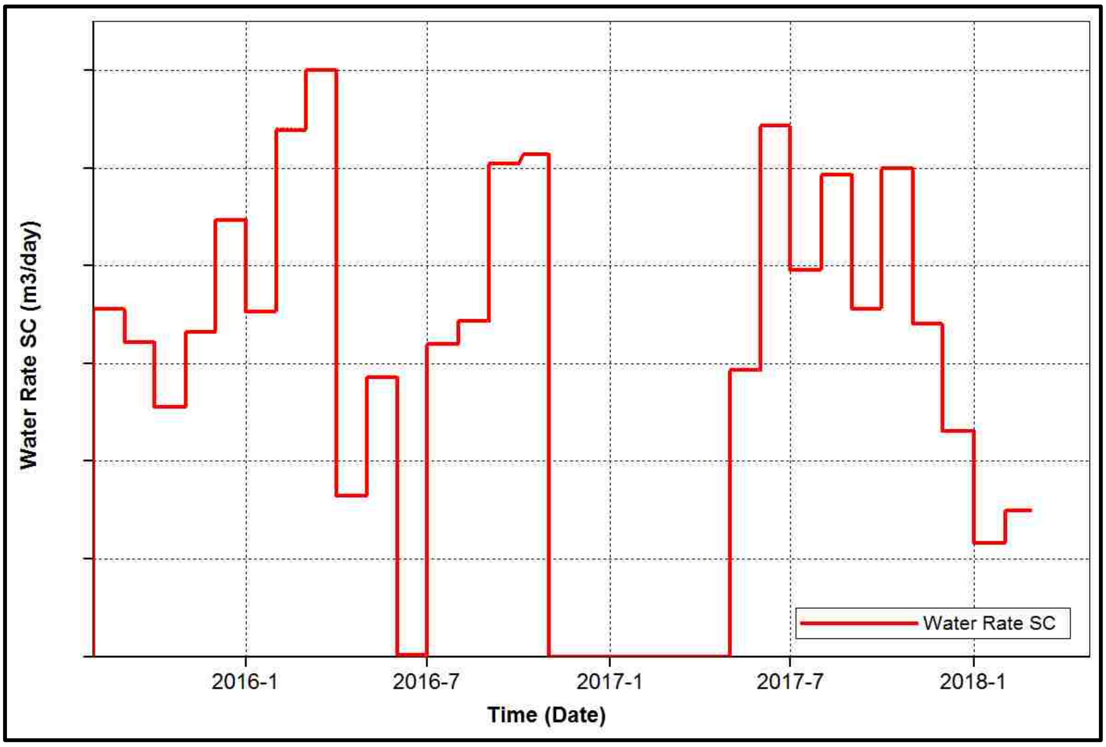

Figure 56. Real monthly steam injection history profile for sector X of YHOF

In order to obtain oil and water production volumes close enough to real data, we changed such parameters of the fractures as fracture permeability and fracture spacing in X, Y and Z direction and fracture porosity. During the history matching process it was observed that fracture permeability and fracture spacing do not have direct relation to oil and water production volumes. This is related to “dual” role of fractures in YHOF: fractures help to distribute steam throughout the reservoir and provide necessary conduits of high permeability for highly viscous oil but also contribute to drastic increase of water cut after the initiation of production and early steam breakthroughs. However, after numerous runs fracture permeability and fracture spacing was indirectly determined. The closest match to real data for cumulative oil and water production is displayed on figure 57. Relative error for both parameters did not exceed 10% and was found to be satisfactory in the conducted history matching process (figures 58-59). Various minor changes of relative permeability curves did not contribute to decrease of the error.

Determination of fracture parameters allowed to obtain sector of YHOF with the most real geological parameters for consecutive validation of fishtail well design hypothetically implemented in this sector.

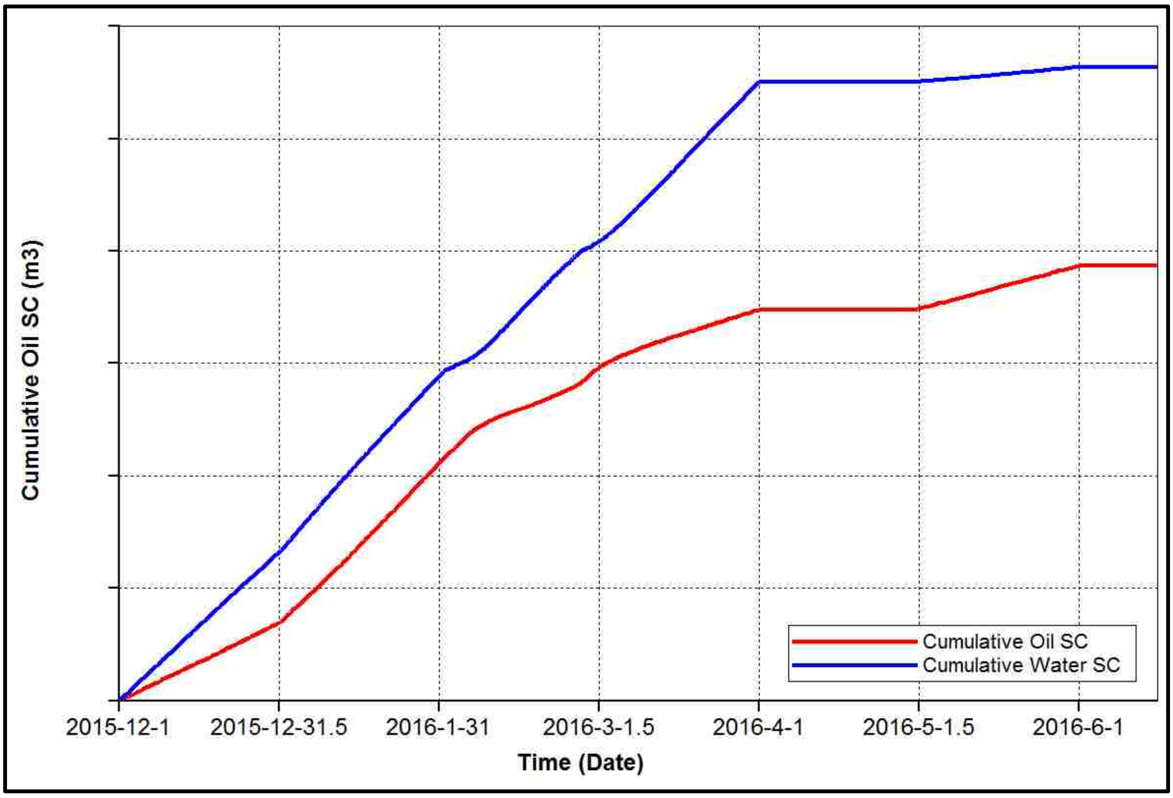

Figure 57. Oil and water production profile that provides the best match with real data

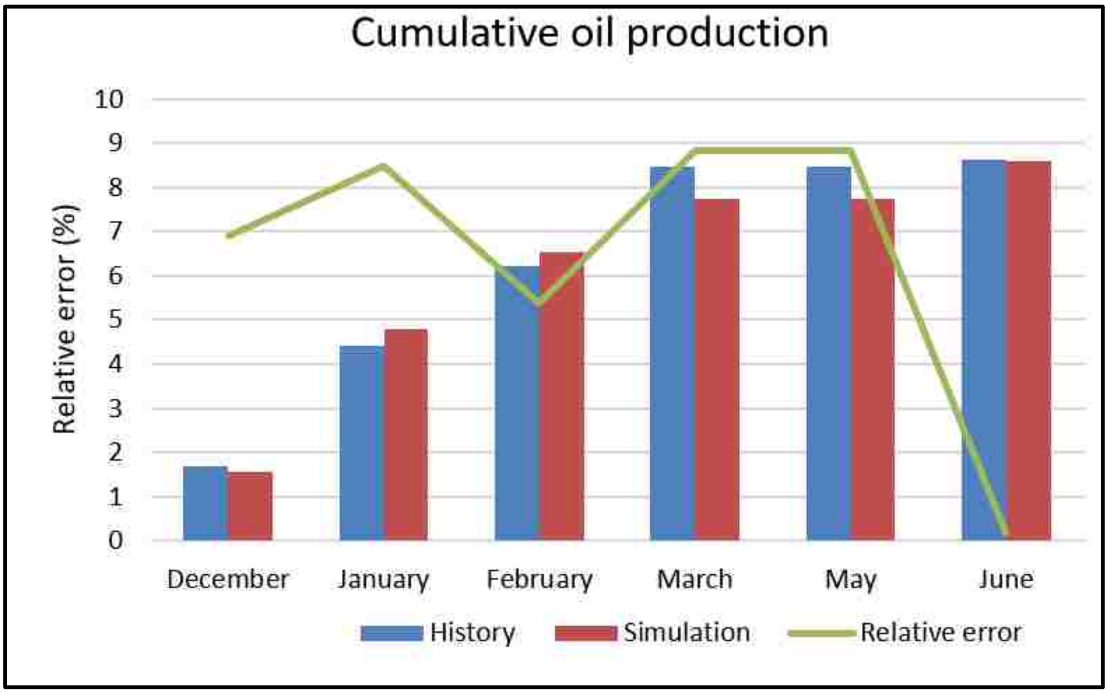

Figure 58. History matching errors for cumulative oil production for sector X of YHOF

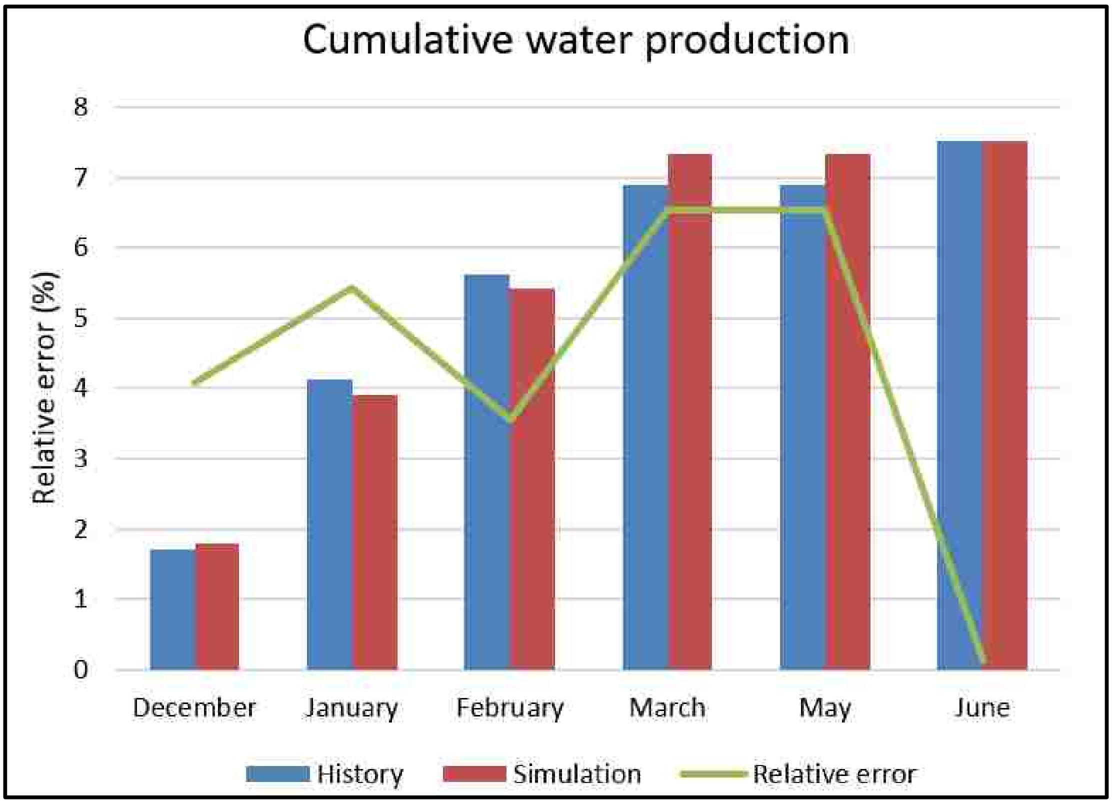

Figure 59. History matching errors for cumulative water production for sector X of YHOF

Fishtail well design was implemented in the history matched sector X of YHOF (figure 60). Fishtail configuration was chosen similar to the one described earlier in this thesis work with four lateral branches extended to the left and right from the well stem. Branches had vertical elevation and horizontal extension in order to “sweep” the maximum possible volume of the reservoir. Generally, branches were chosen to extend vertically up to 5 meters from the upper reservoir boundary. In this simulation, previous location of producer well in SAGD pair (from real data) was picked to be the stem of fishtail well as if a fishtail well was drilled from earlier constructed horizontal well.

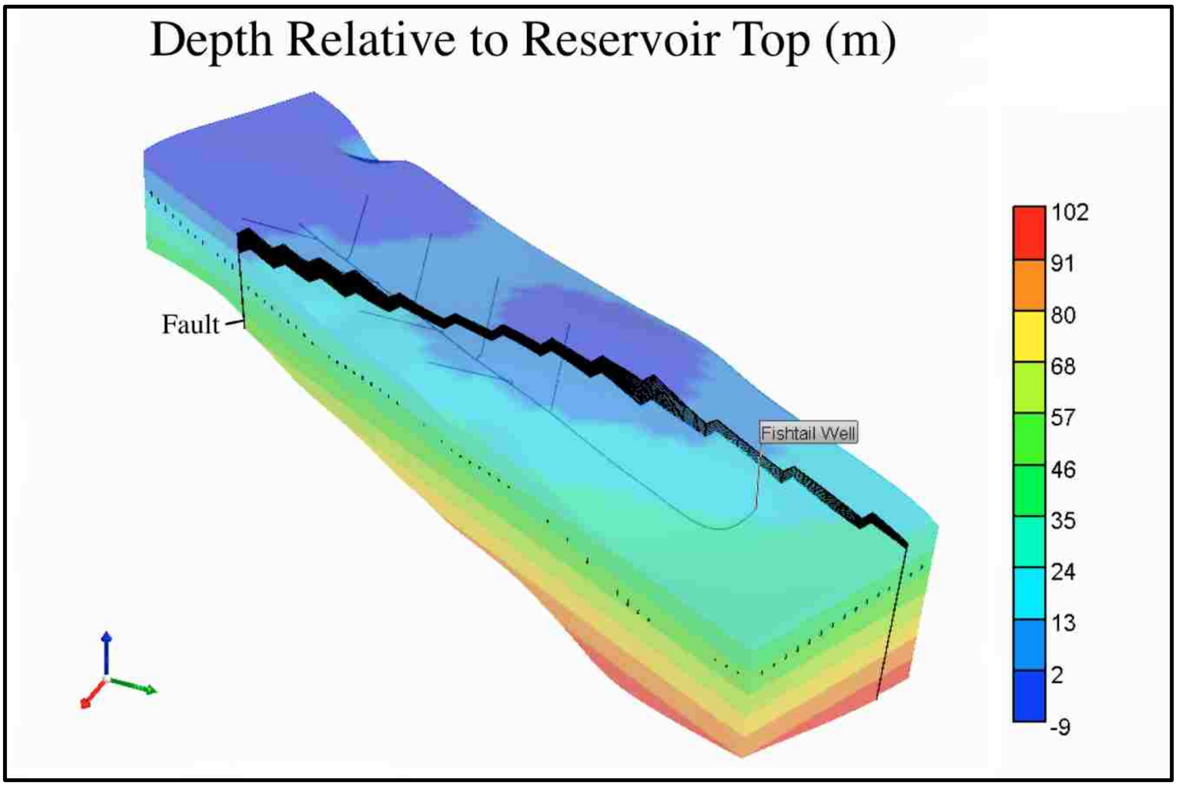

Figure 60. Fishtail well design implemented in sector X of YHOF

Fishtail well design showed to be the most effective development strategy while implemented with cyclic steam stimulation according to results from chapter 6 in this work. Thereby, for validation of fishtail well design efficiency the same development scenario was chosen (CSS). Cycles consisted of injection, soaking and production periods so that relative lengths of the periods were 2:1:3. Three different lengths of a complete cycle (one cycle of injection, one cycle of soaking and one cycle of production) were considered: 4, 2 and 1 month.

Thereby, for 4 month long complete cycle, injection period composed to be 40 days, soaking period – 20 days and production period – 60 days. For 2 month long complete cycle, injection period composed to be 20 days, soaking period – 10 days and production period – 30 days. For 1 month long complete cycle, injection period composed to be 10 days, soaking period – 5 days and production period – 15 days.

Fishtail well design with cyclic steam stimulation was compared with SAGD with simultaneous continuous steam injection and oil production from two wells. Despite the implementation of a supercomputer for calculation of the model, presence of a secondary media and a large number of blocks significantly increase computational time. For example, simulation of 1 year of fishtail well required more than 12 hours for Mike 2 with implemented parallel processing. Simulation of fishtail models for longer periods than 1 year was impossible due to complication related to convergence errors.

However, for the simulated period superiority of a fishtail well design with CSS over conventional SAGD is obvious. Thereby, oil production using fishtail well with 4-long complete cycle regime (40/20/60) first time exceeds cumulative oil production from SAGD wells in 210 days after initiation of development (point C). For 2-month long complete cycle, cumulative oil production first time exceeds oil production from SAGD wells in 114 days (point B). For 1-month long complete cycle, cumulative oil production first time exceeds oil production from SAGD wells in 55 days (point A), during the second complete cycle (figure 61).

Separate attention should be paid to parameter, related to economic assessment of feasibility of fishtail well design – cumulative steam oil ratio. During the considered period, cumulative steam/oil ratio for 4-month long cycle fishtail well never exceeds 2 (figure 62). Peak at 2015/10/01 is caused by “division by zero”, since some volume of steam has already being injected but no oil produced, and therefore entire fraction goes to infinity. After one year of development using fishtail well, cumulative steam/oil ratio composes 0.92 which is a good indicator of fishtail well efficiency. At the same time, after one year of development using SAGD pair, cumulative steam/oil ratio reaches 3.4 and keeps growing.

Also, behavior of water cut trend demonstrates a more effective development during fishtail well implementation (figure 63). Thus, during the first 3 cycles using fishtail well, water cut composes 50-70% (green lines indicate average water cut within the cycle). Water cut that can be observed during SAGD composes 84% after 1 year of development.

Based on information provided earlier, we can recommend fishtail well design with cyclic steam stimulation as a more effective alternative for the considered sector of YHOF.

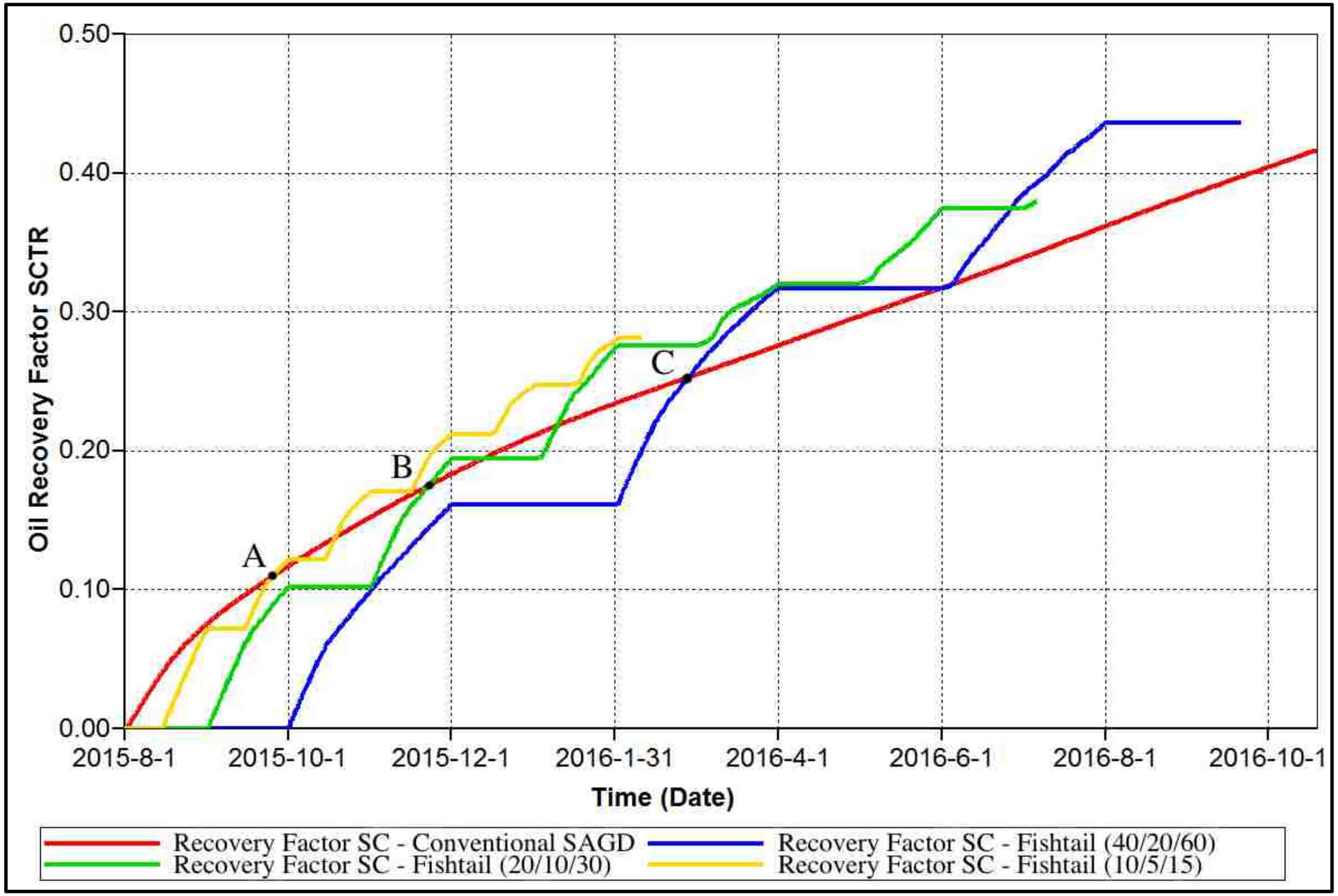
0.50
0.40
0.30
0.20
0.10
0.00
Oil Recovery Factor SCTR
A
B
C
2015-8-1
2015-10-1
2015-12-1
2016-1-31
2016-4-1
2016-6-1
2016-8-1
2016-10-1
Time (Date)
Recovery Factor SC - Conventional SAGD
Recovery Factor SC - Fishtail (20/10/30)
Recovery Factor SC - Fishtail (40/20/60)
Recovery Factor SC - Fishtail (10/5/15)

[redacted]

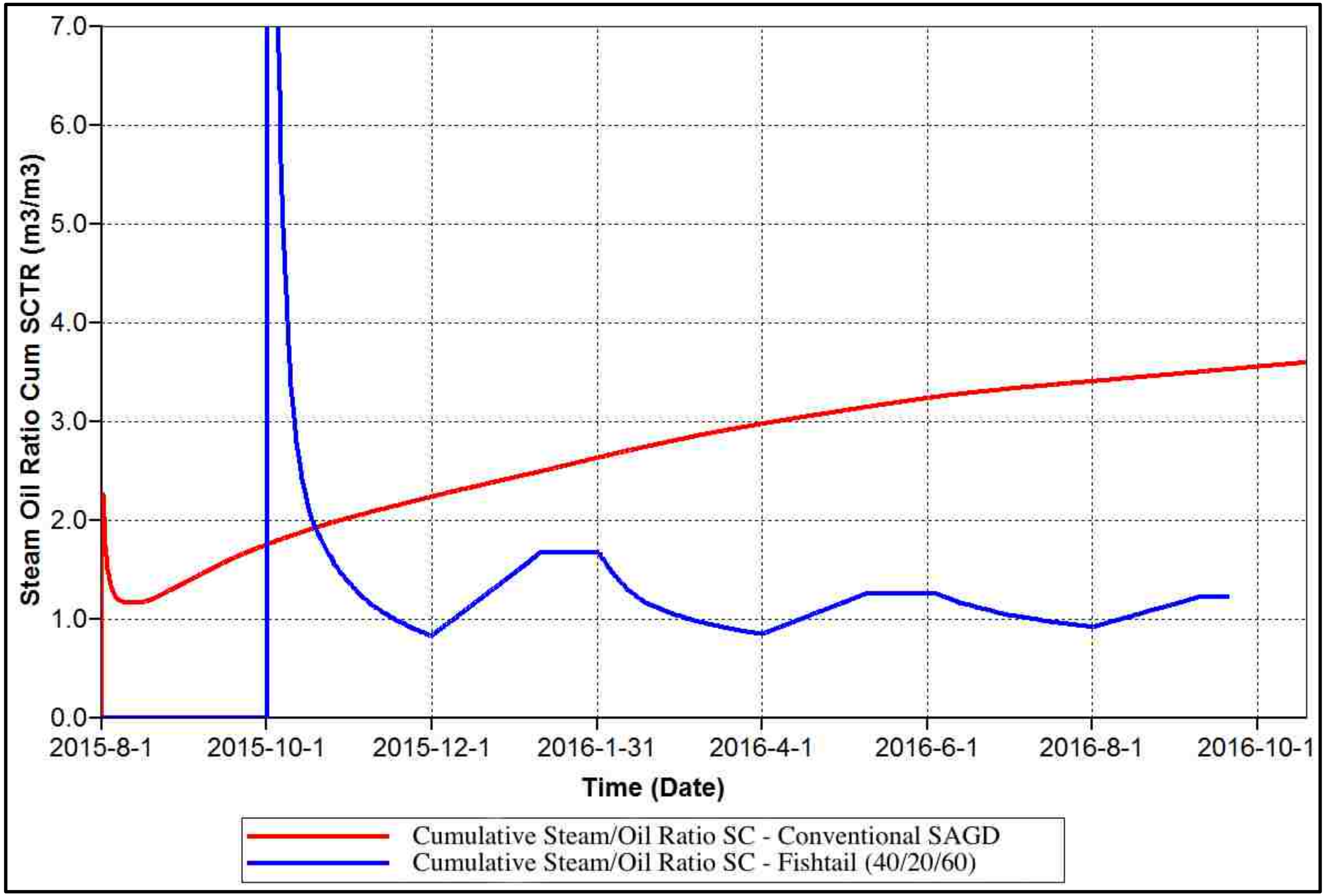
Steam Oil Ratio Cum SCTR (m3/m3)
7.0
6.0
5.0
4.0
3.0
2.0
1.0
0.0
2015-8-1
2015-10-1
2015-12-1
2016-1-31
2016-4-1
2016-6-1
2016-8-1
2016-10-1
Time (Date)
Cumulative Steam/Oil Ratio SC - Conventional SAGD
Cumulative Steam/Oil Ratio SC - Fishtail (40/20/60)

[redacted]

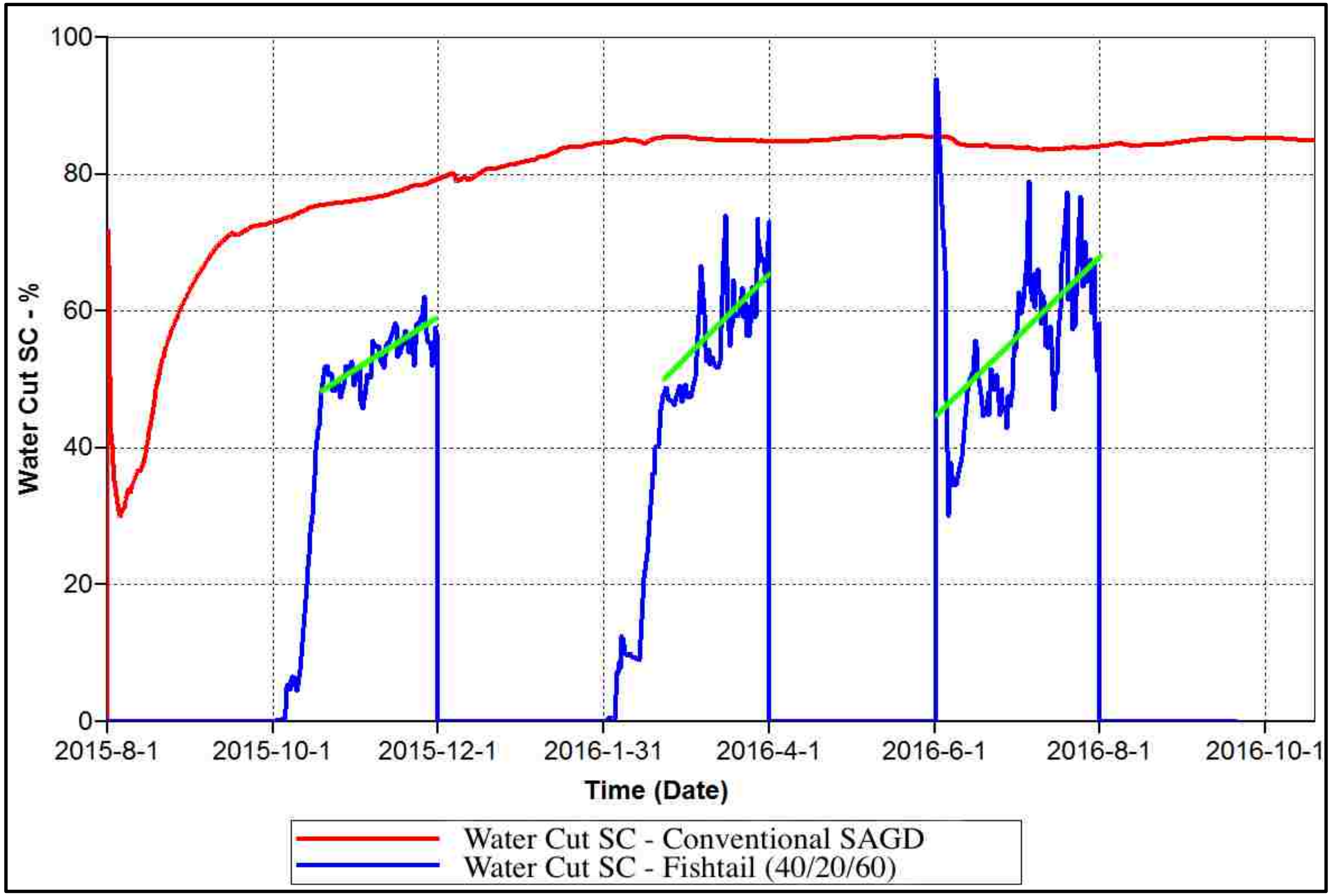
100
80
60
40
20
0
Water Cut SC - %
2015-8-1
2015-10-1
2015-12-1
2016-1-31
2016-4-1
2016-6-1
2016-8-1
2016-10-1
Time (Date)
Water Cut SC - Conventional SAGD
Water Cut SC - Fishtail (40/20/60)

[redacted]

CHAPTER 8. CONCLUSIONS

This research was focused on studying a reservoir “N” in Yarega heavy oilfield (YHOF) for development strategies and production optimization. The primary goal of this research was thus to determine development strategies for reservoir N located in a naturally fractured, heavy oilfield using single, dual porosity and dual permeability models (computational expenses permitting).

Results from this research suggest that steam injection into both the matrix and fractured layers simultaneously was the most effective as the highest amount of heat could be transmitted when the contact between steam and the reservoir rock was the longest.

Increase in fracture permeability resulted in decrease of matrix recovery factor because the fractures acted as permeability super highways within the reservoir. For high-viscosity systems, however, conductive fractures helped distribute heat from the steam throughout the reservoir, and thus the mechanism of matrix recovery is complicated and “ideal” facture permeability is a subjective value, depending on various factors.

While running inverted 5 – point dual porosity dual permeability model, it was observed that increase of the permeability of fractures contributed to higher recovery but balanced by the ratio of matrix to fracture permeability, and that fracture spacing had considerable effect for systems with low matrix permeability.

Results from the 3 dimensional sector model suggest that all effective development technologies in this reservoir should be based on thermal methods of oil recovery. While comparing hot water injection with currently applied steam injection, the superiority of steam is clear. Results from this research suggest that in reservoir N in the YHOF fractures facilitated steam breakthrough in all modes of

SAGD tested. Cyclic steam injection was thus tested, and although the recovery was low, steam breakthrough did not occur and thus can be recommended if the economics of low recovery work out against drilling new producers that are needed when early breakthrough occurs.

We tested five different fishtail scenarios for 3-year forecasting simulation with various lengths of injection, soaking and production periods. The highest recovery was obtained in the case of 10-day long steam injection, 10-day long soaking period and 10-day long production period. After 3 years of development, it resulted in 7% recovery. In comparison we had only 4.5% from continuous steam injection using SAGD wells that is currently implemented in the reservoir N. The fish-tailed well scheme also avoided steam breakthrough. High efficiency of fishtail well design with CSS was additionally validated based on history matched data.

Based on results from this research we thus recommend the use of a fishtail well design to the current development of reservoir N in the YHOF to improve recovery and cumulative oil production. However, an economic analysis will be needed to determine if this scheme can be implemented in a pilot study (as in sector model in reservoir N) prior to full field implementation.

REFERENCES

Akhonizadeh, H., Fattahi, A., (2015) Impact of Well Configuration on Performance of Steam Based Gravity Drainage Processes in Naturally Fractured Reservoirs. Petroleum Exploration and Production Technology Journal. Doi 10.1007/s13202-014-0117-y.

Al Yousef, Z., Al Daif, H., Al Otaibi, M. (2013, November 21). An Overview of Steam Injection Projects in Fractured Carbonate Reservoirs in the Middle East. Journal of Petroleum Science Research. volume 3 issue 3. doi: 10.14355/jpsr.2014.0303.01

Al-Hadhrami, H. S., & Blunt, M. J. (2000, January 1). Thermally Induced Wettability Alteration to Improve Oil Recovery in Fractured Reservoirs. Society of Petroleum Engineers. doi:10.2118/59289-MS

Alvarado, V., Manrique, E. (2010). Enhanced Oil Recovery: Field Planning and Development Strategies. 192 pp.

Azin, R., Kharrat, R., Ghotbi, C., & Vossoughi, S. (2005, January 1). Applicability of the VAPEX Process to Iranian Heavy Oil Reservoirs. Society of Petroleum Engineers. doi:10.2118/92720-MS

Babadagli, T. (2001, January 1). Selection of Proper EOR Method for Efficient Matrix Recovery in Naturally Fractured Reservoirs. Society of Petroleum Engineers. doi:10.2118/69564-MS

Babadagli, T. (2002). Evaluation of EOR methods for heavy-oil recovery in naturally fractured reservoirs. Journal of Petroleum Science and Engineering. 37 (2003) 25– 37

Bagci, A. S. (2007, January 1). SAGD Process In Fractured Heavy Oil Reservoirs. Offshore Mediterranean Conference.

Bahonar, M., Ataei, A., Masoudi, R., & Mousavi Mirkalei, S. M. (2007, January 1). Evaluation of Steam Injection in a Fractured Heavy Oil Carbonate Reservoir in Iran. Society of Petroleum Engineers. doi:10.2118/105299-MS

Baker, R. O., & Kuppe, F. (2000, January 1). Reservoir Characterization for Naturally Fractured Reservoirs. Society of Petroleum Engineers. doi:10.2118/63286-MS

Briggs, P. J., Baron, P. R., Fulleylove, R. J., & Wright, M. S. (1988, February 1). Development of Heavy-Oil Reservoirs. Society of Petroleum Engineers. doi:10.2118/15748-PA

Britton, M. W., Martin, W. L., Leibrecht, R. J., & Harmon, R. A. (1983, March 1). The Street Ranch Pilot Test of Fracture-Assisted Steamflood Technology. Society of Petroleum Engineers. doi:10.2118/10707-PA

Chan, M. Y. S., Fong, J., & Leshchyshyn, T. (1997, January 1). Effects Of Well Placement And Critical Operating Conditions On The Performance of Dual Well SAGD

Well Pair In Heavy Oil Reservoir. Society of Petroleum Engineers. doi:10.2118/39082-MS

Chérif Khelifa, Aziez Zeddouri, Fayçal Djabes. “Influence of Natural Fractures on Oil Production of Unconventional Reservoirs”, Energy Procedia, Volume 50, 2014, Pages 360-367

Chordia, M., & Trivedi, J. J. (2010, January 1). Diffusion in Naturally Fractured Reservoirs- A- Review. Society of Petroleum Engineers. doi:10.2118/134589-MS

Chu, C. (1990, January 1). Prediction of Steamflood Performance in Heavy Oil Reservoirs Using Correlations Developed by Factorial Design Method. Society of Petroleum Engineers. doi:10.2118/20020-MS

Civan, F., & Rasmussen, M. L. (2005, January 1). Determination of Parameters for Matrix-Fracture Transfer Functions from Laboratory Data. Society of Petroleum Engineers. doi:10.2118/94267-MS

Civan, F., & Rasmussen, M. L. (2006, January 1). Determining Parameters of Matrix-Fracture Interface Fluid Transfer from Laboratory Tests. Society of Petroleum Engineers. doi:10.2118/104028-MS

Clemens, T., & Wit, K. (2001, January 1). The Effect of Fracture Spacing on Gas/Oil Gravity Drainage in Naturally Fractured Reservoirs. Society of Petroleum Engineers. doi:10.2118/71507-MS

Closmann, P. J., & Seba, R. D. (1983, June 1). Laboratory Tests on Heavy Oil Recovery by Steam Injection. Society of Petroleum Engineers. doi:10.2118/10778-PA

Cook, A.C., Johnson, K.R., 1970. “Early joint formation in sediments.” Geol. Mag., v. 107, No. 4, p. 361-368.

Creux, P., Meyer, V., Cordelier, P. R., Franco, F., & Montel, F. (2005, January 1). Diffusivity In Heavy Oils. Society of Petroleum Engineers. doi:10.2118/97798-MS

Das, S. K. (2007, January 1). Application of thermal processes in heavy oil carbonate reservoirs. Society of Petroleum Engineers. doi:10.2118/105392-MS

Edmunds, N., Barrett, K., Solanki, S., Cimolai, M., & Wong, A. (2009, September 1). Prospects for Commercial Bitumen Recovery from the Grosmont Carbonate, Alberta. Petroleum Society of Canada. doi:10.2118/09-09-26

Eker, E., Uzun, I., & Kazemi, H. (2017, February 20). Numerical Simulation of Dual-Porosity Multiphase Flow Using Poroelasticity Theory. Society of Petroleum Engineers. doi:10.2118/182728-MS

Farah, N., Ding, D. Y., & Delorme, M. (2016, August 1). Extension of the Multiple Interacting Continua Method to Discrete Fracture Models for Unconventional Low Permeability Reservoir Simulations. Unconventional Resources Technology Conference. doi:10.15530/URTEC-2016-2443586

Fatemi, Mobeen. (2009). Simulation Study of Steam Assisted Gravity Drainage (SAGD) in Fractured Systems. Oil & Gas Science and Technology - Revue de l'IFP. 64. 477-487. 10.2516/ogst/2009012.

Fatemi, S. M., Kharrat, R., & Vossoughi, S. (2011, January 1). Investigation of Steam Assisted Gravity Drainage (SAGD) and Expanding Solvent-SAGD (ES-SAGD) Processes in

Fattahi, A., Akhondzadeh, H., Derahman, M.N., Yunan, M.H., Namazi, S. (2012). Impact of reservoir heterogeneity on Steam Assisted Gravity Drainage in heavy oil fractured reservoirs. Energy exploration and exploitation journal. Vol 30, pp 553-566.

Farog, A., A.Mustafa, H., Mukhtar, E., Elblaoula, H., A. Yassin, B., Tagwa, M., … Abdalla, F. (2016, April 25). Implementation of Chemical EOR as Huff and Puff to Improve Oil Recovery for Heavy Oil Field by Chemical Treatment SEMAR Cast Study Bamboo Oil Field. Society of Petroleum Engineers. doi:10.2118/182792-MS

Fridman, A., Timonina, N. “Prospects of Development of Oil Producing Industry in the Republic of Komi”, Izvestiya Komi, UDK 553.982, 2011

Fung, L. S.-K., Simulation of block-to-block processes in naturally fractured reservoirs”, Annual SPE Meeting, November 1991.

Gabitto, J. F. (1998, January 1). Matrix-Fracture Mass Transfer. Society of Petroleum Engineers. doi:10.2118/39702-MS

Gautam, P. S., & Mohanty, K. K. (2002, January 1). Role of Fracture Flow in Matrix-Fracture Transfer. Society of Petroleum Engineers. doi:10.2118/77336-MS

Geiger, S., Dentz, M., & Neuweiler, I. (2013, May 27). A Novel Multi-Rate Dual-Porosity Model for Improved Simulation of Fractured and Multiporosity Reservoirs. Society of Petroleum Engineers. doi:10.2118/148130-PA

Golf-Racht, T.D., (1986). Fundamentals of Fractured Reservoir Engineering. Developments in Petroleum Science. New York.

Gong, B., Karimi-Fard, M., & Durlofsky, L. J. (2006, January 1). An Upscaling Procedure for Constructing Generalized Dual-Porosity/Dual-Permeability Models from Discrete Fracture Characterizations. Society of Petroleum Engineers. doi:10.2118/102491-MS

Hoteit, H. (2011, January 1). Proper Modeling of Diffusion in Fractured Reservoirs. Society of Petroleum Engineers. doi:10.2118/141937-MS

Hughes, R. G., & Blunt, M. J. (1999, January 1). Pore-Scale Modeling of Multiphase Flow in Fractures and Matrix/Fracture Transfer. Society of Petroleum Engineers. doi:10.2118/56411-MS

Jamili, A., Willhite, G. P., & Green, D. (2011, December 1). Modeling Gas-Phase Mass Transfer Between Fracture and Matrix in Naturally Fractured Reservoirs. Society of Petroleum Engineers. doi:10.2118/132622-PA

Kalinina, A., Kalinin, E. “Geological and Economical Assessment of Complex Use of Yarega Oil”, Izvestiya Komi, Issue 3, 2014.

Konoplev, U. “Method of Technological Parameter Determination During Thermo-Mining Development”, GIAB, #1, 2018.

Kostyuchenko, S.V., Savenkov, S.A., Evlanova, Y.A., Karachurin, N.T., Ganopolsky, R.M, Badrizlov, A.A., Chudinov. S.S., 2017. “Computational technology for hydrodynamic modelling of large oil and gas fields with parallelization on sectoral models for clusters.” Rosneft. Udk 622.276.1/4.001.57.

Kuneevsky, V. V., Osnos, V. B., Vankov, Y. V., Larionov, V. M., & Saifullin, E. R. (2017, October 16). Heat and Mass Transfer Processes Caused by Natural Thermal Convection in Oil-Containing Media. Society of Petroleum Engineers. doi:10.2118/187685-MS

Kyte, J. R. (1970, June 1). A Centrifuge Method To Predict Matrix-Block Recovery in Fractured Reservoirs. Society of Petroleum Engineers. doi:10.2118/2729-PA

Labastie, A., Aquitaine, E. (September 1991). Capillary Continuity Between Blocks in Fractured Reservoir. 65th Annual Technical Conference and Exhibition of Petroleum Engineering. New Orleans. September, 1990.

Listed, N. (1987, January 1). 1987 Reports. World Petroleum Congress.

Lu, J., & Qu, J. (2017, November 13). A New Dual-Permeability Model for Naturally Fractured Reservoirs. Society of Petroleum Engineers. doi:10.2118/188553-MS

Lu, J., Zhu, T., & Tiab, D. (2009, January 1). Pressure Behavior of Horizontal Wells in Dual-Porosity, Dual-Permeability Naturally Fractured Reservoirs. Society of Petroleum Engineers. doi:10.2118/120103-MS

Makurat, A., & Gutierrez, M. (1996, January 1). Fracture Flow and Fracture Cross Flow Experiments. Society of Petroleum Engineers. doi:10.2118/36732-MS

McQuillan, H., 1973. Small-scale fracture density in Asmari Formation in southwest Iran and its relation to bed thickness and structural setting. American Association of Petroleum Geologists. Bull., v. 45, No. 1, p. 1-38.

Nabipour, M. Escrochi, S. Ayatollahi, F. Boukadi, M. Wadhahi, R. Maamari, A. Bemani, Laboratory investigation of thermally-assisted gas–oil gravity drainage for secondary and tertiary oil recovery in fractured models, Journal of Petroleum Science and Engineering, Volume 55, Issues 1–2, 2007, Pages 74-82.

Mahmoud, T., & Rao, D. N. (2008, January 1). Range of Operability of Gas-Assisted Gravity Drainage Process. Society of Petroleum Engineers. doi:10.2118/113474-MS.

Mollaei, A., Maini, B. B., & Jalilavi, M. (2007, January 1). Investigation of Steam Flooding in Naturally Fractured Reservoirs. International Petroleum Technology Conference. doi:10.2523/IPTC-11087-MS

Narr, W., Schechter, D., Thompson, L. (2006). Naturally Fractured Reservoir Characterization. Society of Petroleum Engineers. ISBN: 978-1-55563-112-3. 115 pp.

Nikitin, M., Gladkov, P., Kolonskikh, A., Petukhov, A., Mikheev, A. “Analysis of Reological Properties of Yaregskoye Field Heavy High-Viscosity Oil”, UDK 622.276, Saint Petersburg, 2012.

Penney, R. K., Moosa, R., Shahin, G. T., Hadrami, F., Kok, A., Engen, G., … Kharusi, B. (2005, January 1). Steam Injection in Fractured Carbonate Reservoirs: Starting a New Trend in EOR. International Petroleum Technology Conference. doi:10.2523/IPTC-10727-MS

Pickup, G. E., Ringrose, P. S., Corbett, P. W. M., Jensen, J. L., & Sorbie, K. S. (1994, January 1). Geology, Geometry, and Effective Flow. Society of Petroleum Engineers. doi:10.2118/28374-MS

Rangel-German, E. R., & Kovscek, A. R. (2003, January 1). Time-Dependent Matrix-Fracture Shape Factors for Partially and Completely Immersed Fractures. Society of Petroleum Engineers. doi:10.2118/84411-MS

Rangel-German, E. R., & Kovscek, A. R. (2004, January 1). Microvisual Analysis of Matrix-Fracture Interaction. Society of Petroleum Engineers. doi:10.2118/92133-MS

Rusin, L., Chuprov, I., Morozyuk, O., Durkin S. (2005). Technological Principles of Abnormally Heavy Oilfield and Bitumen Development. Second edition. Institute of Computer Research. Moscow, Izhevsk.

Ruzin, L. “Features and Innovative Areas of the Development of High-Viscosity Oil Resourses”, Izvestiya Komi, UDK 622.276(470.13), 2010.

Sabathier, J. C., Bourbiaux, B. J., Cacas, M. C., & Sarda, S. (1998, January 1). A New Approach of Fractured Reservoirs. Society of Petroleum Engineers. doi:10.2118/39825-MS

Saidi, A. M. (1983, January 1). Simulation of Naturally Fractured Reservoirs. Society of Petroleum Engineers. doi:10.2118/12270-MS

Sarma, P., & Aziz, K. (2006, September 1). New Transfer Functions for Simulation of Naturally Fractured Reservoirs with Dual Porosity Models. Society of Petroleum Engineers. doi:10.2118/90231-PA

Sawhney, G. S., Liebe, H., & Butler, R. M. (1995, January 1). Vertical Injection Wells For Sagd: A Practical Option Or Not? Petroleum Society of Canada. doi:10.2118/95-01-06

Schulte, W. M., & de Vries, A. S. (1985, February 1). In-Situ Combustion in Naturally Fractured Heavy Oil Reservoirs. Society of Petroleum Engineers. doi:10.2118/10723-PA

Shen, G., & Shen, X. (2017, August 28). Numerical Simulation on Steam Fingering in Steam Assisted Gravity Drainage of Heavy Oil. American Rock Mechanics Association.

Song, X., Zhu, Y., Liu, Q., Chen, J., Ren, D., Li, Y., Liao, M. (1998, January 1). Identification and Distribution of Natural Fractures. Society of Petroleum Engineers. doi:10.2118/50877-MS.

Sonier, F., Souillard, P., & Blaskovich, F. T. (1988, November 1). Numerical Simulation of Naturally Fractured Reservoirs. Society of Petroleum Engineers. doi:10.2118/15627-PA.

Stearns, D.W., Friedman, M., 1972. "Reservoir in structured rock in stratigraphic oil and gas fields classification, exploration methods and case histories." American Association of Petroleum Geologists. Mem. 16, p. 82-106.

Su, S., Gosselin, O., Parvizi, H., & Giddins, M. A. (2013, June 10). Dynamic Matrix-Fracture Transfer Behavior in Dual-Porosity Models. Society of Petroleum Engineers. doi:10.2118/164855-MS.

Suzuki, A., Nibori, Y., Fomin, S., Chugunov, S., Hashida, T. (2015, April 19). Characterization of mass/heat transfer in fractured geothermal reservoirs by means of mathematical model for complex system. Proceedings World Geothermal Congress 2015, Melbourne, Australia.

Tang, G.-Q., Inouye, A., Lowry, D., & Lee, V. (2011, January 1). Recovery Mechanism of Steam Injection in Heavy Oil Carbonate Reservoir. Society of Petroleum Engineers. doi:10.2118/144524-MS

Tamer, M., & Gates, I. D. (2009, January 1). Impact of Well Configuration on Performance of Steam-Based Gravity Drainage Processes. Petroleum Society of Canada. doi:10.2118/2009-046

Telnova, K. "Palynological and Faunistic Complexes from Adjacent Late Mid-Devonian Depositions of Timan-Pechora Province", Vestnik, #12, 2005.

Thakur, G. C. (1997, January 1). Heavy Oil Reservoir Management. Society of Petroleum Engineers. doi:10.2118/39233-MS.

Van Heel, A. P., Boerrigter, P. M., & van Dorp, J. J. (2008, August 1). Thermal and Hydraulic Matrix-Fracture Interaction in Dual-Permeability Simulation. Society of Petroleum Engineers. doi:10.2118/102471-PA.

Vologodskiy, K., Telkov, V., Aksenov, M., Khramov, D., Rymarenko, K., Lachugin, D., & Gaidukov, L. (2013, June 11). Specifics and Challenges of Heavy oil Production in

Northen Siberia Illustration Based on Biggest Heavy Oil Project in Russia. Society of Petroleum Engineers. doi:10.2118/165552-MS.

Witherspoon, P. A., Tsang, Y. W., Long, J. C. S., & Noorishad, J. (1981, January 1). New Approaches To Problems Of Fluid Flow In Fractured Rock Masses. American Rock Mechanics Association.

Wu, Y.-S., & Pruess, K. (1988, February 1). A Multiple-Porosity Method for Simulation of Naturally Fractured Petroleum Reservoirs. Society of Petroleum Engineers. doi:10.2118/15129-PA.

Yang, G., & Butler, R. M. (1992, August 1). Effects Of Reservoir Heterogeneities On Heavy Oil Recovery By Steam-Assisted Gravity Drainage. Petroleum Society of Canada. doi:10.2118/92-08-03.

VITA

German Albertovich Abzaletdinov was born in 1995, in Vuktyl, Russia. He received his bachelor’s degree in petroleum engineering from Ukhta State Technical University. Later, he decided to join the Craft and Hawkins Department of Petroleum Engineering at Louisiana State University to pursue graduate education. He is currently a candidate for Master of Science in petroleum engineering and plans to graduate in August 2018.